Pancreatic Neuroendocrine Neoplasms (PNENs)

10

Javier Casillas, Joe U. Levi,
John I. Lew, Roberto Ruiz-Cordero,
and Monica T. Garcia-Buitrago

Contents

J. Casillas (✉)
University of Miami Miller School of Medicine,
Department of Radiology, Jackson Memorial
Hospital, 1611 NW 12 Avenue,
WW-279, Miami, FL 33136, USA
e-mail: jcasilla@med.miami.edu

J.U. Levi • J.I. Lew
University of Miami Miller School of Medicine,
Department of Surgery, Jackson Memorial Hospital,
Clinical Research Building, 410L, 1120N.W.
14 th Street, Miami, FL 33136, USA

R. Ruiz-Cordero
Department of Pathology, Jackson Memorial
Hospital, Holtz Center, 2042E,
1611 NW 12 Avenue, Miami, FL 33136, USA

M.T. Garcia-Buitrago
University of Miami Miller School of Medicine,
Department of Pathology, Jackson Memorial
Hospital, Holtz Center, 2042E,
1611 NW 12 Avenue, Miami, FL 33136, USA

J. Casillas et al., *Multidisciplinary Teaching Atlas of the Pancreas: Radiological, Surgical, and Pathological Correlations*, DOI 10.1007/978-3-662-46745-9_10

10.1 Self-Assessment Questions

1. **All of the following are histologic characteristics of well-differentiated pancreatic neuroendocrine neoplasms (PNENs), *except***:
   a. Composed of uniform polygonal cells that resemble islet cells.
   b. Have round or ovoid nuclei that have stippled, salt-and-pepper chromatin and eosinophilic cytoplasm.
   c. Endocrine differentiation may be confirmed with chromogranin A.
   d. Amyloid may be identified in some insulinomas.
   e. Hormonal activity always correlates with immunohistochemical staining of the tumor.
2. **All of these statements about imaging of PNEN are incorrect, *except***:
   a. Transabdominal ultrasound has a higher sensitivity in the detection of PNEN than intraoperative ultrasound.
   b. Usually, PNENs are best identified by computed tomography on the venous phase.
   c. PNENs are usually hyperattenuating on arterial and venous phase computed tomography images.
   d. These tumors are isointense to the normal pancreas on MR T2-weighted imaging.
   e. Overall sensitivity of octreotide scan in the detection of PNEN is between 60 and 50 %.
3. **The following statements are correct regarding insulinomas, *except***:
   a. The most common location of insulinomas is the head of the pancreas.
   b. Insulinomas are the most common functioning PNEN.
   c. 10 % of insulinomas demonstrate malignant behavior.
   d. Classic clinical triad of insulinomas: hypoglycemic symptoms, low blood glucose, and relief of symptoms after administration of glucose.
   e. Insulinomas are usually small at the time of diagnosis (<2 cm).
4. **Which statement about gastrinomas is *correct***?
   a. Gastrinomas are as common as insulinomas.
   b. 30 % of gastrinomas demonstrate malignant behavior.
   c. More common in the duodenum than in the pancreas.
   d. Zollinger-Ellison syndrome is responsible for 10 % of cases of peptic ulcer disease.
   e. Gastrinomas have a low concentration of somatostatin receptors.
5. **Glucagonomas are associated with all of these, *except***:
   a. Dermatitis
   b. Diabetes
   c. Dizziness
   d. Deep vein thrombosis
   e. Depression
6. **Watery diarrhea, hypokalemia, and achlorhydria are associated with**:
   a. Somatostatinoma
   b. Glucagonoma
   c. Gastrinoma
   d. VIPoma
   e. Insulinoma
7. **The following statements about somatostatinomas are true, *except***:
   a. These tumors most frequently occur in the pancreas or periampullary region of the duodenum.
   b. Duodenal somatostatinomas are more likely to be associated with neurofibromatosis type 1.
   c. These tumors inhibit the intestinal absorption and release of insulin, glucagon, gastrin, and pancreatic enzymes
   d. These tumors may be associated with cholelithiasis.
   e. At the time of diagnosis, the tumor metastases are rare.
8. **The following tumors are associated with MEN-1 syndrome, *except***:
   a. Parathyroid adenoma
   b. Medullary thyroid carcinoma
   c. Carcinoid tumor of the lung
   d. Anterior pituitary adenoma
   e. Endocrine tumor of the pancreas

9. **The following statements about PNEN treatment and prognosis are true**, ***except***:
   a. Most reliable indicators of malignancy and poor prognosis are tumor size and cytologic atypia.
   b. PNENs are classified under the same TNM staging as pancreatic ductal carcinoma.
   c. Poor prognostic factors are vascular or neural invasion, high mitotic rate, and high Ki-67 index.
   d. Surgical resection is the only curative treatment for PNEN.
   e. Metastatic disease may be managed medically with octreotide and/or α-interferon.
10. **Which statement about von Hippel-Lindau syndrome (VHL) is *true*?**
   a. PNEN occurs in 30–40 % of patients with VHL.
   b. PNENs in patients with VHL syndrome are nonfunctioning.
   c. Mean age of PNEN presentation in VHL is 20 years.
   d. PNENs are the most common pancreatic manifestations of VHL.
   e. Frequency of metastatic disease in patients with VHL and PNEN is high.

Answers: 1. e, 2. c, 3. a, 4. c, 5. c, 6. d, 7. e, 8. b, 9. a, 10. b

10.2 Introduction

- Pancreatic neuroendocrine neoplasms (PNENs) are predominantly well-differentiated pancreatic or peripancreatic tumors that demonstrate neuroendocrine differentiation.
- Arises from multipotential epithelial cells in the pancreatic ductal epithelium.
- Classified on the basis of clinical symptoms, size, biological behavior, and histologic parameters.
- Clinically are categorized as nonfunctional or functional.
- PNENs smaller than 0.5 cm are defined as microadenomas.
- Prevalence: approximately 1 in 100,000 people.
- 3 % of all pancreatic neoplasms.
- Most often occur in the third to sixth decades of life.
- No significant gender predilection.
- Most occur sporadically.

- **Hereditary endocrinopathies associated with PNEN (1–2 %)**
  – Multiple endocrine neoplasia type 1 (MEN-1)
  – Von Hippel-Lindau (VHL)
  – Neurofibromatosis type 1 (NFT1)
  – Tuberous sclerosis (TS)

10.3 Histopathology

10.3.1 Macroscopic Appearance (Figs. 10.1 and 10.2)

- Usually solitary, well-demarcated, tan to pink soft tissue tumors.
- The masses may be hard and gray-white when they exhibit fibrosis or amyloid deposition.
- Sizes range from a few millimeters up to 20 cm; average range 1–5 cm.
- Cystic degeneration: due to necrosis 5–10 %; containing clear or hemorrhagic fluid.
- Vascular invasion: adverse prognostic factor.
- Obstruction of the pancreatic duct (benign or malignant tumors).
- Obstruction of the common bile duct (malignant tumors).

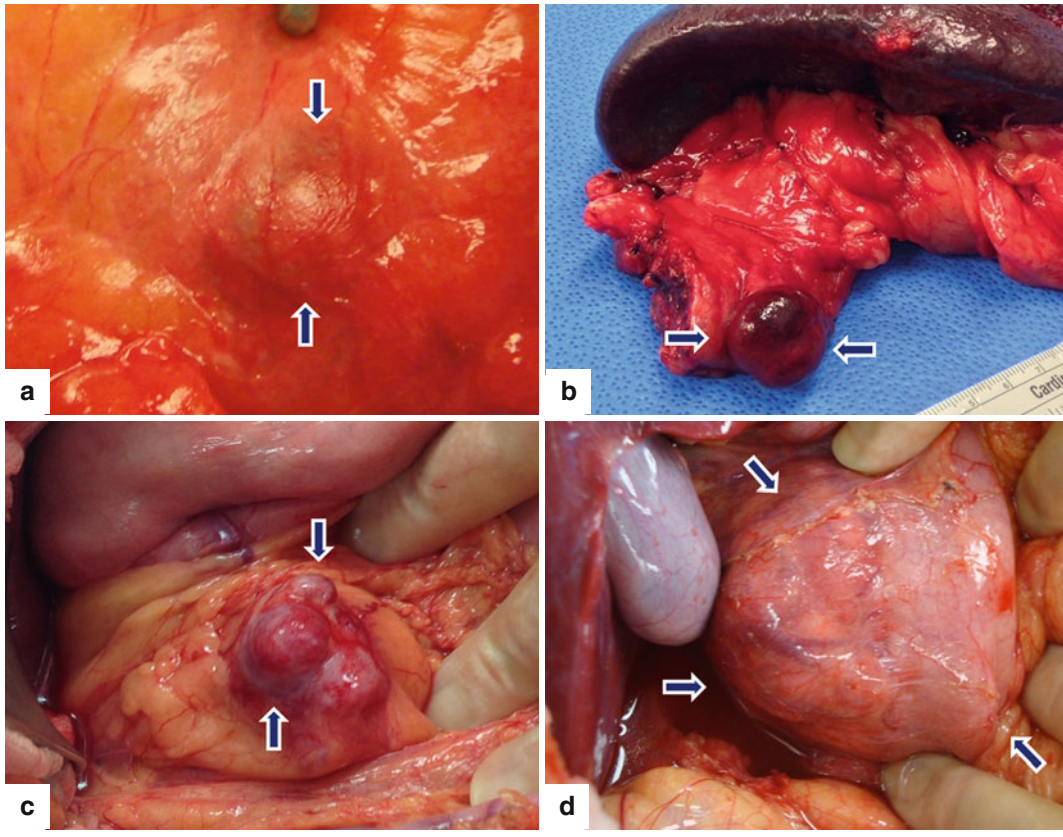

Fig. 10.1 PNEN macroscopic appearance. Intraoperative and surgical speciments of four nonfunctional PNENs show (**a**) a small mass bulging on the serosal surface (*arrows*), (**b**) a small, round, purple mass (*arrows*), (**c**) a small mass with lobulated contours (*arrows*), and (**d**) a medium-sized, pale pink, firm mass with smooth borders (*arrows*)

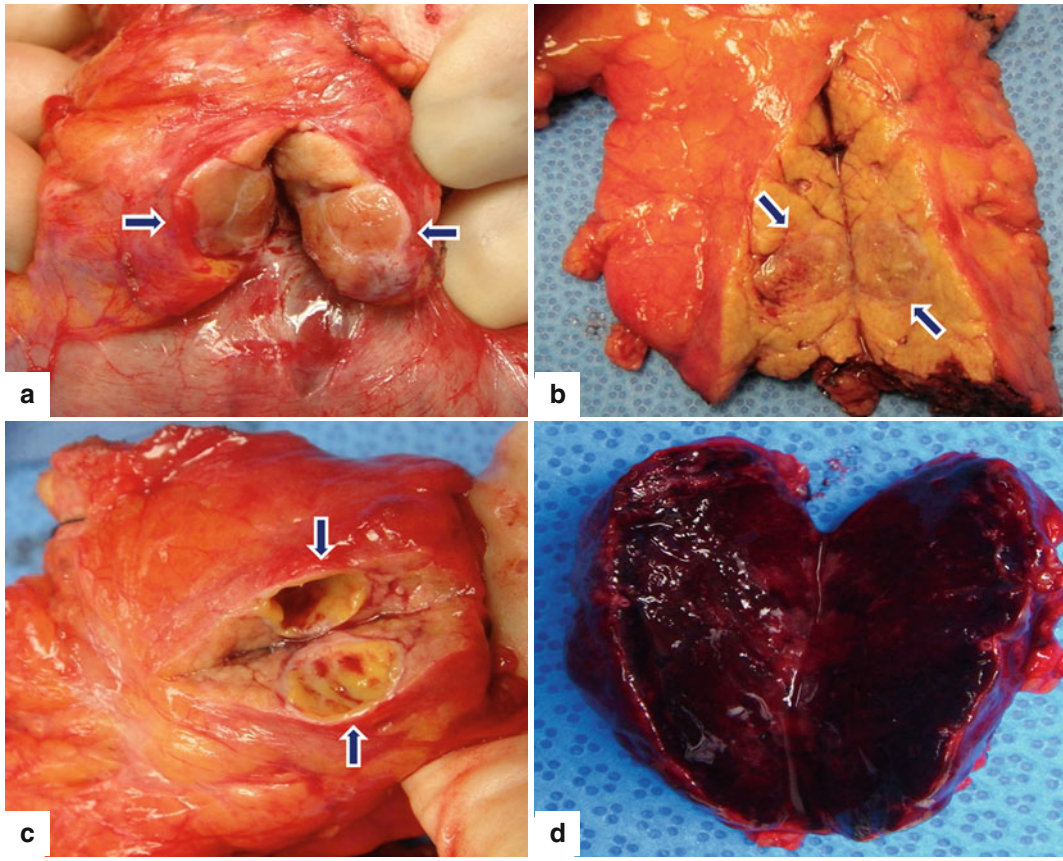

Fig. 10.2 PNEN macroscopic appearance – cross section. Photographs of four bivalved specimens demonstrate (**a**, **b**) light tan masses with a soft, fleshy homogeneous parenchyma (*arrows*), (**c**) a cystic mass with a thick capsule (*arrows*), and (**d**) a completely hemorrhagic mass with friable parenchyma

10.3.2 Microscopic Appearance (Fig. 10.3)

- Uniform polygonal cells arranged in a nested pattern.
- Round to oval nuclei that have stippled, **"salt-and-pepper" chromatin** and scant eosinophilic granular cytoplasm.
- Growth patterns: solid, trabecular, glandular, acinar, cystic, papillary, and angiomatoid.
- Variable amounts of collagenous stroma and sclerosis.
- Tumor differentiation refers to the extent of resemblance to the normal cellular counterpart (well or poorly differentiated).
- Tumor grade refers to the degree of biologic aggressiveness (low, intermediate, and high grades) and is based on the mitotic count and the proliferative index by Ki-67 immunohistochemistry.
- Tumor stage refers to the extent of spread of the tumor.

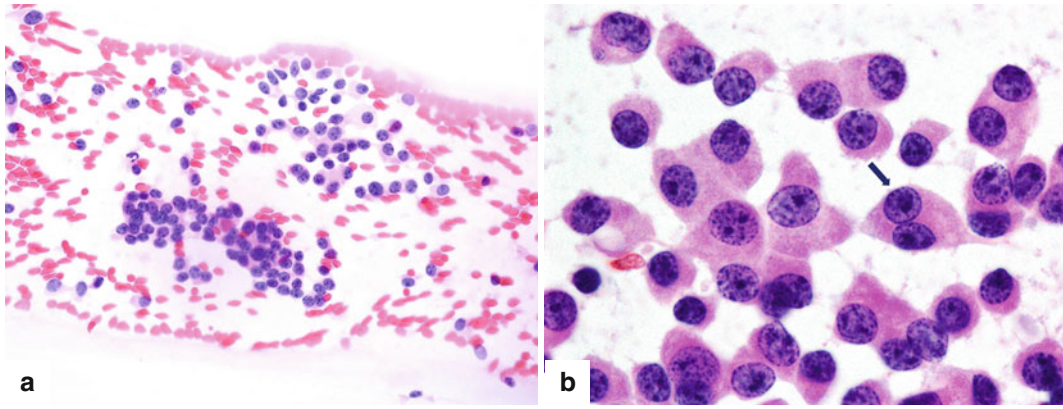

Fig. 10.3 Cytologic features: specimens demonstrate loosely cohesive groups (**a**) and isolated oval cells (**b**) with round, eccentrically located nuclei with the characteristic chromatin stippling ("salt-and-pepper"). The nuclei are mildly enlarged with well-defined nuclear borders. The *arrow* in (**b**) points to a binucleated cell (H&E, 10×, 100×)

10.3.3 Immunohistochemical Endocrine Markers (Fig. 10.4)

- **Chromogranin A**: positive (protein found in secretory granules)
- **Synaptophysin**: positive (membrane glycoprotein found in presynaptic vesicles)
- **Ki-67**: used to assess the proliferative rate

Practical Pearls

- In functional PNEN, the hormonal activity does not always correlate with immunohistochemical staining of the tumor.
- Most nonfunctioning PNENs can show focal immunohistochemical staining for several peptides.

Features of Well-Differentiated PNEN

- Tumor confined to pancreas
- Usually do not metastasize
- No necrosis
- Low grade: low mitotic rate (less than 2 mitoses per 10 high-power fields) and low Ki-67 proliferative index (less than 3 % of Ki-67 staining)
- Intermediate grade: intermediate mitotic rate (between 2 and 20 mitoses per 10 high-power fields) and intermediate Ki-67 proliferative index (3–20 % of Ki-67 staining)
- Strong positivity for chromogranin and synaptophysin

Mutations of Common Oncogenes or Tumor-Suppressor Genes

- K-ras
- PTEN
- RET
- BRAF
- Rb
- CDKN2a/p16 DNA mismatch repairs and P53 are absent

Features of Poorly Differentiated PNEN

- Infiltrative growth pattern.
- Areas of necrosis can be seen.
- Cells are small or large in size with irregular nuclei, scant cytoplasm, and abundant mitoses (>20 per 10 high-power fields).
- Positive stain for chromogranin and synaptophysin (sometimes only focally).
- High Ki-67 proliferative index (>20 %).

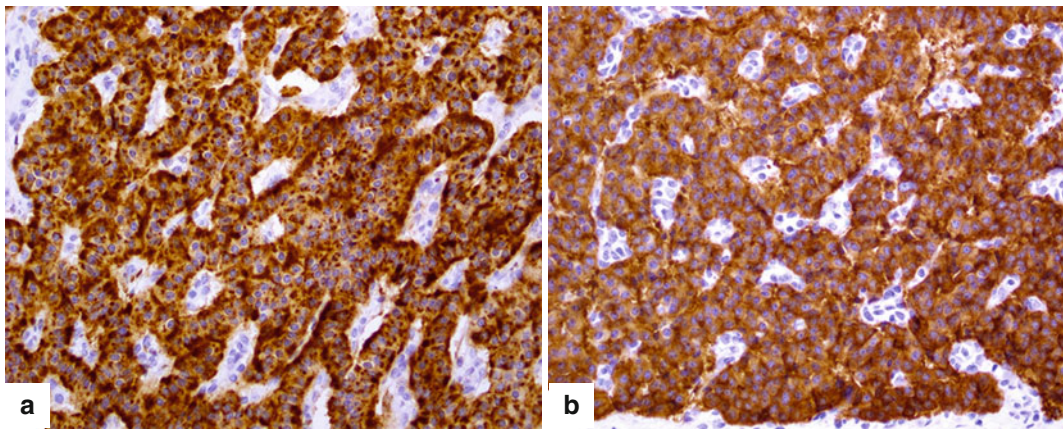

Fig. 10.4 Immunohistochemistry. The neurosecretory granules in neuroendocrine cells stain strongly positive for chromogranin (**a**) (20×) and synaptophysin (**b**) (20×) however, a faint or focal staining can be observed in poorly differentiated tumors

10.3.4 World Health Organization (WHO) Classification (Fig. 10.5)

The 2010 WHO classification recommends to use the term "neuroendocrine carcinoma" in the absence of metastases, only for poorly differentiated neoplasms (small cell carcinomas and large cell carcinomas) (Table 10.1).

- Well-differentiated endocrine neoplasm
  - Low grade; grade 1
  - Intermediate grade; grade 2
- Poorly differentiated endocrine carcinoma
  - High grade; grade 3

- **Classification is based on mitotic rate and cell proliferation (measured with the Ki-67 labeling index) (Fig. 10.6). Once the tumor shows cytologic features of high-grade carcinoma, it should be categorized as small cell carcinoma or large cell carcinoma.**

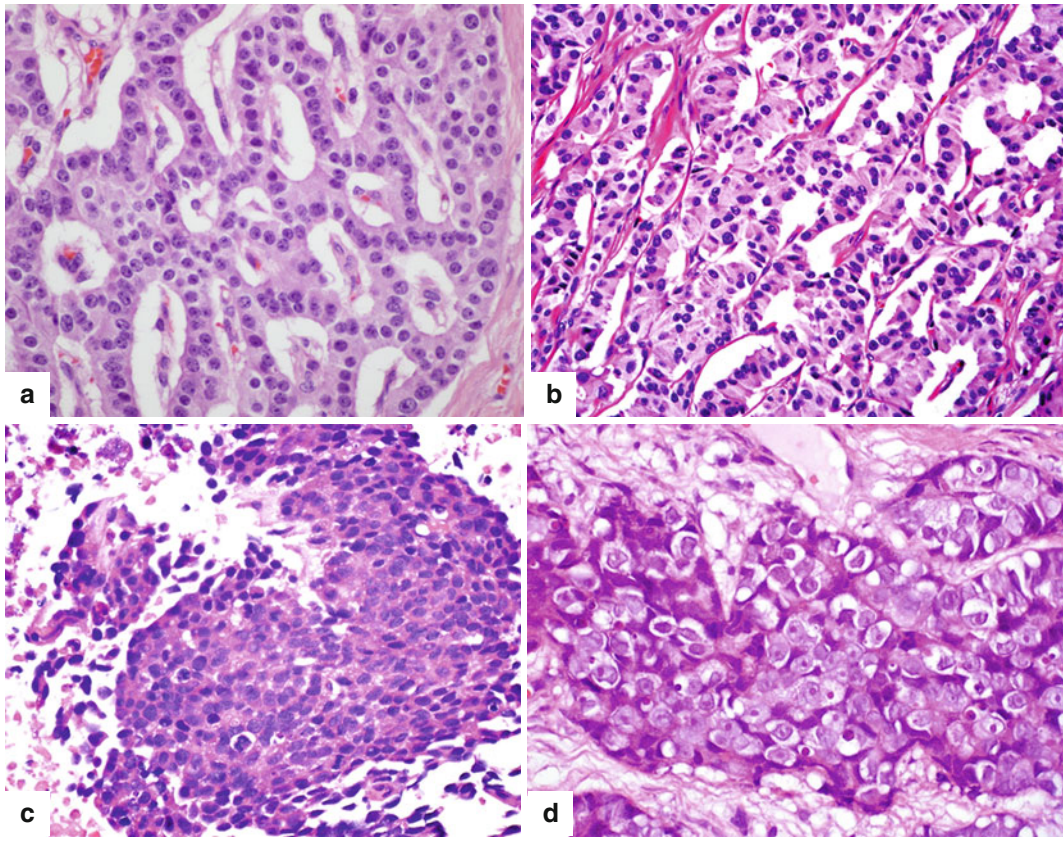

Fig. 10.5 Classification. PNENs are classified based on their degree of differentiation: well-differentiated low grade (**a**) (20×) and well-differentiated intermediate grade (**b**) (20×); or poorly differentiated carcinoma [small cell (**c**) (20×) or large cell neuroendocrine carcinoma (**d**) (60×)]. Well-differentiated tumors retain an organoid formation with a glandular pattern and abundant cytoplasm; intermediate-grade tumors display a more trabecular pattern; and poorly differentiated tumors are arranged in sheets of small or large cells with scant cytoplasm, prominent nucleoli, condensed chromatin and necrosis

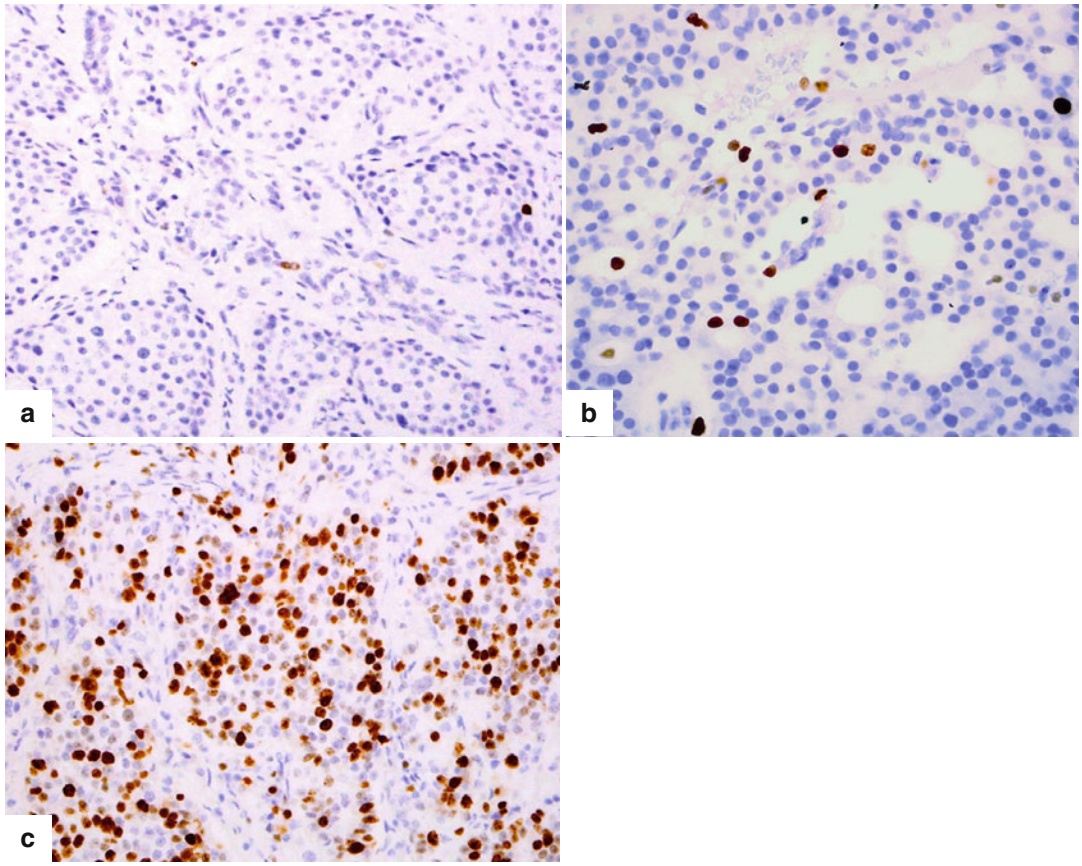

Fig. 10.6 Proliferative index. Immunohistochemistry for Ki-67 illustrates the proliferative rate of three different tumors: (**a**) <1 % expression grade 1 PNEN, (**b**) approximately 3 % expression grade 2 PNEN, and (**c**) >80 % expression grade 3 PNEN

Table 10.1 WHO Nomenclature for Pancreatic Neuroendocrine Neoplasms

Differentiation	ENETS/WHO 2010 Classifications and grading		Features	
			Mitoses/10 HPF	Ki-67 proliferative index (%)
Well-differentiated	Neuroendocrine neoplasm, grade 1 (G1)		<2	<3
	Neuroendocrine neoplasm, grade 2 (G2)		2–20	3–20
Poorly differentiated	Neuroendocrine carcinoma, grade 3 (G3)	Small cell carcinoma	>20	>20
		Large cell carcinoma		

10.4 Nonfunctional PNEN

10.4.1 Epidemiology

- Usually sporadic
- More common than functional PNEN; representing up to 50–75 % of the cases
- Most common PNEN in MEN-1 and VHL syndrome
- Mean age of presentation: 55 years
- Slight female predominance
- 60 % incidence of malignancy
- Patients who have nonfunctional PNEN that are smaller than 2 cm are mostly cured by surgery

- Many of these tumors secrete pancreatic polypeptide or other hormones without associated clinical symptoms.
- May also produce an inert precursor hormone or low levels of an effective hormone.

10.4.2 Clinical Presentation

- Nonfunctional PNENs remain clinically silent until they reach a noticeable size and provoke symptoms by tumor mass effect.

Associated Symptoms and Signs
- Abdominal pain
- Weight loss
- Anorexia
- Nausea
- Abdominal mass
- Jaundice (rare)
- Pruritus

Practical Pearls
- Silent, nonfunctional PNENs may eventually be discovered incidentally by abdominal imaging performed for another cause or during screening of a patient with MEN-1 syndrome.
- Although nonfunctional PNENs secrete a number of substances such as chromogranin, neuron-specific enolase, pancreatic polypeptide, and ghrelin. They do not present clinically with a hormonal syndrome as compared to the functional neoplasms.

10.4.3 Laboratory Evaluation

- **Chromogranin A** (**CgA**): most commonly secreted and measured hormone associated with all types of PNEN (normal value <93 ng/ml). Sensitivity of 50 %
- **Chromogranin A**: useful marker for detecting residual or recurrent disease in treated patients

Practical Pearls
- Chromogranin A can also be elevated in patients with carcinoid tumors, pheochromocytoma, neuroblastoma, medullary thyroid cancer, some pituitary tumors, and in amine precursor uptake and decarboxylation (APUD) tumors.
- False-positive elevations of chromogranin A (CgA) are often seen in patients taking proton pump inhibitors or experiencing impaired hepatic or renal function or non-neuroendocrine tumors (i.e. testicular cancer).

10.4.4 Imaging

- On average, nonfunctional PNENs are larger than functional PNENs
- Average size: 5–6 cm
- Usually solitary, except if they are associated with familial syndromes
- Shape: round or oval, well-circumscribed or poorly defined margins
- Calcifications and vascular invasion may be present
- Even distribution throughout the pancreas
- Diffuse involvement of the entire pancreas is rare
- Metastases at the time of diagnosis (60–80 %), presenting as peripancreatic lymph nodes and/or liver masses

10.4.4.1 Ultrasound (US), Endoscopic Ultrasound (EUS), Intraoperative Ultrasound (IOUS)
(Figs. 10.7–10.16)

Findings
- Well-circumscribed, round or oval, hypoechoic mass with smooth margins
- Color Doppler: hypervascular or hypovascular

Signs of Malignancy
- Ill-defined margins
- Enlarged peripancreatic nodes
- Liver metastases: hyperechoic or hypoechoic
- Pancreatic duct obstruction (rare)
- Biliary obstruction (rare)

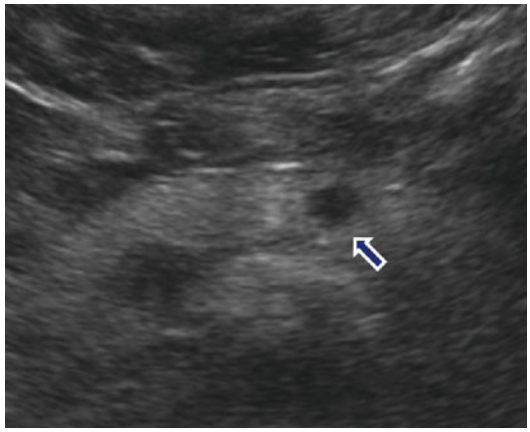

Fig. 10.7 Nonfunctional PNEN on US. A 41-year-old male with right upper quadrant pain. Incidental finding in an abdominal ultrasound. Transverse image shows a small, well-circumscribed, hypoechoic mass in the pancreatic body (*arrow*)

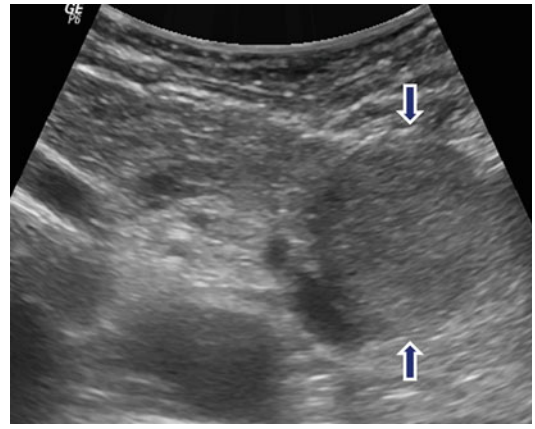

Fig. 10.8 Nonfunctional PNEN on US. A 62-year-old male with history of left quadrant pain. Transverse image reveals a round, well-defined, homogeneous, slightly hypoechoic mass in the tail of the pancreas (*arrows*)

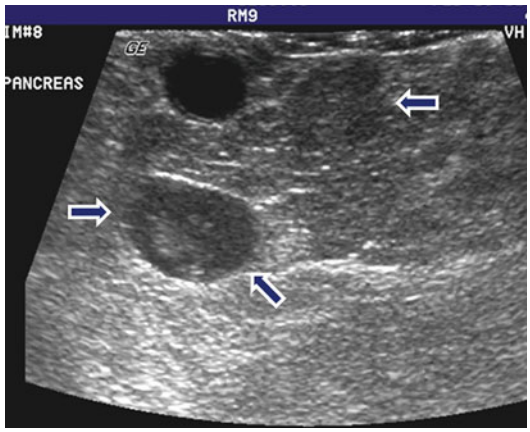

Fig. 10.9 Multiple nonfunctional PNENs on US. A 37-year-old male patient with history of MEN-1 syndrome. IOUS transverse image shows two small, well-defined hypoechoic masses in the pancreatic neck (*arrows*)

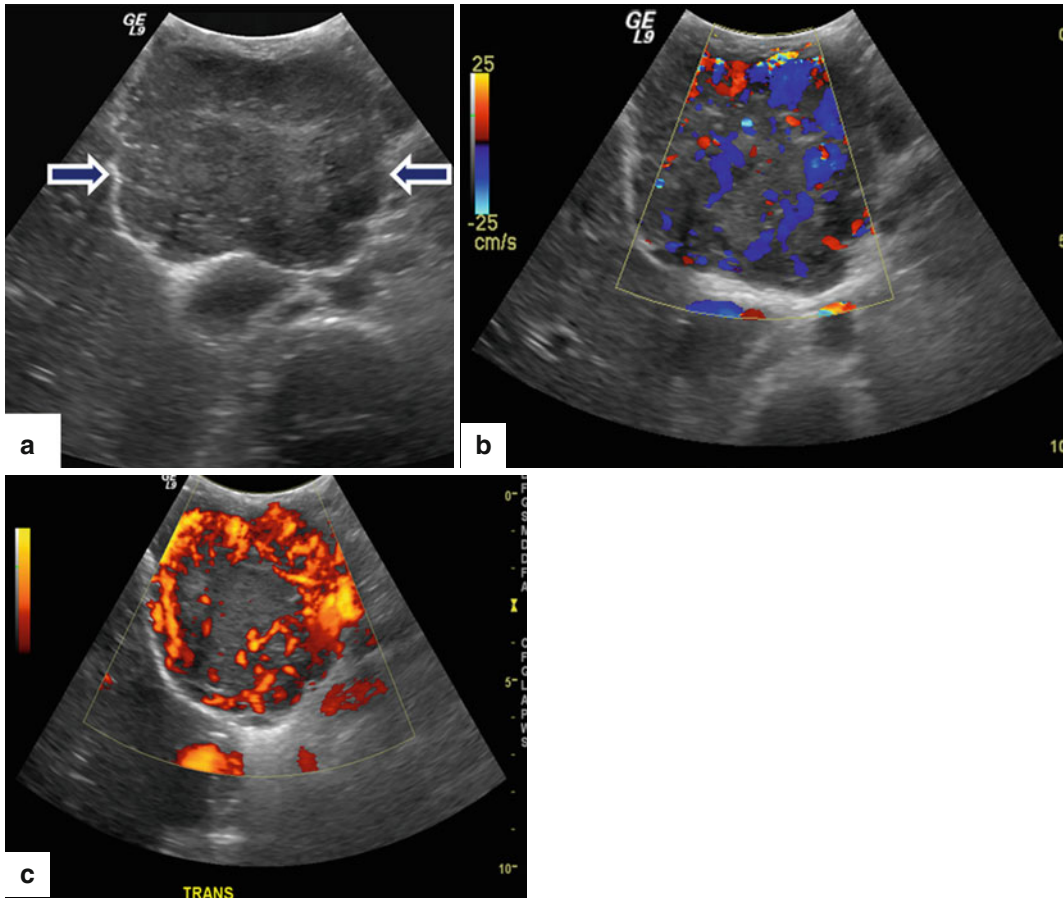

Fig. 10.10 Nonfunctional PNEN on US. An 18-year-old with history of von Hippel-Lindau disease. IOUS gray scale and color power Doppler transverse (**a**–**c**) images show a large homogeneous, hypoechoic, lobulated, hypervascular mass in the pancreatic head (*arrows*)

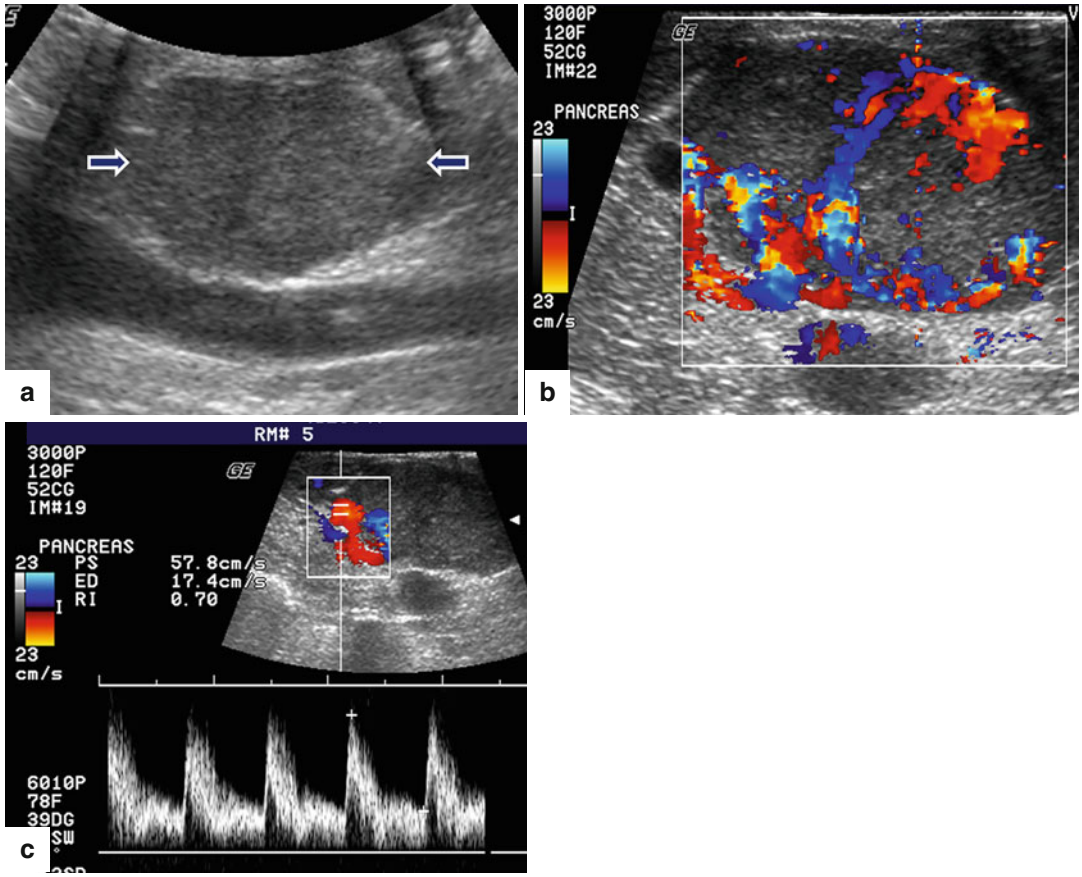

Fig. 10.11 Nonfunctional PNEN on US. A 50-year-old female patient with an incidental pancreatic finding. IOUS longitudinal gray scale (**a**) and color Doppler spectral (**b**, **c**) images show an ovoid, hypoechoic mass with prominent arterial supply in the pancreatic head anterior to the inferior vena cava (*arrows*)

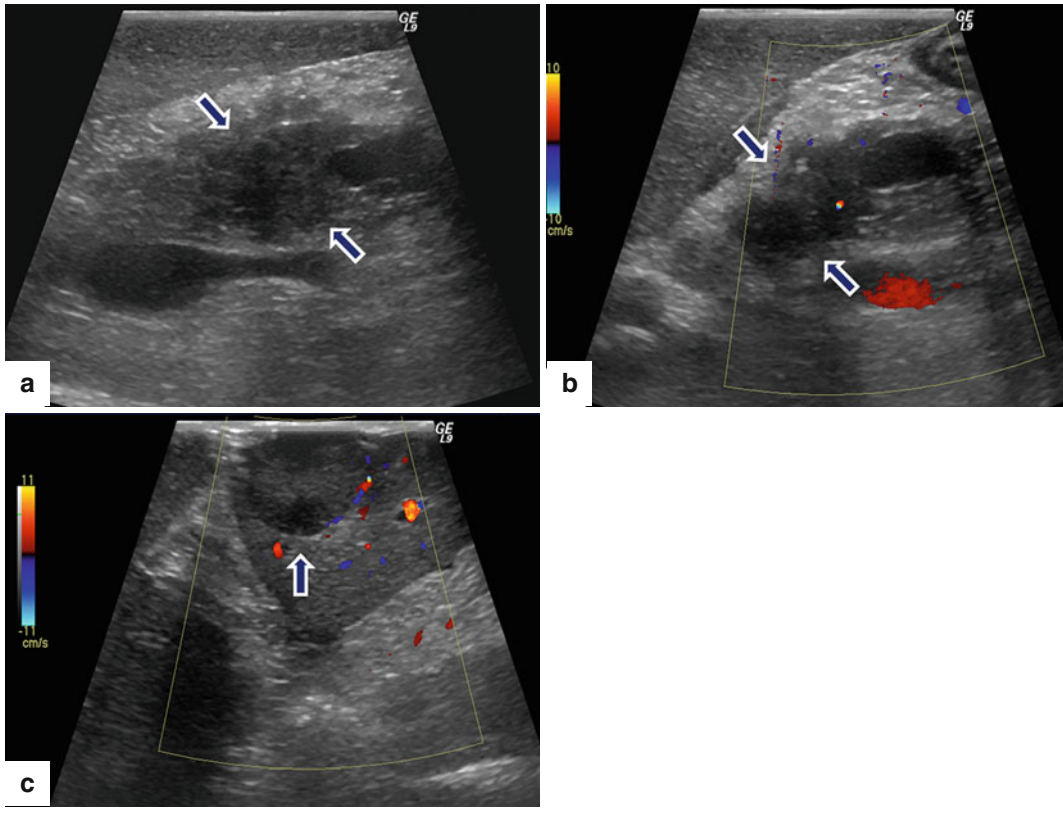

Fig. 10.12 Malignant nonfunctional PNEN on US. A 65-year-old female with history of epigastric pain and weight loss. Transverse (**a**) and sagittal (**b**, **c**) images demonstrate a hypoechoic mass with poorly defined margins in the pancreatic head (**a**, **b**) (*arrows*) and a hypoechoic, avascular metastatic deposit in the liver (**c**) (*arrow*)

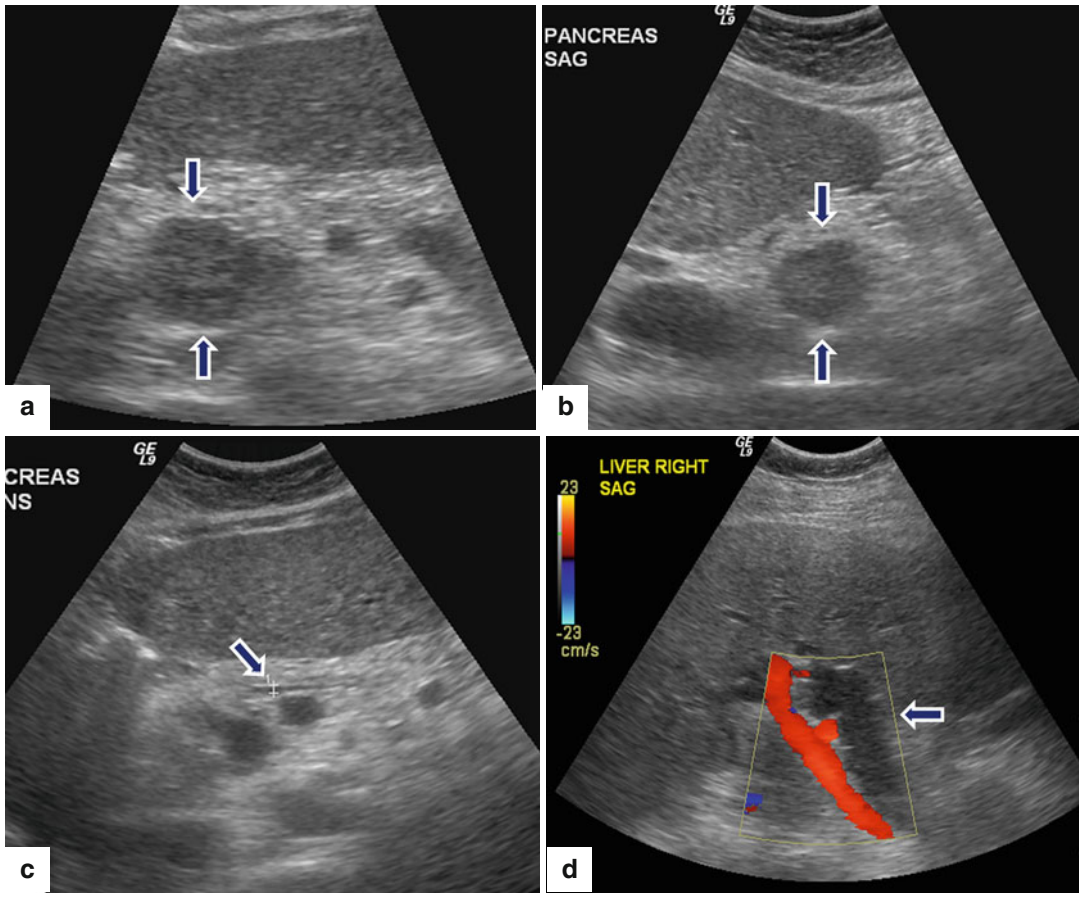

Fig. 10.13 Malignant nonfunctional PNEN on US. A 72-year-old male with history of epigastric pain and weight loss. Transverse (**a**) and sagittal (**b**) images show a round, hypoechoic mass, with ill-defined margins in the pancreatic head (*arrows*). Transverse images show mild dilatation of the pancreatic duct (**c**) (*arrow*) and obstruction of the common bile duct (**d**) (*arrow*) associated with this mass

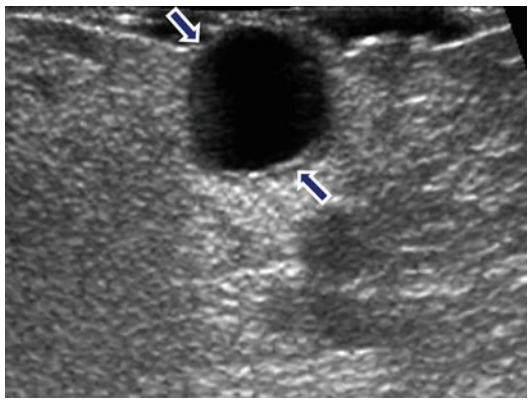

Fig. 10.14 Cystic nonfunctional PNEN on US. A 41-year-old male with MEN-1 syndrome. IOUS transverse image demonstrates a small cystic mass with mild asymmetric wall thickening (*arrows*)

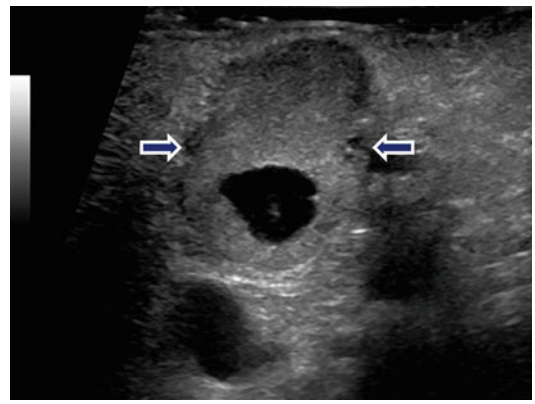

Fig. 10.15 Complex nonfunctional PNEN on US. A 53-year-old female with an incidental finding on a CT of the chest. IOUS transverse image reveals a complex mass with solid and cystic components in the pancreatic body (*arrows*)

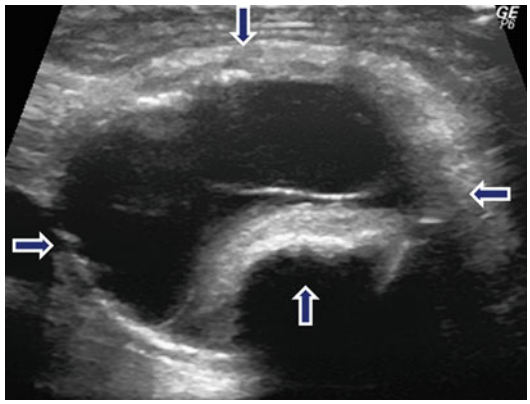

Fig. 10.16 Complex nonfunctional PNEN on US. A 72-year-old male with abdominal pain. IOUS transverse image displays a complex septated cystic mass (*arrows*) with a coarse calcification in the pancreatic body

10.4.4.2 Computed Tomography (CT) (Figs. 10.17–10.43)

Contrast-Enhanced Computed Tomography (CECT) Protocol

- Arterial phase images obtained at 20–25 s after the injection of nonionic intravenous contrast
- Portal venous phase at 55–50 s after injection

Findings

- Well-circumscribed margins, smooth or lobulated
- Tumor enhancement:
  - Small lesion: homogeneous enhancement
  - Large lesion: heterogeneous enhancement (cystic degeneration, necrosis, fibrosis)
  - Calcifications (punctuate, coarse)

Signs of Malignancy

- Large size
- Poorly defined margins
- Arterial vascular encasement (gastroduodenal, hepatic, splenic arteries)
- Venous invasion: (splenic vein, portal vein)
- Enlarged peripancreatic nodes: hypervascular, homogeneous or heterogeneous
- Hepatic metastases: hypervascular, homogeneous or heterogeneous, or peripheral rim enhancing
- Biliary obstruction

Practical Pearls

- Pancreatic duct dilatation associated with parenchymal atrophy and/or pancreatic lipodystrophy distal to a PNEN is rarely seen. These findings may be associated with either benign or malignant tumors.
- Intraductal PNENs without a pancreatic parenchymal lesion may also occur but are exceptionally rare (Fig. 10.41).

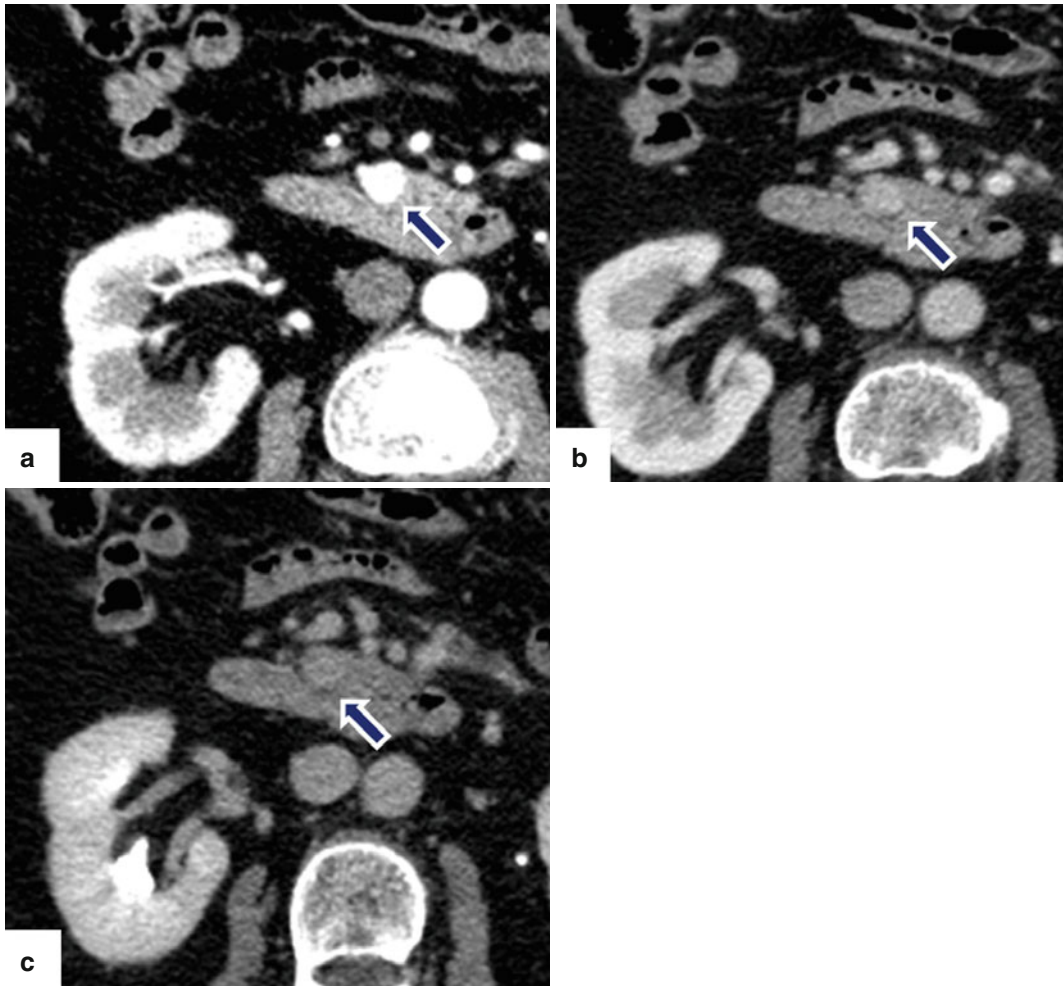

Fig. 10.17 Small nonfunctional PNEN in the pancreatic head on CECT. A 45-year-old female with incidental finding. CECT arterial (**a**), portal (**b**), and delayed phase axial (**c**) images show small, hypervascular mass in the pancreatic head (*arrows*). Note that in the different phases, this mass matches the enhancement pattern of the aorta

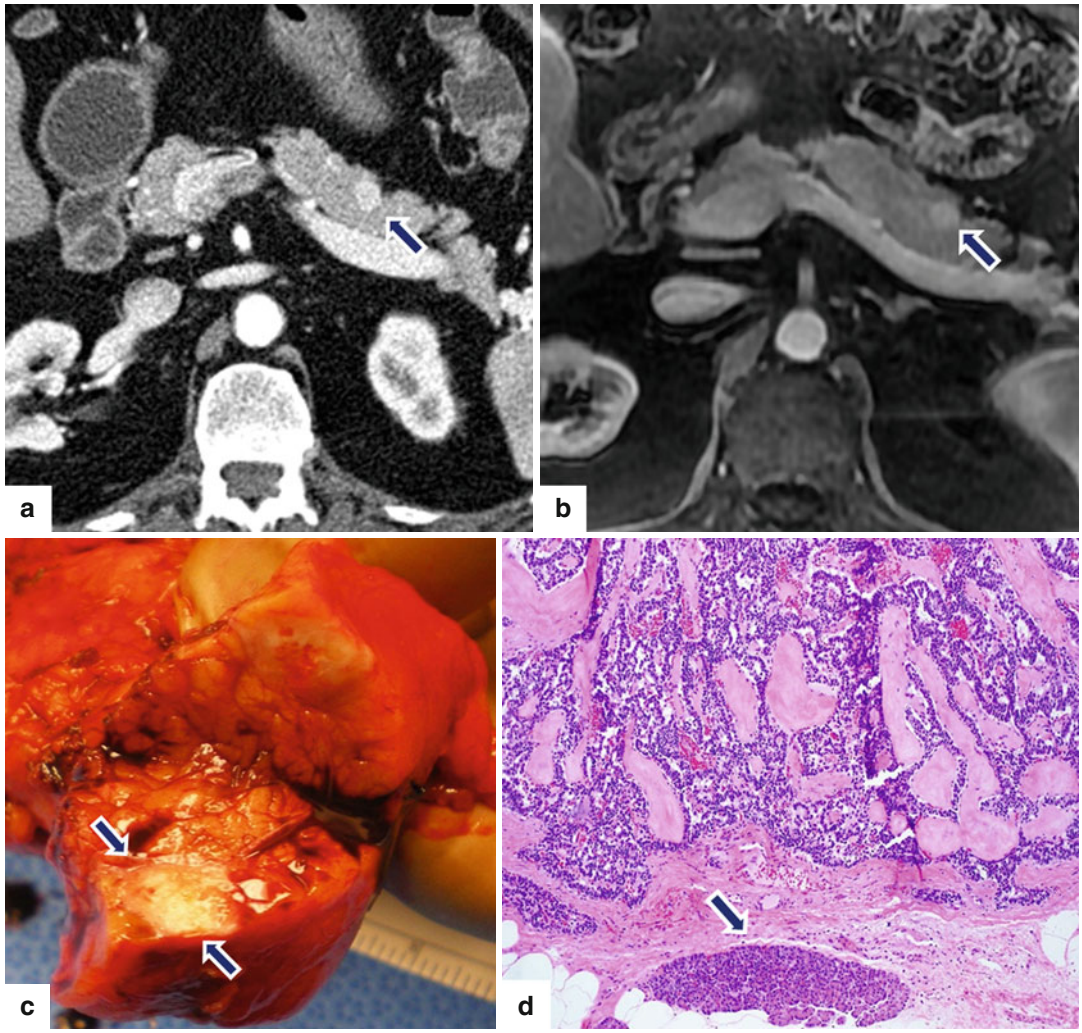

Fig. 10.18 Small nonfunctional PNEN in the pancreatic body on CT and MR. A 67-year-old male with history of nausea and vomiting. Incidental finding on an abdominal CT. CECT arterial axial (**a**) and contrast-enhanced fast spin gradient echo T1-weighted axial (**b**) images demonstrate a small, well-circumscribed, hypervascular mass in the pancreatic body (*arrows*). The patient underwent a distal pancreatectomy. Photograph of the bivalved specimen (**c**) demonstrates a small, ill-defined, yellow-tan mass (*arrows*). Microscopic examination (**d**) reveals a well-differentiated neuroendocrine neoplasm with hyalinized trabecular areas and a pseudocapsule adjacent to a small residual pancreatic lobule (*arrow*)

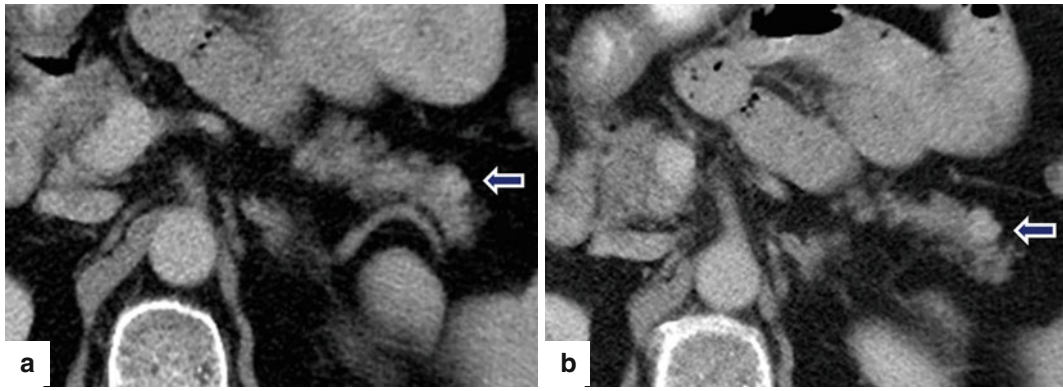

Fig. 10.19 Small nonfunctional PNEN in the pancreatic tail on CT. A 45-year-old female with incidental finding. CECT axial (**a**, **b**) images reveal an 8 mm lobulated hypervascular mass in the pancreatic tail (*arrows*)

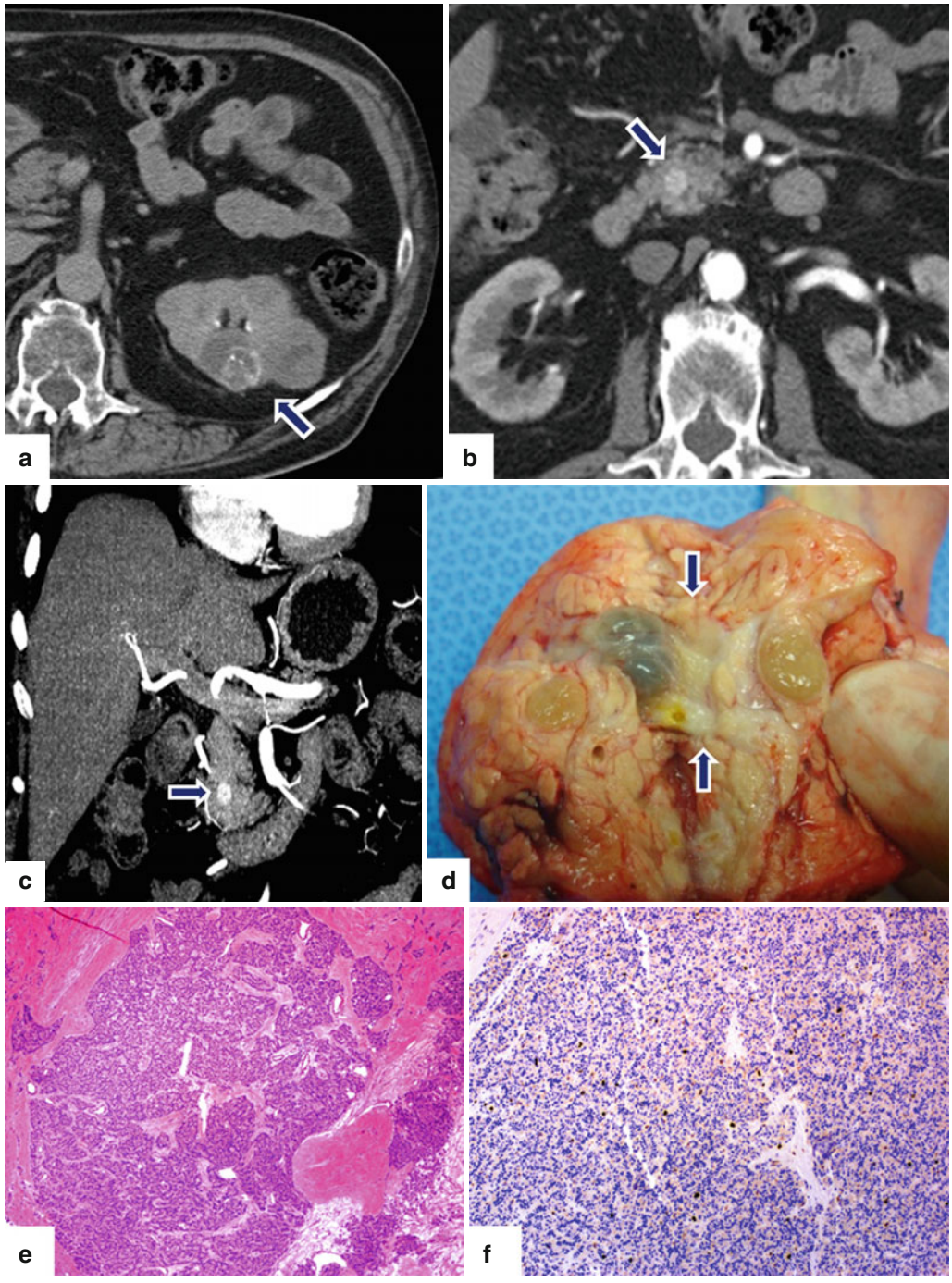

Fig. 10.20 Small nonfunctional PNEN versus pancreatic metastases on CT. A 56-year-old male with history of renal carcinoma. CECT performed 3 years prior (**a**) revealed a complex bilobulated renal cell carcinoma of the left kidney (*arrow*). The patient underwent a partial nephrectomy. Follow-up abdominal CECT axial (**b**) and coronal MIP (**c**) images show a small hypervascular mass in the head of the pancreas (*arrows*). Differential diagnosis included a metastatic deposit from the previous renal carcinoma versus a nonfunctional PNEN. Patient underwent a pancreaticoduodenectomy. Photograph of the gross specimen (**d**) shows a yellow-greenish fleshy tumor (*arrows*). Histological sections show (**e**) (H&E, 4×) a well-differentiated neuroendocrine neoplasm with a very low Ki-67 proliferative index of < 1% (**f**) (immunohistochemistry, 10×)

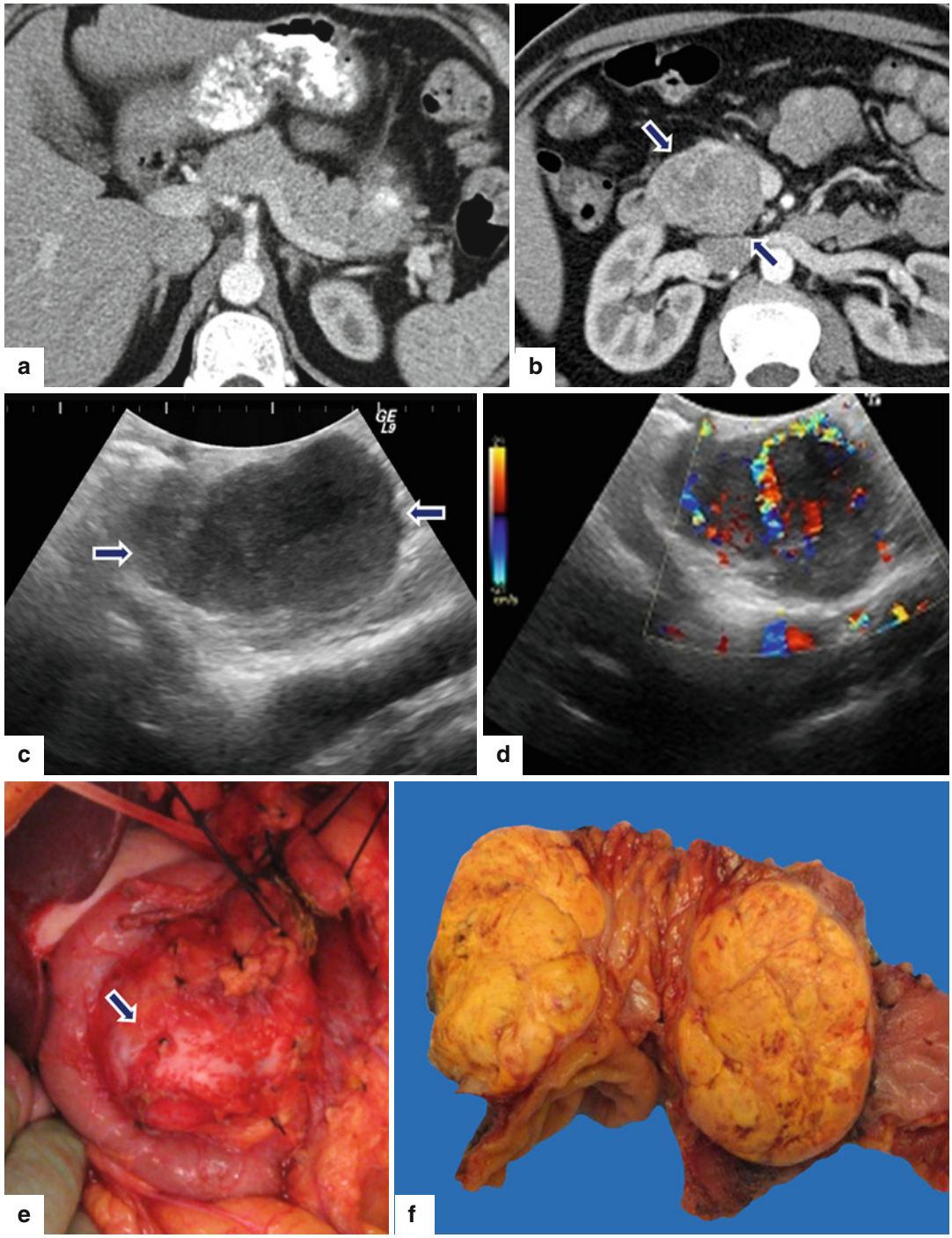

Fig. 10.21 Large nonfunctional PNEN in the pancreatic head on CT. A 44-year-old female complaining of right upper quadrant pain. CECT axial (**a**, **b**) images demonstrate a large hypervascular, heterogeneous mass in the pancreatic head. Note the absence of dilatation of the pancreatic duct and common bile duct associated with this mass. IOUS gray scale and color Doppler transverse (**c**, **d**) images demonstrate a well-differentiated, hypoechoic, partially vascular, solid mass. Intraoperative photograph (**e**) demonstrates a large pancreatic head mass abutting the duodenum (*arrows*). Photograph of the bivalved mass (**f**) demonstrates a fleshy, yellow, soft mass.

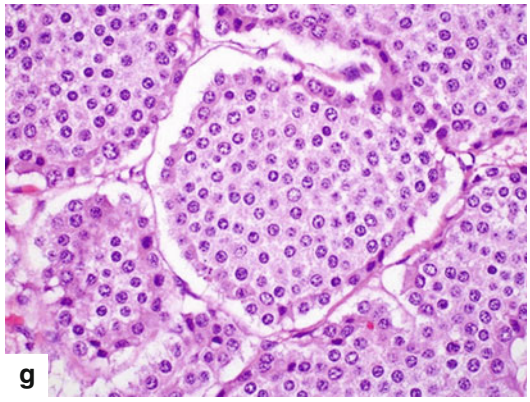

Fig. 10.21 (continued)Histological section (**g**) (H&E, 40x) shows cells with abundant eosinophilic cytoplasm arranged in a nesting pattern. The nuclei display a "salt-and-pepper" appearance of the chromatin

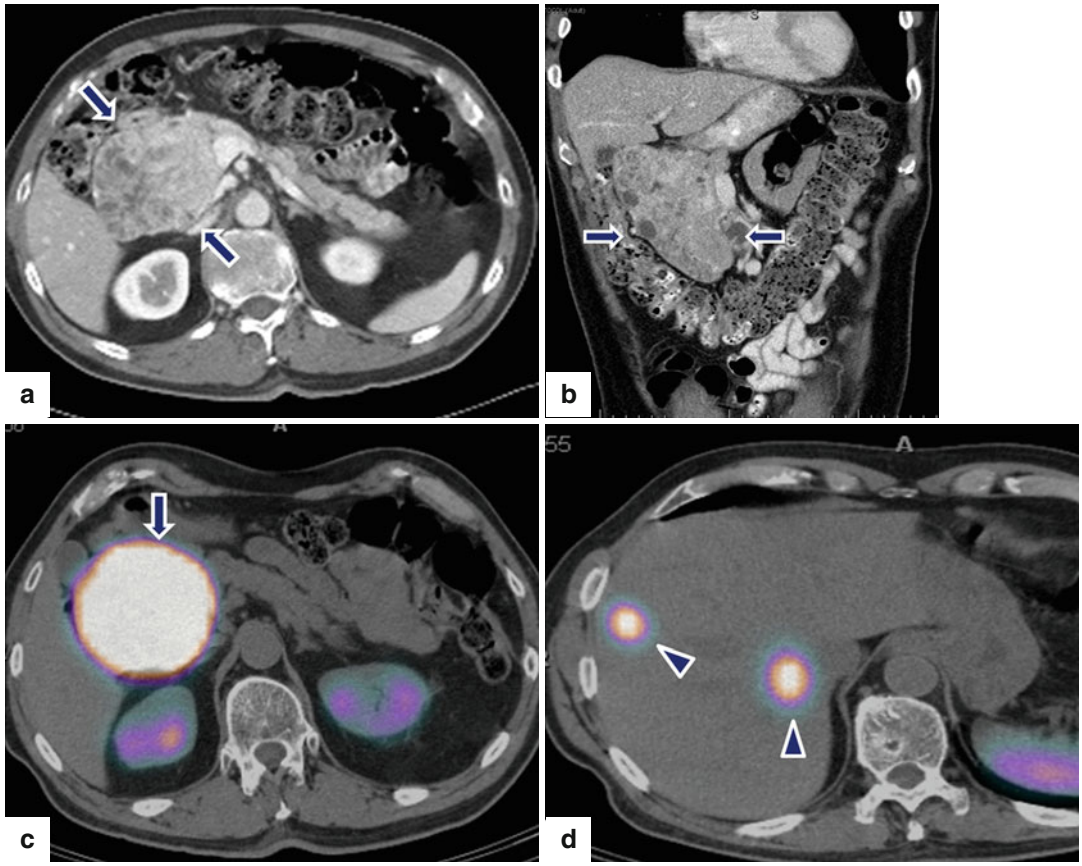

Fig. 10.22 Large nonfunctional PNEN in the pancreatic head on CECT and octreotide scan. A 69-year-old male undergoing abdominal CT workup for an aortic bruit was found to have a mass in the head of pancreas and two small masses in the right lobe of the liver. CECT axial (**a**) and coronal (**b**) images show a large, hypervascular, heterogeneous mass involving the pancreatic head (*arrows*). Octreotide scan (**c**, **d**) shows intense uptake of the radiotracer by this mass (*arrows*) and two hot spots in the right lobe of the liver (*arrowheads*).

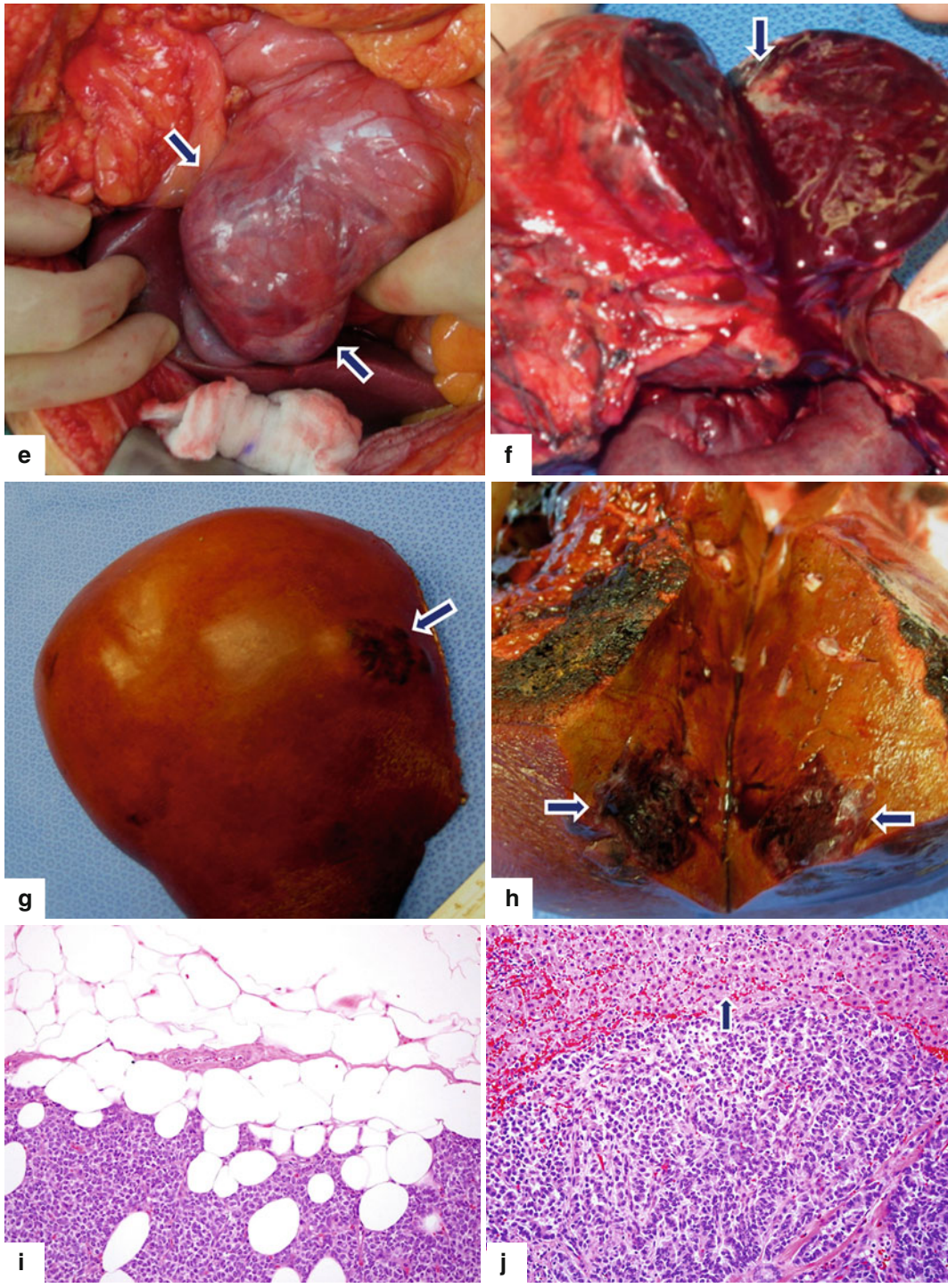

Fig. 10.22 (continued) Patient underwent a pancreaticoduodenectomy and a right lobe hepatectomy. Intraoperative photograph (**e**) shows a large, bilobulated, red mass with smooth serosal surface that is located in the pancreatic head (*arrows*). Photograph of the bivalved specimen (**f**) shows a large tumor mass with red, hemorrhagic parenchyma and peripheral scarring (*arrow*). Photograph of the resected right lobe of the liver (**g**) shows a round area with irregular raised borders (*arrow*) located in segment VIII. A cross section of the mass reveals (**h**) an ill-defined, mahogany-brown tumor (*arrows*). Histological sections showed an intermediate-grade (grade 2) neuroendocrine carcinoma of the pancreas extending into the peripancreatic adipose tissue (**i**) and metastatic carcinoma to two lymph nodes and to the liver (**j**) (*arrow*) (H&E, 20×)

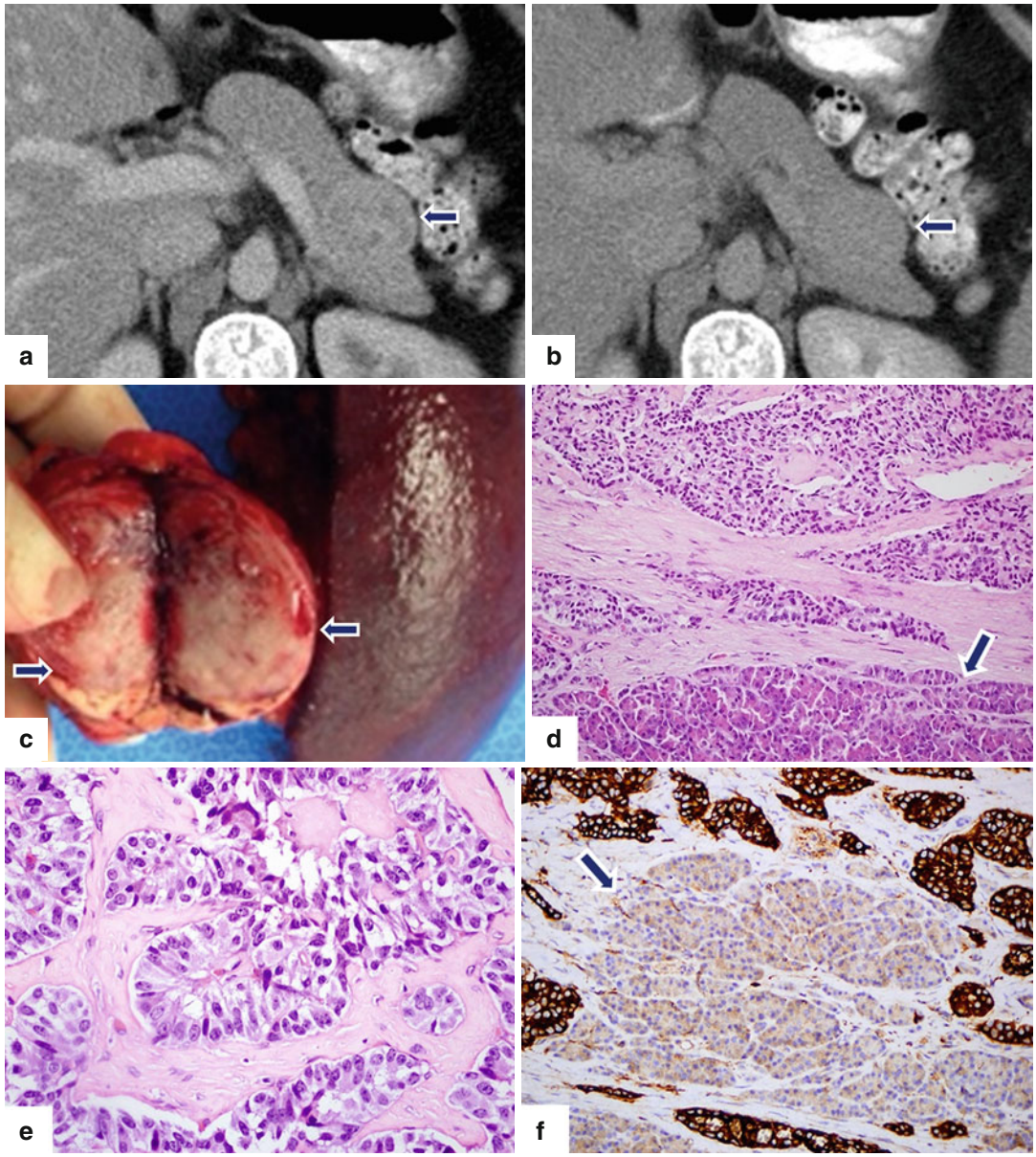

Fig. 10.23 Large nonfunctional PNEN in the pancreatic tail on CECT. A 37-year-old female with history of pelvic pain who underwent an abdominal CT that showed an incidental finding in the pancreas. CECT axial arterial (**a**) and delayed phase (**b**) images demonstrate a round hypervascular mass with heterogeneous attenuation involving the tail of the pancreas (*arrows*). Note that this mass became isodense with the rest of the pancreas in the delay phase (*arrowheads*). A distal pancreatectomy and splenectomy was performed on this patient. Photograph of the bivalved specimen (**c**) shows a soft, tan, and partially hemorrhagic tumor (*arrows*). Histopathological examination demonstrated a well-differentiated neuroendocrine neoplasm (grade 1) infiltrating the pancreas (**d**) (*arrow*) with a nesting and trabecular pattern (**e**) (H&E, 50×). Tumor cells are strongly positive for synaptophysin (**f**) (Immunohistochemistry, 20×). Note the residual pancreatic lobule surrounded by tumor cells (**f**) (*arrow*).

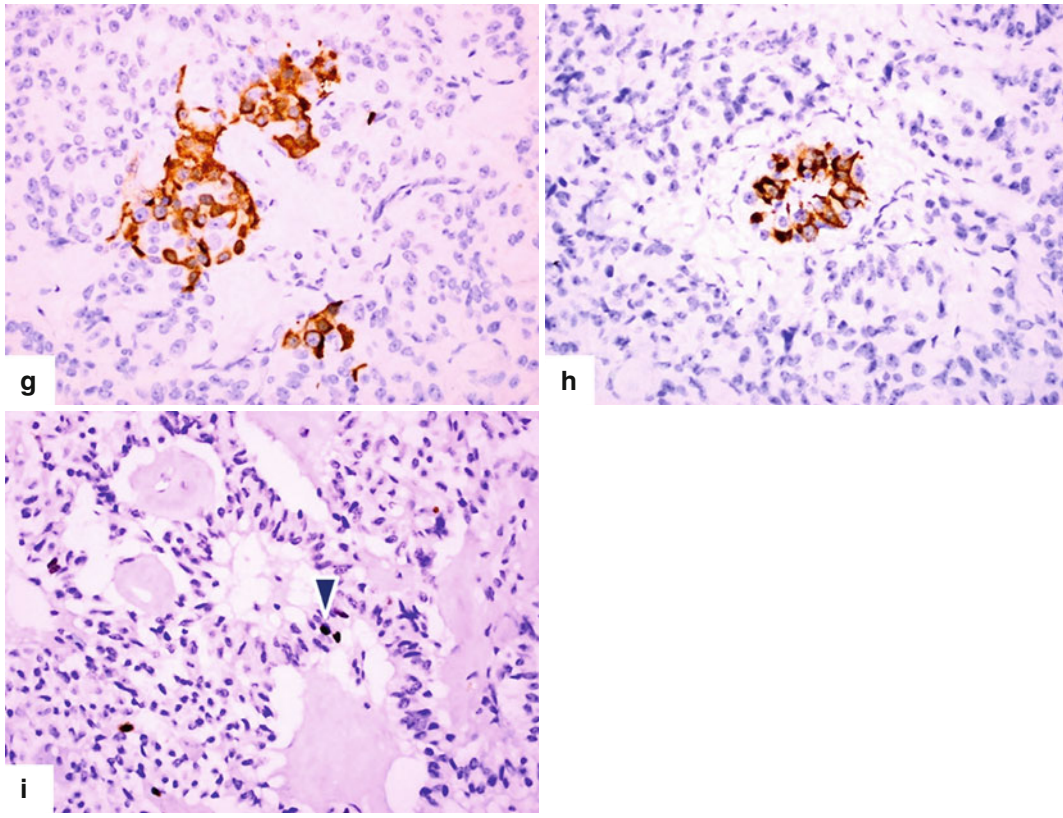

Fig. 10.23 (continued) The tumor cells were focally positive for glucagon (**g**) and insulin (**h**), Ki-67 proliferative index was <3 % (**i**) (*arrowhead*) (Immunohistochemistry, 50×)

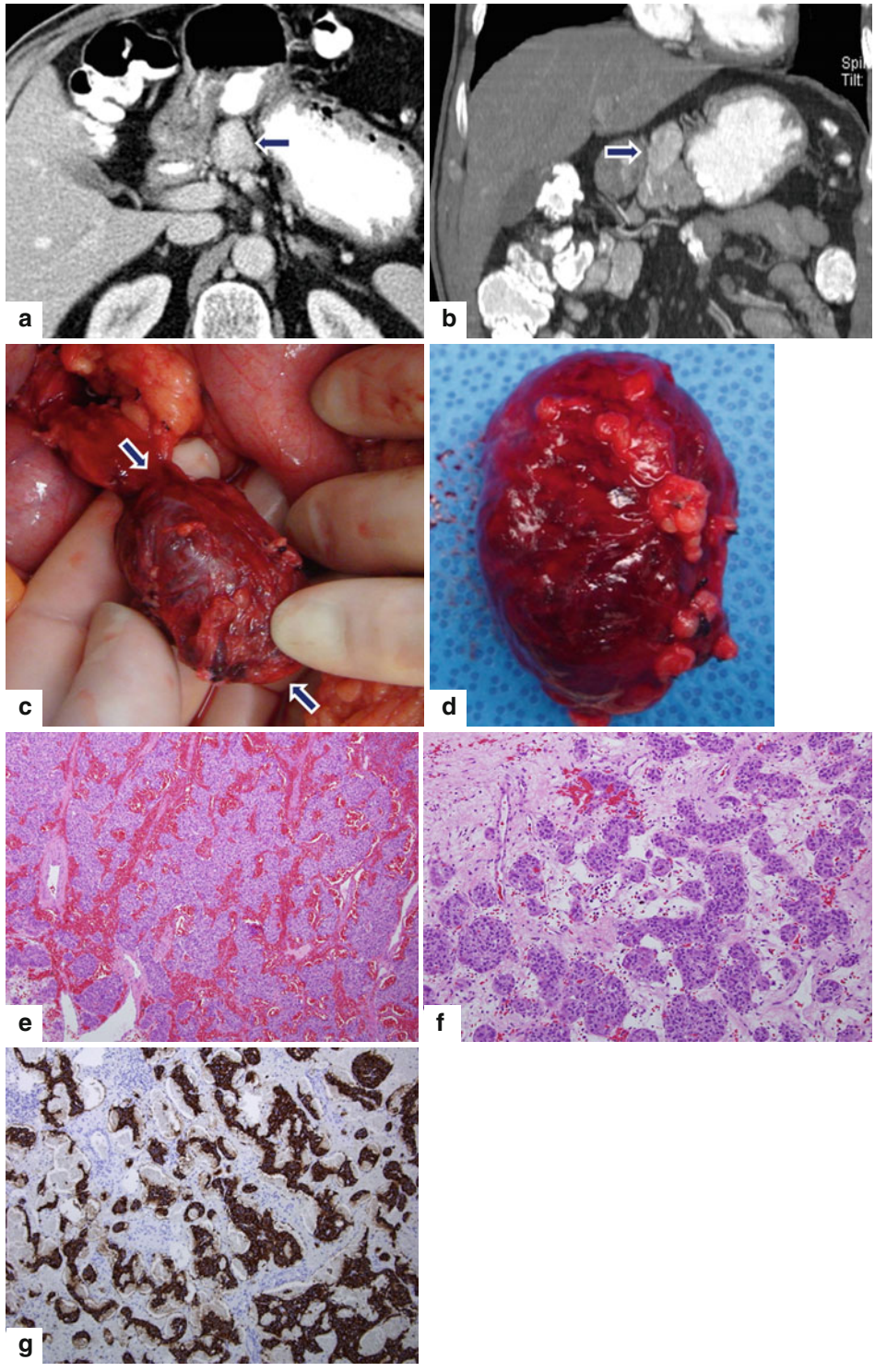

Fig. 10.24 Exophytic PNEN on CT. A 77-year-old male with history of diabetes and recent 12 lb weight loss. CECT axial (**a**) and coronal (**b**) images show an exophytic, ovoid, hypervascular, homogeneous mass arising in the neck of the pancreas (*arrows*). Intraoperative and gross photographs (**c**, **d**) show an oval, well-circumscribed, pedunculated pancreatic mass (*arrows*) with a smooth serosal surface. Histological sections show highly vascular areas with abundant hemorrhage (**e**) (H&E, 10×) and areas with tumor cells arranged in an organoid pattern (**f**) (H&E, 20×). Mitoses were not identified. Immunohistochemistry for synaptophysin (**g**) highlights the tumor cells

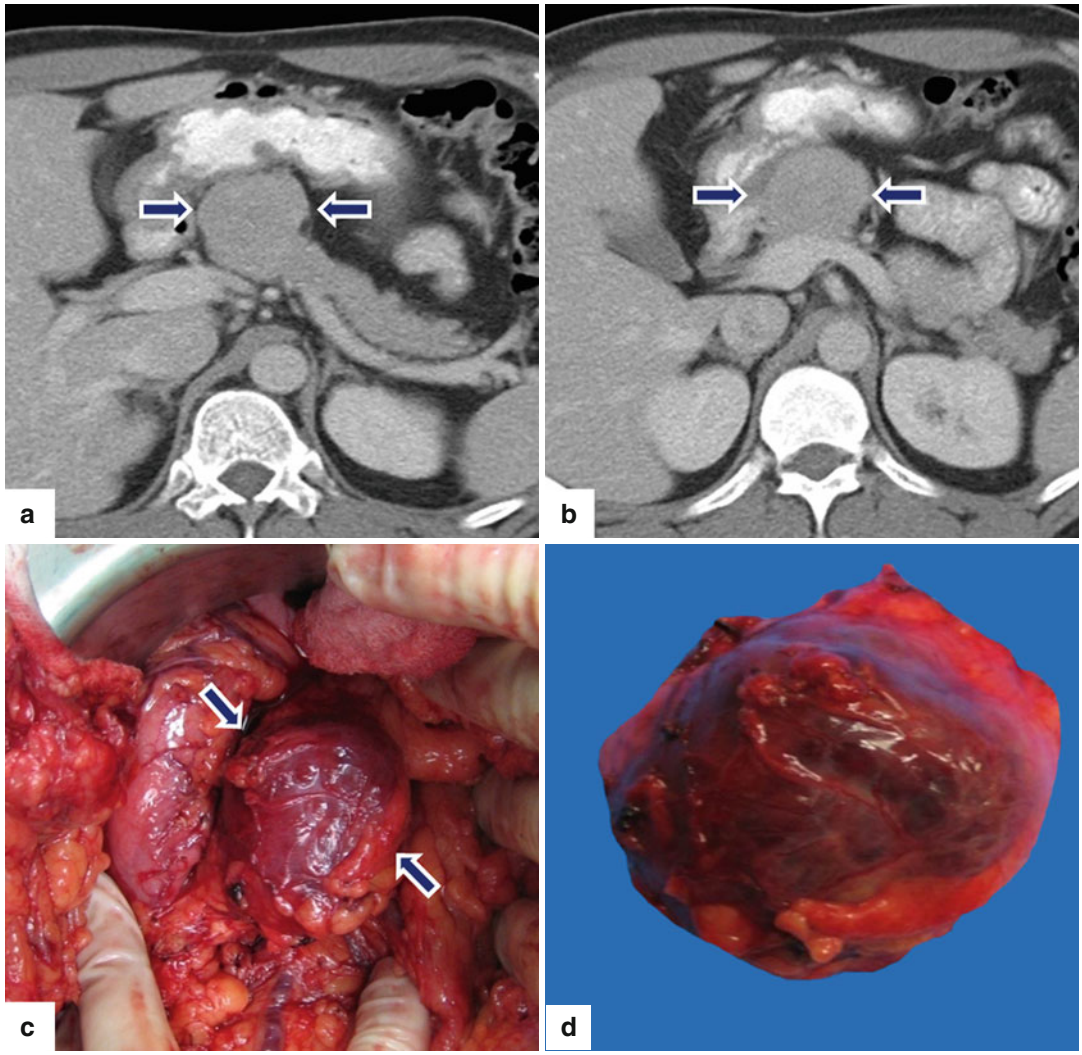

Fig. 10.25 Exophytic PNEN on CT. A 38-year-old male with history of small bowel neuroendocrine tumor resected 8 years prior. Annual CT surveillance found an incidental pancreatic mass. CECT axial (**a**, **b**) images reveal an exophytic, isodense mass arising in the pancreatic neck (*arrows*). Intraoperative photograph (**c**) reveals a round to oval, purple mass (*arrows*). Patient underwent a central pancreatectomy. Photograph of the gross specimen (**d**) demonstrates the oval mass with a smooth serosal surface. Final pathology: well-differentiated PNEN

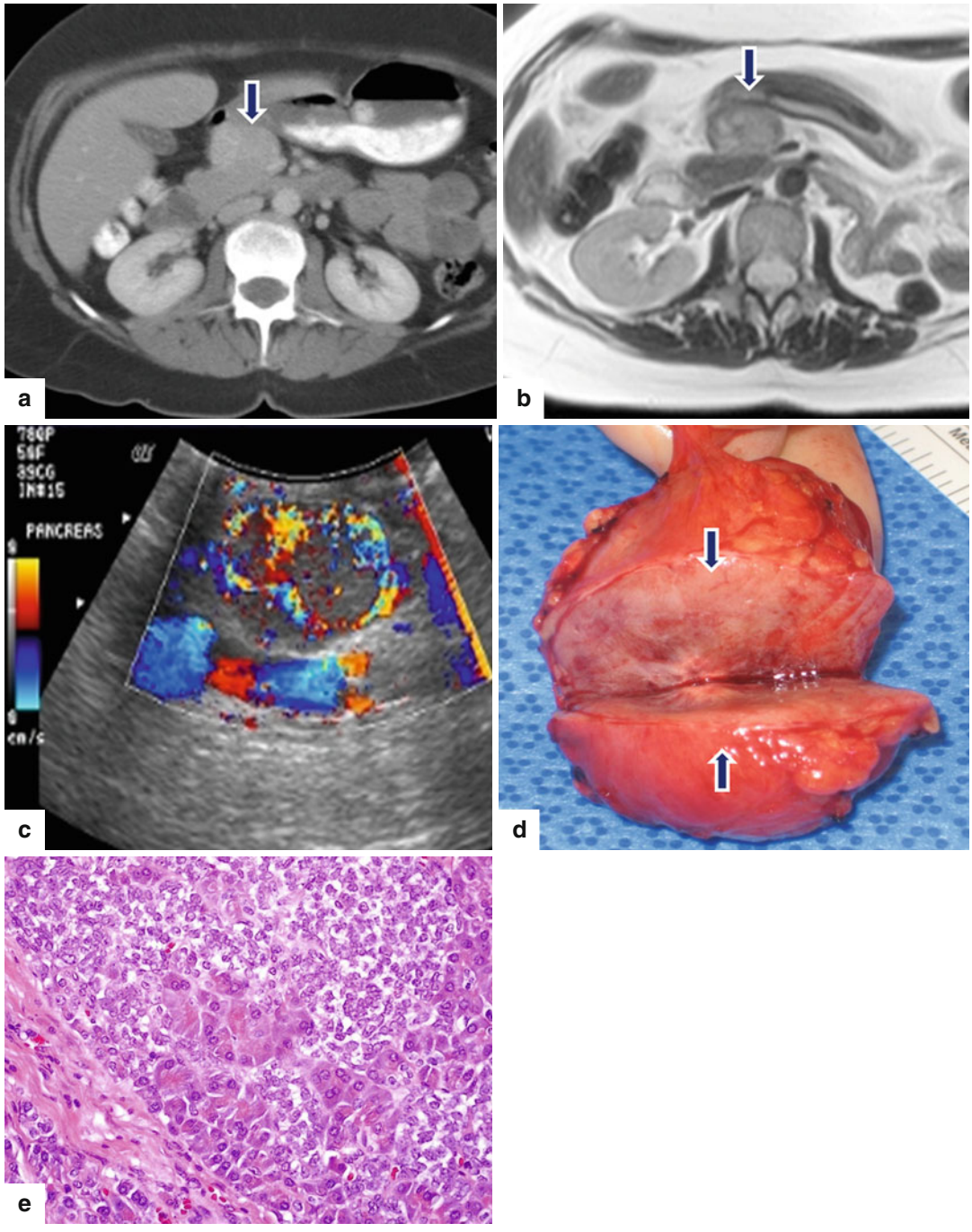

Fig. 10.26 Exophytic PNEN on CT and MR. A 50-year-old female with history of renal stones. Surveillance abdominal CT demonstrated a pancreatic mass. CECT axial (**a**) image shows a homogeneous, exophytic, hypervascular mass arising from the anterior aspect of the pancreatic head (*arrow*). T2WI axial (**b**) image confirms the presence of an exophytic pancreatic mass with heterogeneous signal intensity (*arrow*). IOUS axial (**c**) image shows a hypervascular pancreatic mass. Photograph of the bivalved specimen (**d**) demonstrates a round, well-circumscribed mass with a fleshy appearance and a central stellate scar (*arrows*). Microscopic examination demonstrated a well-differentiated neuroendocrine neoplasm, grade 2. The tumor cells are arranged in sheets (**e**) (H&E, 40×)

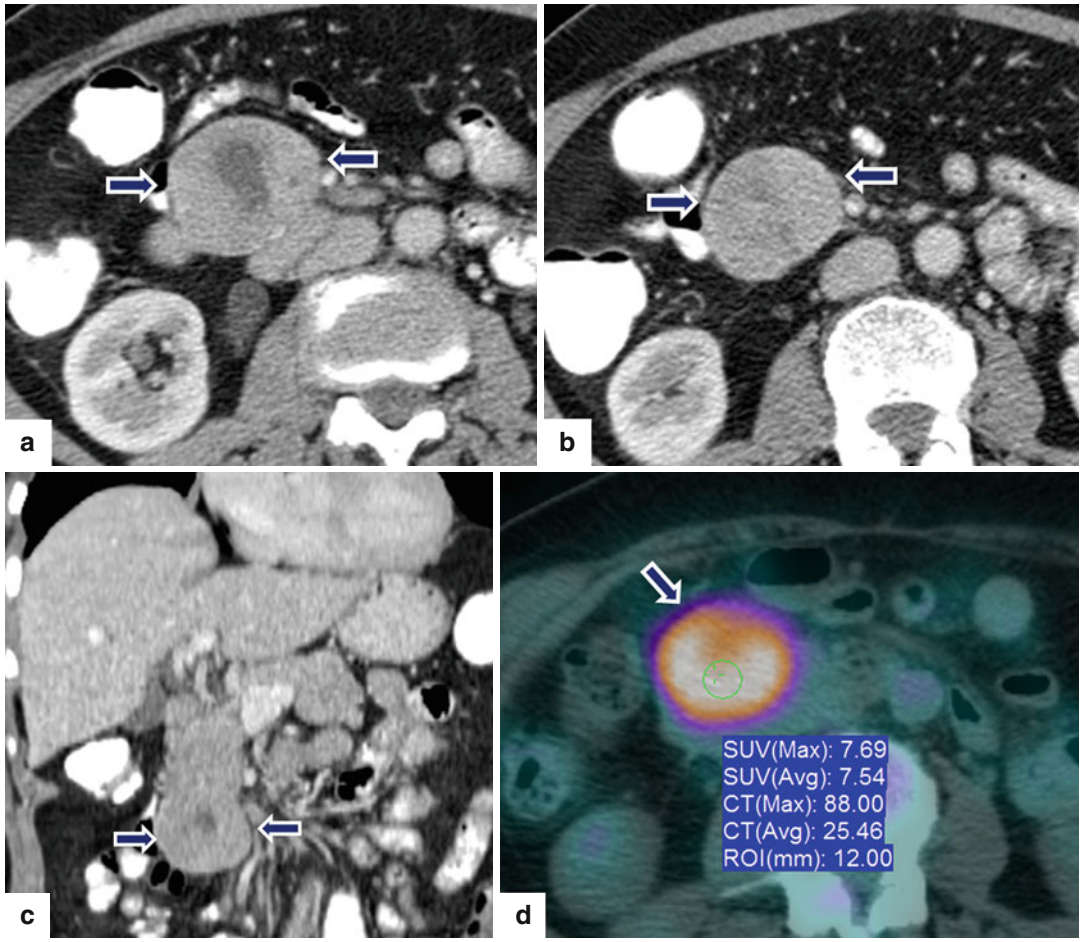

Fig. 10.27 Pedunculated necrotic PNEN on CT and PET/CT. A 71-year-old female with history of mild epigastric pain. CECT axial (**a**, **b**) and coronal (**c**) images show a large round exophytic, hypervascular mass with central necrosis arising from the inferior aspect of the pancreatic head (*arrows*). PET/CT axial (**d**) image shows avid FDG uptake by this mass (*arrow*)

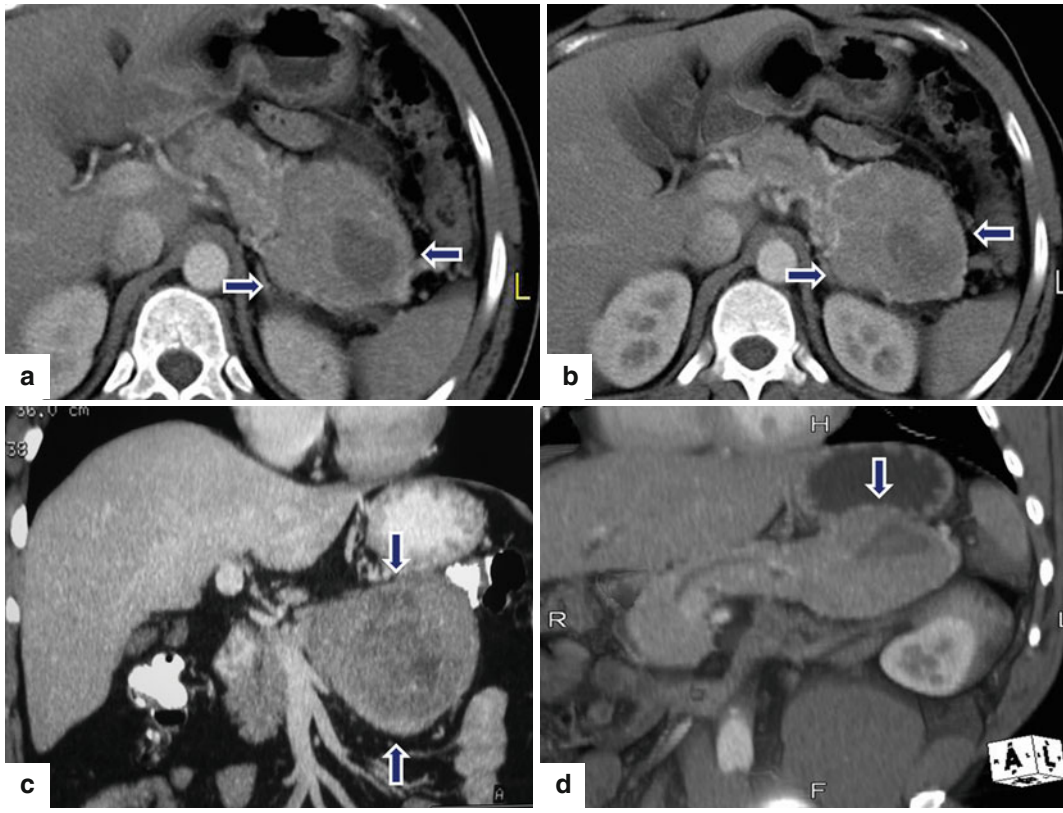

Fig. 10.28 Partially necrotic PNEN on CT. A 41-year-old male complaining of abdominal pain. CECT axial (**a**, **b**) and coronal (**c**, **d**) images demonstrate a well-defined, oval, heterogeneously attenuating mass with central necrosis involving the tail of the pancreas (*arrows*). Patient underwent a distal pancreatectomy and splenectomy. Final pathology: large, well-differentiated pancreatic neuroendocrine neoplasm, grade 1, with mild nuclear atypia without mitosis

Fig. 10.29 Cystic PNEN on CT. A 62-year-old male with history of prostatic carcinoma. Surveillance abdominal CT found an incidental mass in the pancreas. CECT axial (**a**) image demonstrates a round cystic mass with a thick peripheral enhancing rim (*arrow*). Patient underwent a distal pancreatectomy and splenectomy. Photograph of the bivalved gross specimen (**b**) shows a friable mass with a thick periphery wall (*arrows*) and central hemorrhage. Histologic examination revealed a well-differentiated neuroendocrine carcinoma (**c**, **d**) (H&E 10×, 20×) with metastasis to one peripancreatic lymph node (**e**) (H&E, 20×). Immunohistochemistry for insulin (**f**) (20×) and glucagon (**g**) (20×) is negative in the tumor cells and highlights the beta and alpha cells of a residual islet of Langerhans (**f**) (*arrowhead*) respectively. The tumor was nonfunctional

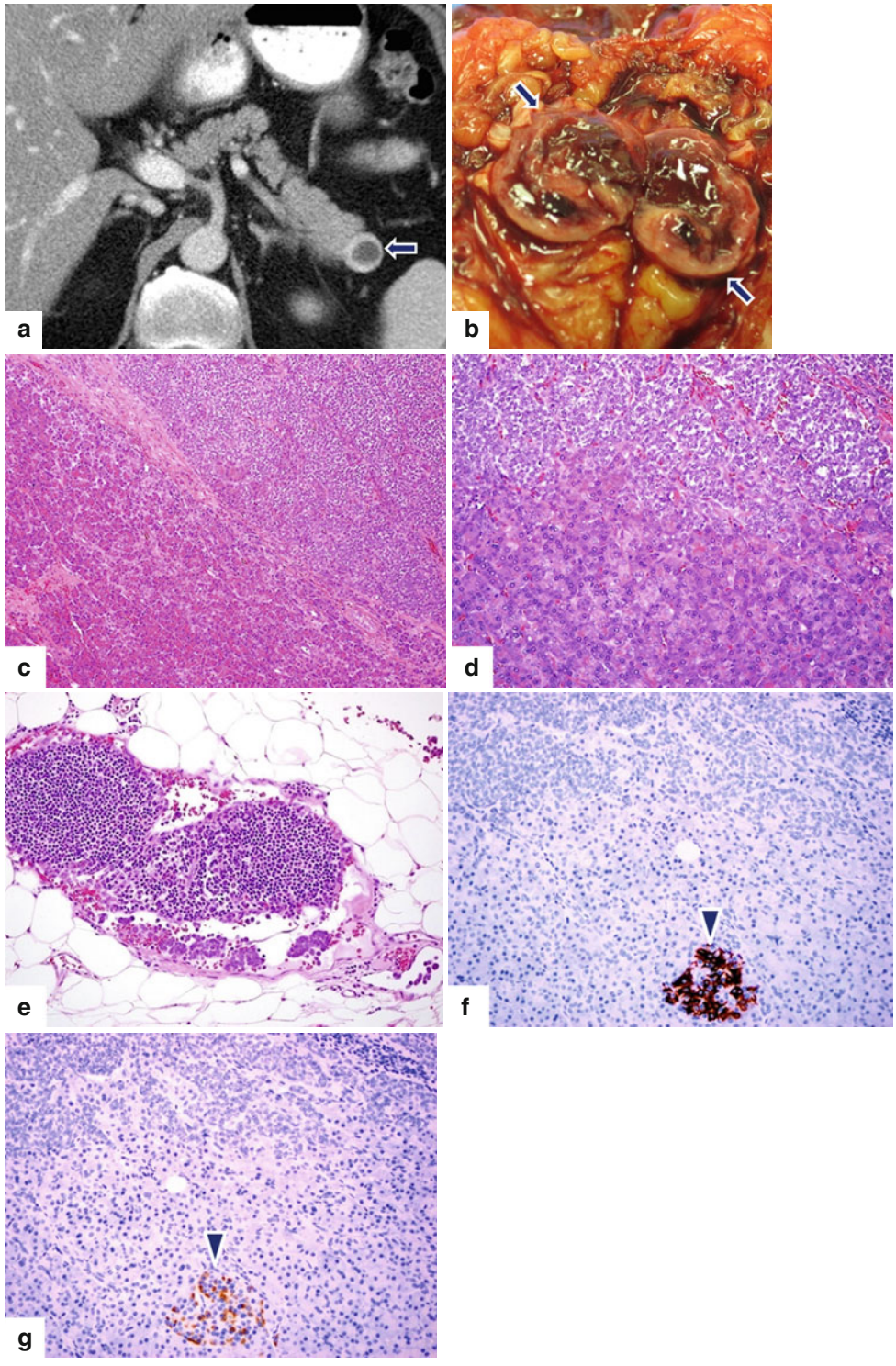
a
b
c
d
e
f
g

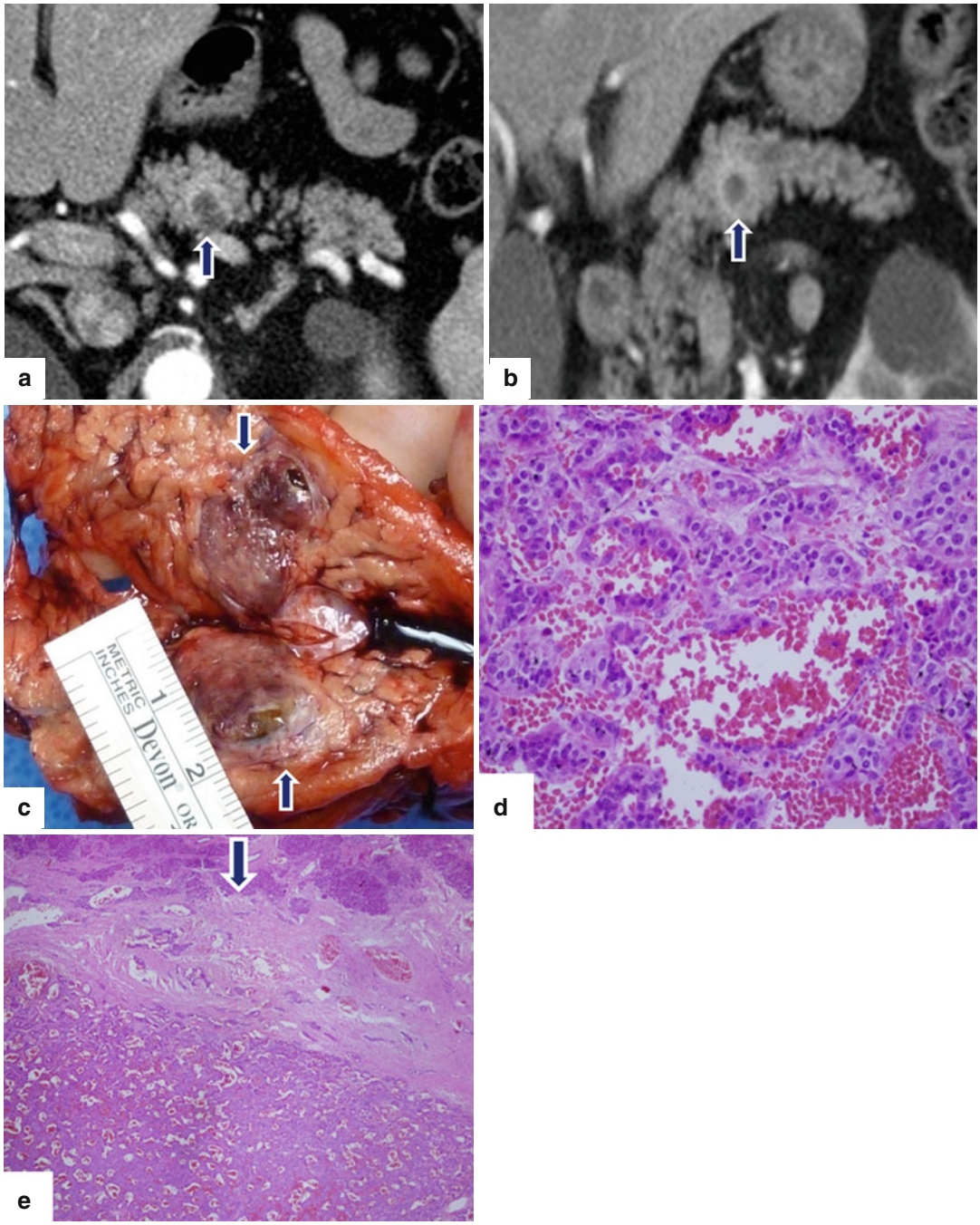

Fig. 10.30 Cystic PNEN on CT. A 58-year-old male with vague periumbilical pain. Abdominal CT found an incidental mass in the pancreas. CECT axial (**a**) and coronal (**b**) images reveal a cystic mass with a thick enhancing capsule (*arrows*). Photograph of the bivalved gross specimen (**c**) shows a partially hemorrhagic, ill-defined mass (*arrows*). Histological sections show (**d**) (H&E, 50×) areas of tumor cells with trabecular arrangement and hemorrhage. Solid areas (**e**) (H&E, 10×) show cells with focal pseudoglandular arrangement and dense fibrotic areas (**e**, *arrow*). Final diagnosis: well-differentiated, neuroendocrine neoplasm, grade 1.

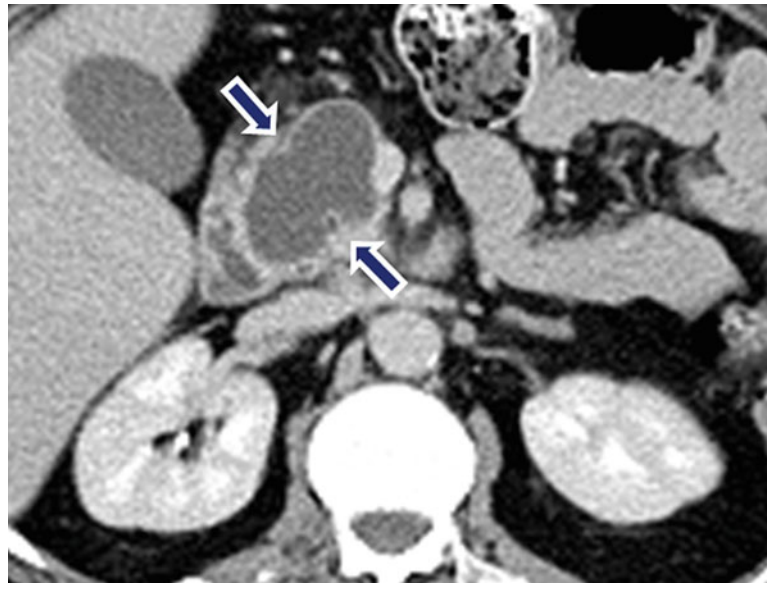

Fig. 10.31 Cystic PNEN on CT. A 46-year-old male with epigastric discomfort. CECT axial image shows an ovoid cystic mass with a thin enhancing wall involving the pancreatic head (*arrows*). Final pathology: well-differentiated neuroendocrine neoplasm

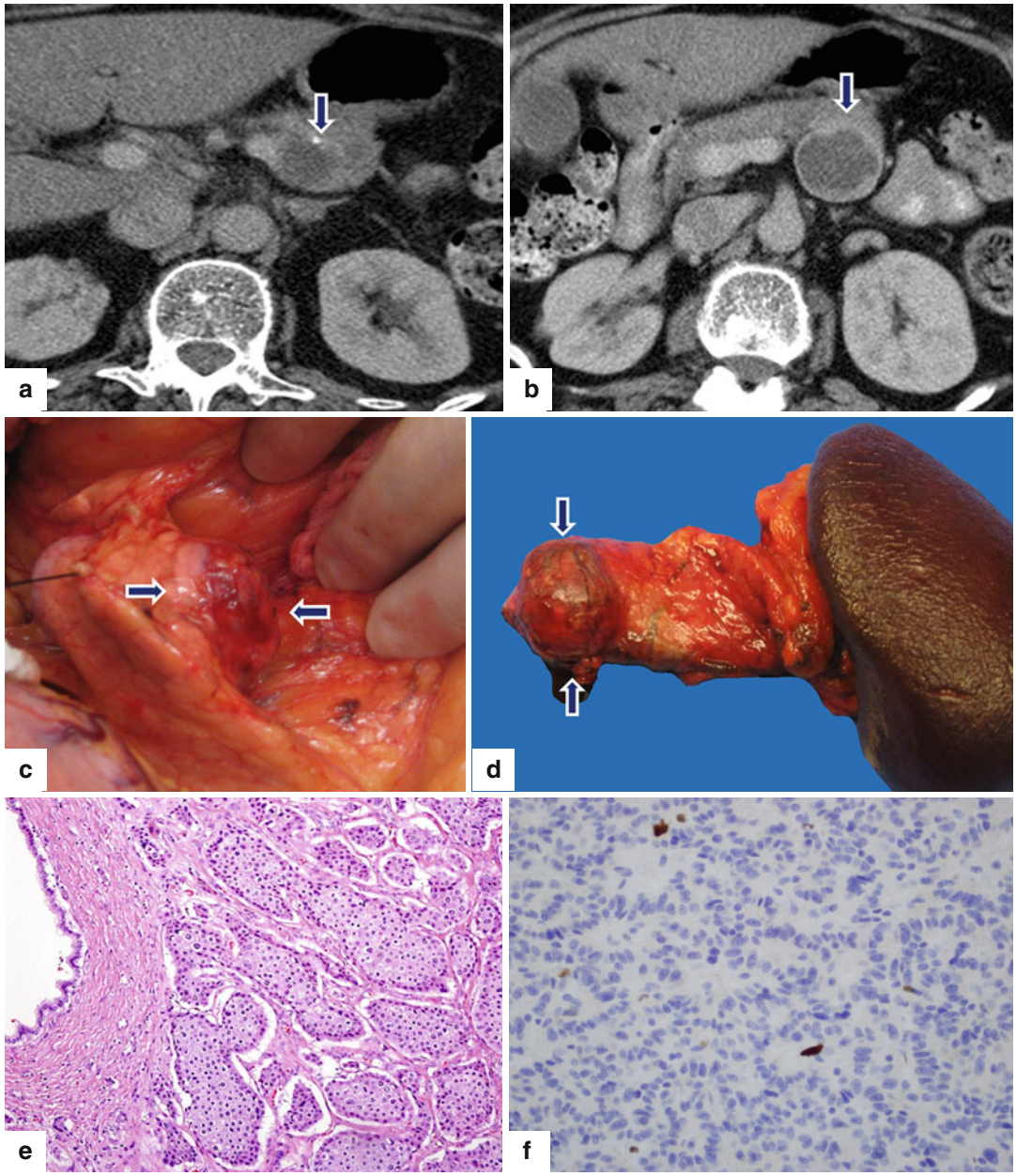

Fig. 10.32 Cystic nonfunctional PNEN on CT. A 61-year-old female with history of rheumatoid arthritis. Incidental pancreatic mass was found during an abdominal CT examination. CECT axial (**a**, **b**) images demonstrate an exophytic, round, cystic mass with a punctate calcification and enhancing wall involving the body of the pancreas (*arrows*). Intraoperative photograph (**c**) demonstrates an exophytic mass (*arrows*). Patient underwent a distal pancreatectomy and splenectomy. Photograph of the gross specimen (**d**) demonstrates a red, round mass with smooth serosal surface (*arrows*). Histological sections of the mass show a well-differentiated, neoplasm, grade 1, (**e**) (H&E, 20×) with a nesting pattern and a low Ki-67 proliferative index (**f**) (Immunohistochemisty, 40×)

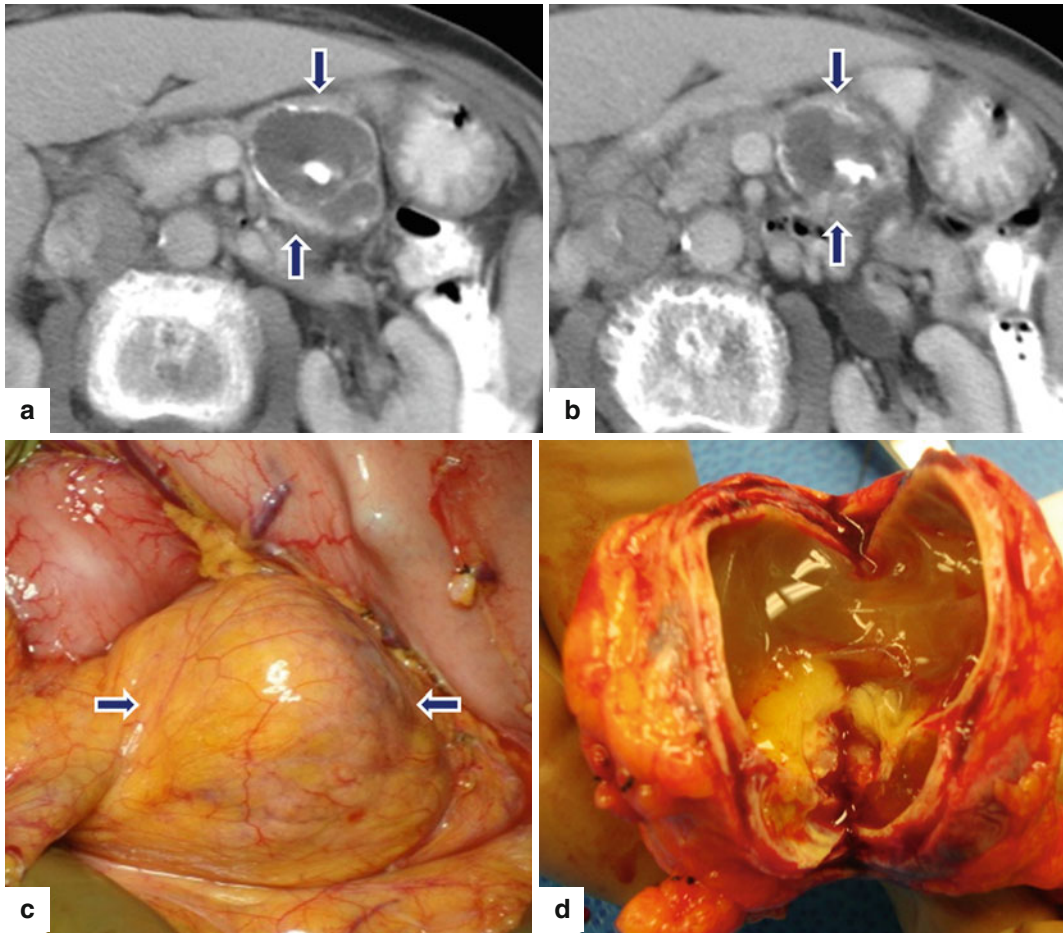

Fig. 10.33 Complex nonfunctional PNEN with calcifications and cystic changes. A 60-year-old female with epigastric pain. CECT axial (**a**, **b**) images demonstrate a complex cystic mass with thin peripheral and coarse central calcifications involving the body of the pancreas (*arrows*). Intraoperative photograph (**c**) demonstrates a yellow mass with smooth serosal surface (*arrows*). Photograph of the bivalved specimen (**d**) demonstrates a neuroendocrine neoplasm with internal yellow, mucoid-like material and an irregular inner surface.

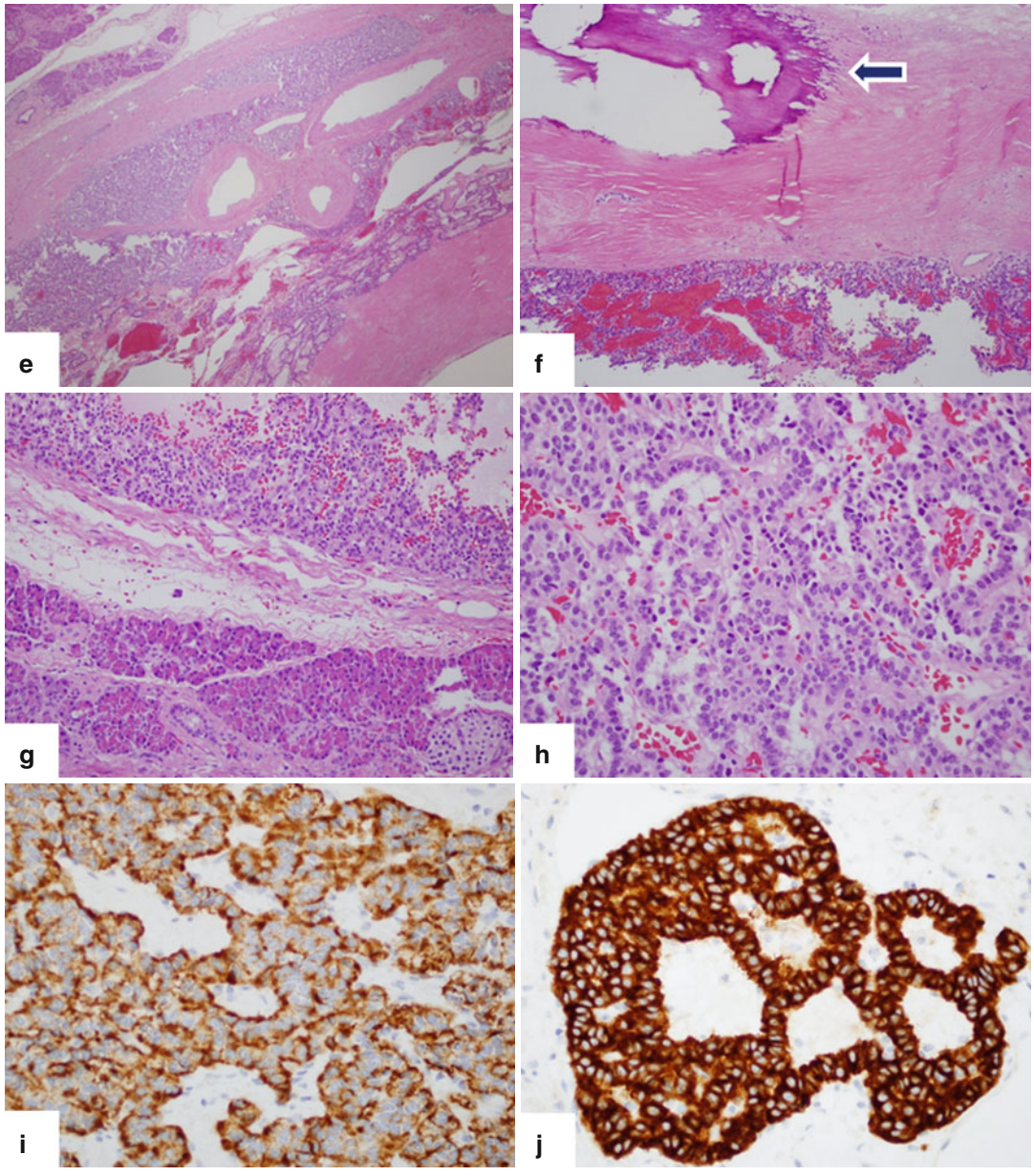

Fig. 10.33 (continued) Histological sections (**e**–**h**), (H&E, 10x, 40x) show a neuroendocrine neoplasm with extensive fibrosis, calcifications (**f**) (*arrow*), and cystic changes. Chromogranin (**i**) and synaptophysin (**j**) immunostains were positive (immunostains, 40x, 60x)

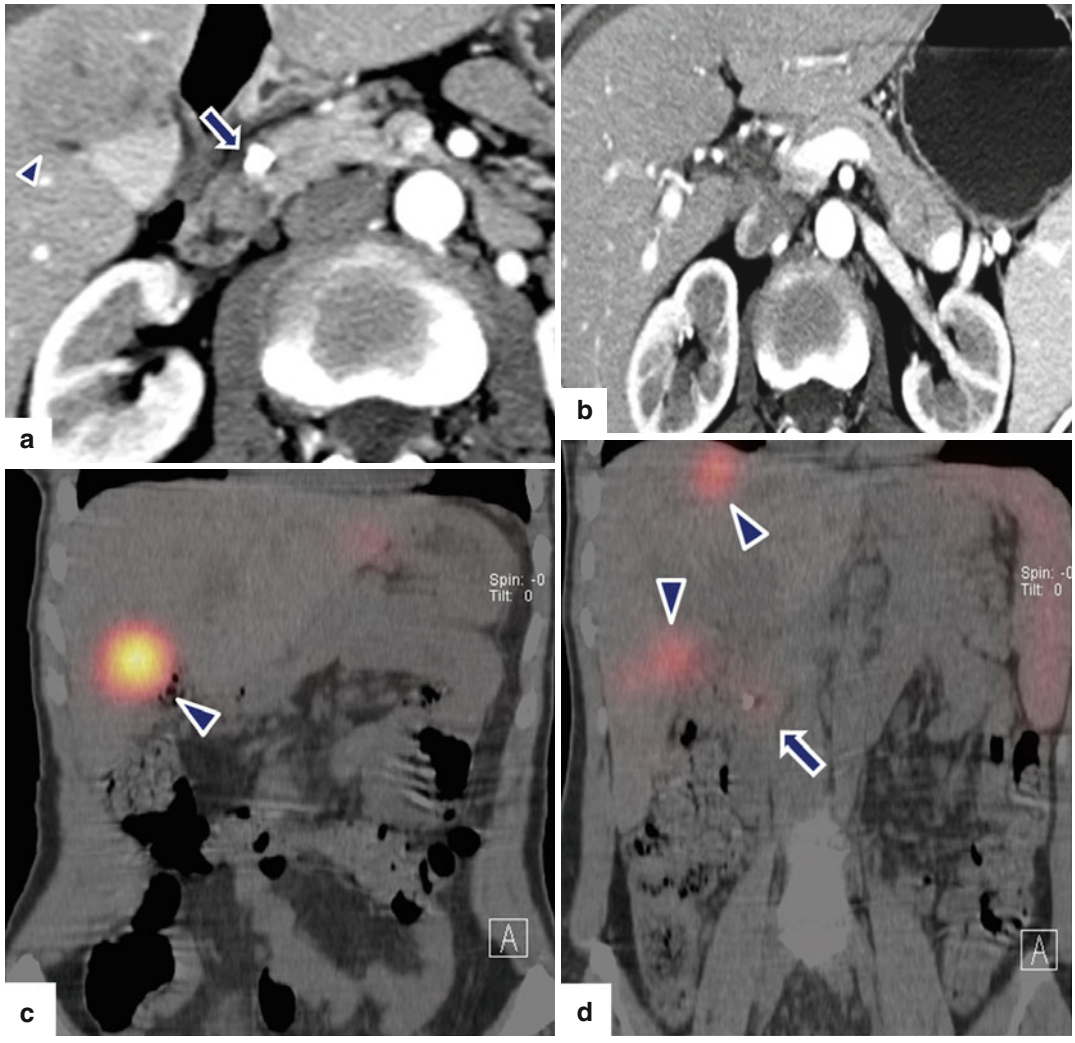

Fig. 10.34 Small, malignant, calcified PNEN with liver metastasis on CT. A 55-year-old female with history of epigastric pain. Upper GI endoscopy showed a duodenal ulcer. Results of ulcer biopsy were negative for malignancy. CECT axial (**a**, **b**) images show a coarse calcification in the pancreatic head (*arrow*). Note a normal pancreatic duct in the body and tail of the pancreas and the presence of a hepatic mass of heterogeneous attenuation in the right lobe (**a**) (*arrowhead*). PET/CT coronal (**c**, **d**) images show three sites of focus with intense increased uptake of FDG in the right lobe of the liver (*arrowheads*) and a focus of subtle increased uptake in the head of the pancreas (*arrow*) around the pancreatic calcification.

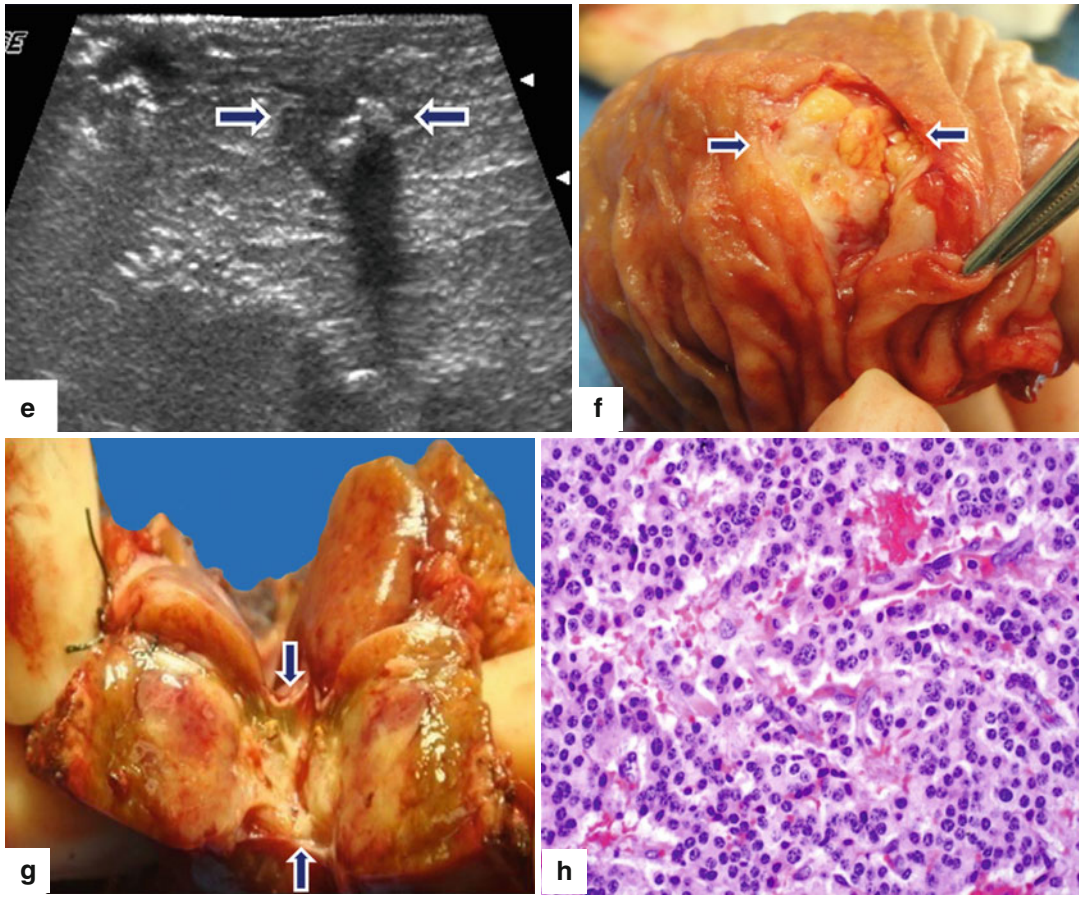

Fig. 10.34 (continued) IOUS transverse (**e**) image shows a well-defined, small, hypoechoic mass with a coarse calcification in the pancreatic head (*arrows*). The patient underwent a pancreaticoduodenectomy and a right lobe hepatectomy. Photographs of the duodenum and pancreas (**f**, **g**) show a fleshy, yellow-white mass with calcifications (*arrows*). Histological section (**h**) (H&E, 60×) shows a neuroendocrine neoplasm, grade 1, composed of uniform cells with nuclei displaying a "salt-and-pepper" chromatin pattern

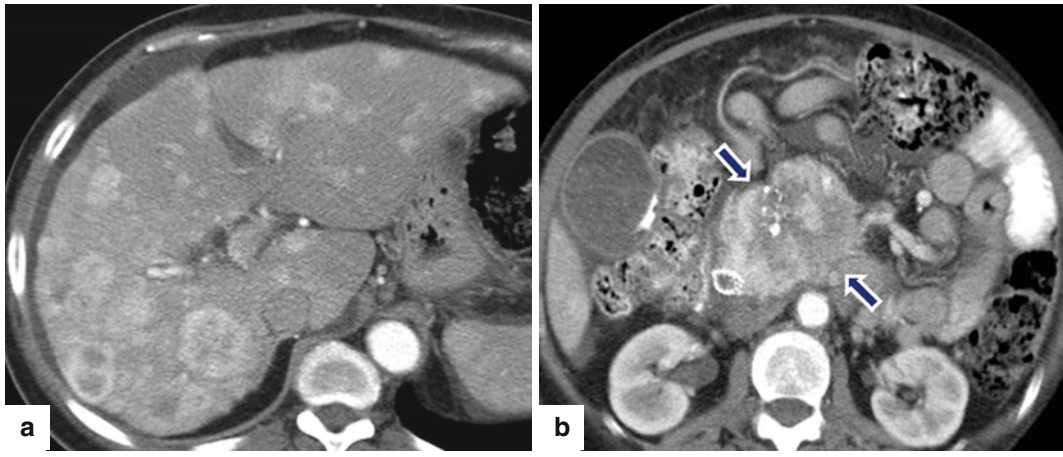

Fig. 10.35 Malignant, calcified nonfunctional PNEN on CT. A 55-year-old female with epigastric pain and weight loss. CECT axial (**a**, **b**) images reveal multiple hypervascular hepatic metastases with central necrosis and a large, hypervascular, heterogeneous mass with coarse calcifications in the pancreatic head (*arrows*). Patient underwent a percutaneous biopsy of the pancreatic mass. Final pathology: neuroendocrine neoplasm, grade 2

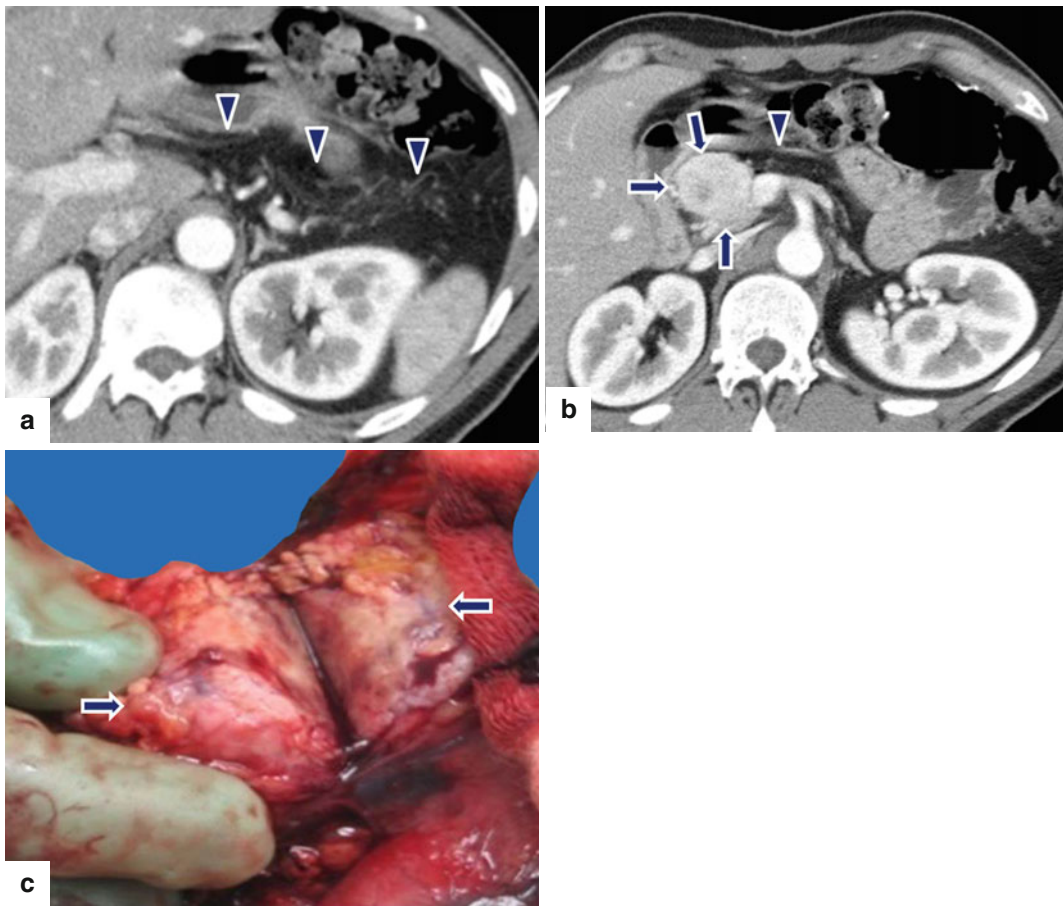

Fig. 10.36 Nonfunctional PNEN associated with pancreatic lipodystrophy. A 45-year-old female patient with an incidental pancreatic finding on chest CT. CECT axial (**a**, **b**) images demonstrate an ovoid heterogeneous, hypervascular mass in the head and neck of the pancreas (**b**) (*arrows*) associated with complete fatty replacement (**a**) (*arrowheads*) of the body and tail of the pancreas. Patient underwent a pancreaticoduodenectomy. Photograph of the bivalved specimen (**c**) shows a solid, partially hemorrhagic mass in the pancreas (*arrows*)

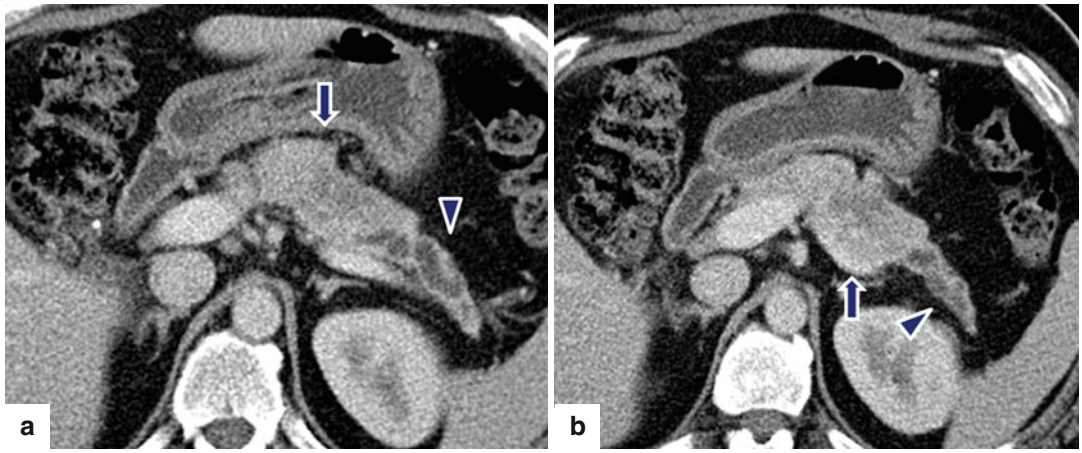

Fig. 10.37 Nonfunctional PNEN associated with obstruction of the pancreatic duct on CT. A 45-year-old male with an incidental pancreatic mass found while undergoing a cholecystectomy. CECT axial (**a**, **b**) images display a vascular mass of heterogeneous attenuation involving the pancreatic body (*arrows*). Note the dilatation of the pancreatic duct distal to this mass (*arrowheads*) and the atrophy of the pancreatic parenchyma. The patient underwent a distal pancreatectomy and splenectomy. Final pathology: well-differentiated neuroendocrine neoplasm, 5.1 cm in diameter, grade 2

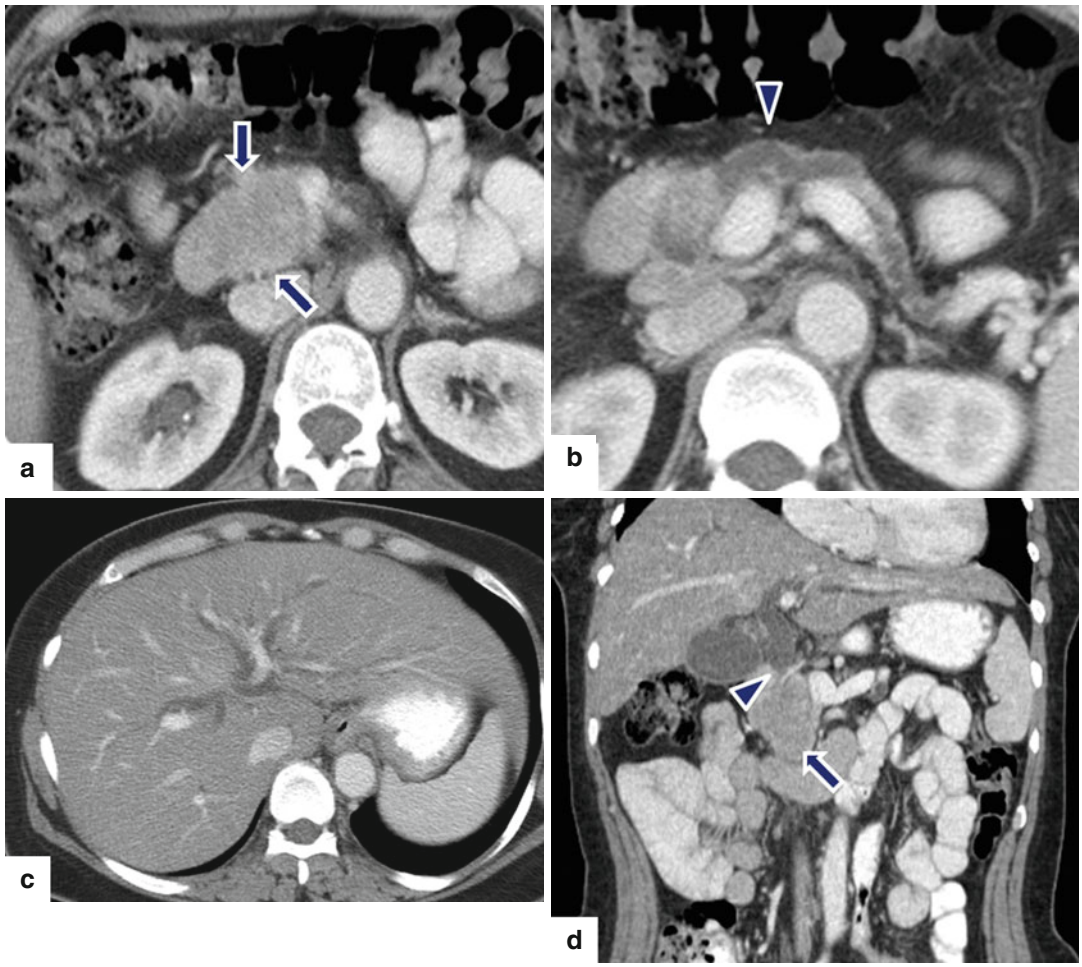

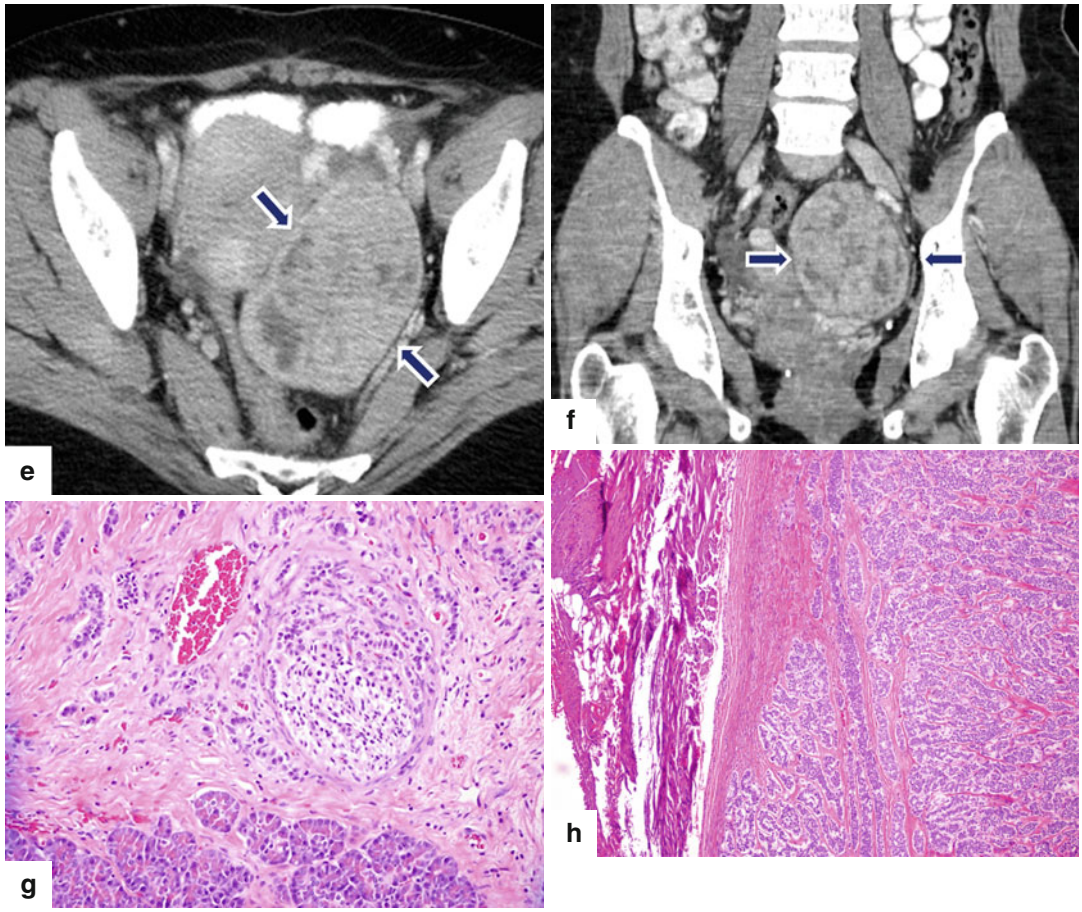

Fig. 10.38 (continued) CECT axial (**e**) and coronal (**f**) images of the pelvis reveal a hypervascular and heterogeneous attenuation on the left side of the pelvic mass (*arrows*). Patient underwent a pancreaticoduodenectomy and resection of the pelvic mass. Microscopic examination (**g**) (H&E, 10x) showed a well-differentiated neuroendocrine carcinoma. Metastatic neuroendocrine carcinoma to the ovary (**h**) (H&E, 10x)

Fig. 10.38 Malignant, nonfunctional PNEN associated with obstruction of the biliary system and pancreatic duct and pelvic metastases on CT. A 51-year-old female with acute onset of painless jaundice. CECT axial (**a–c**) and coronal (**d**) images reveal a well-defined mass with heterogeneous attenuation involving the pancreatic head (*arrows*) associated with obstruction of the pancreatic duct (*arrowhead*) and dilatation of the intrahepatic biliary system secondary to the obstruction of the common bile duct (*arrowhead*).

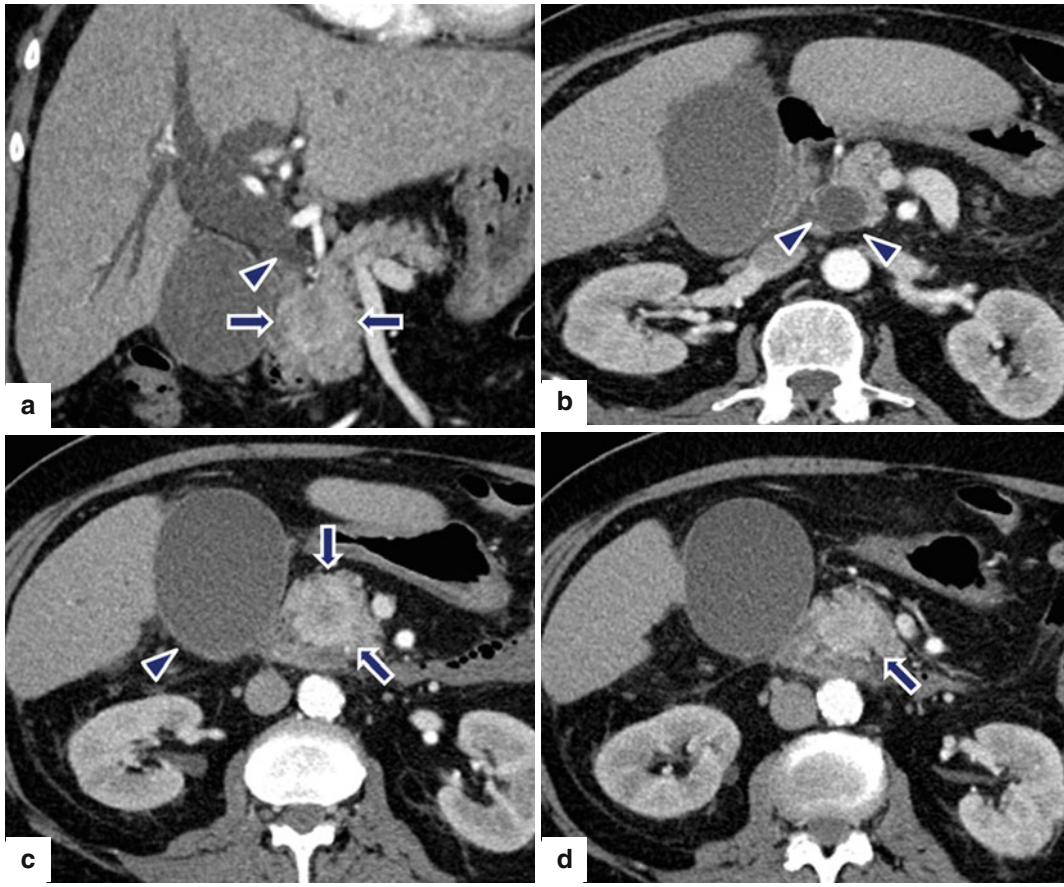

Fig. 10.39 Malignant, nonfunctional PNEN associated with obstruction of the biliary system on CT. A 72-year-old male with history of jaundice, weight loss, and vomiting. CECT coronal (**a**) and axial (**b–d**) images demonstrate dilatation of the intra- and extrahepatic biliary system (**a**, **b**) (*arrowheads*) and gallbladder (**c**) secondary to an ill-defined hypervascular mass involving the head of the pancreas (**c**, **d**) (*arrows*). Note the extension of this mass into the peripancreatic fatty tissues, atrophy of the body and tail of the pancreas, and the absence of dilatation of the pancreatic duct. Patient underwent a Whipple procedure. Final pathology: poorly differentiated neuroendocrine carcinoma, large cell type, with lymphovascular invasion and extension into the peripancreatic soft tissues

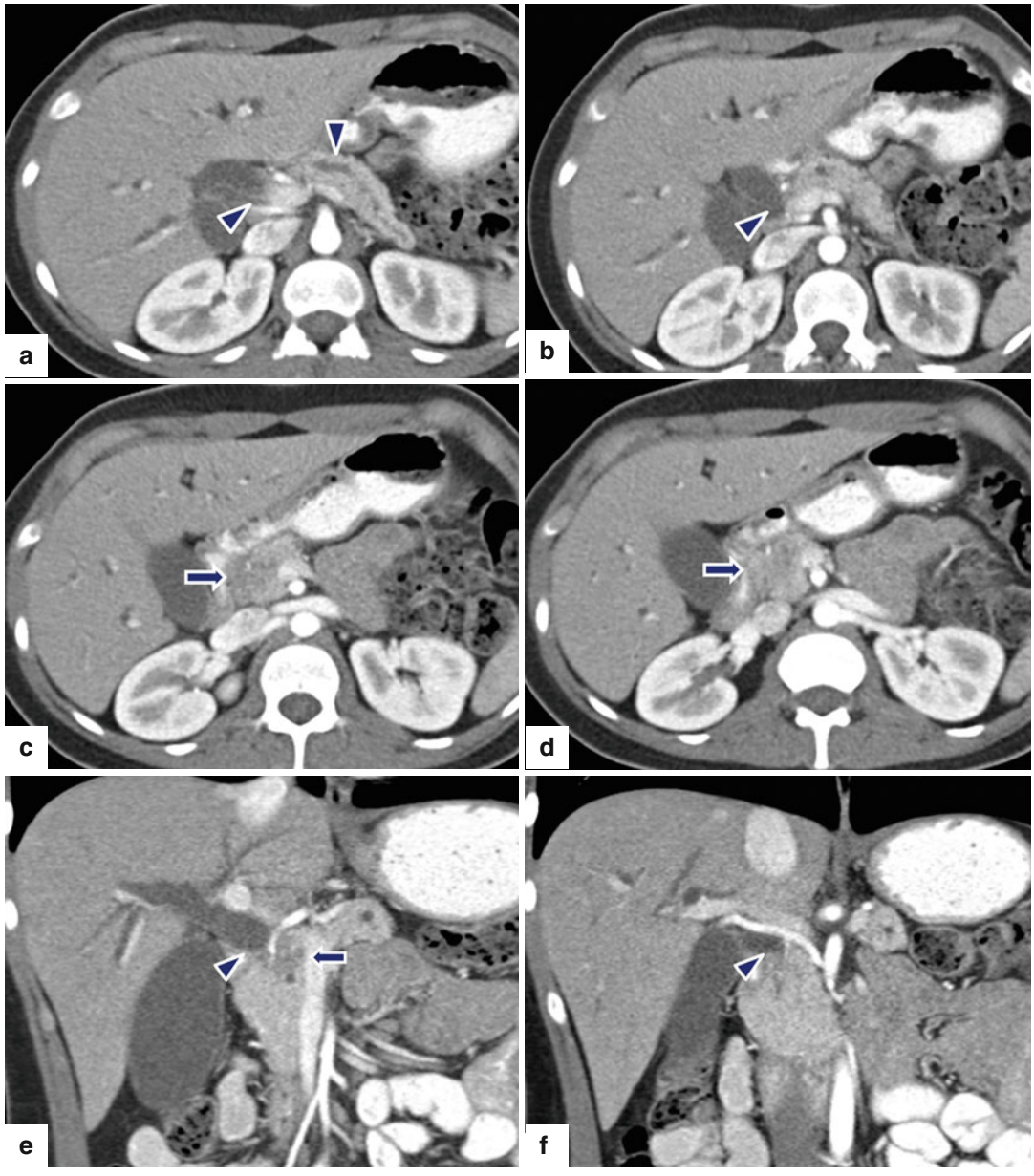

Fig. 10.40 Nonfunctional PNEN associated with obstruction of the biliary system and pancreatic duct on CT. A 20-year-old female patient with history of acute onset of painless jaundice and pruritus. CECT axial (**a–d**) and coronal (**e**, **f**) images show an ill-defined mass with heterogeneous attenuation involving the head of the pancreas (**c–e**) (*arrows*) and encasing the gastroduodenal artery, causing obstruction of the common bile duct (**a**, **b**, **e**, **f**) (*arrowheads*) and pancreatic duct (**a**) (*arrowhead*). The patient underwent a pancreaticoduodenectomy.

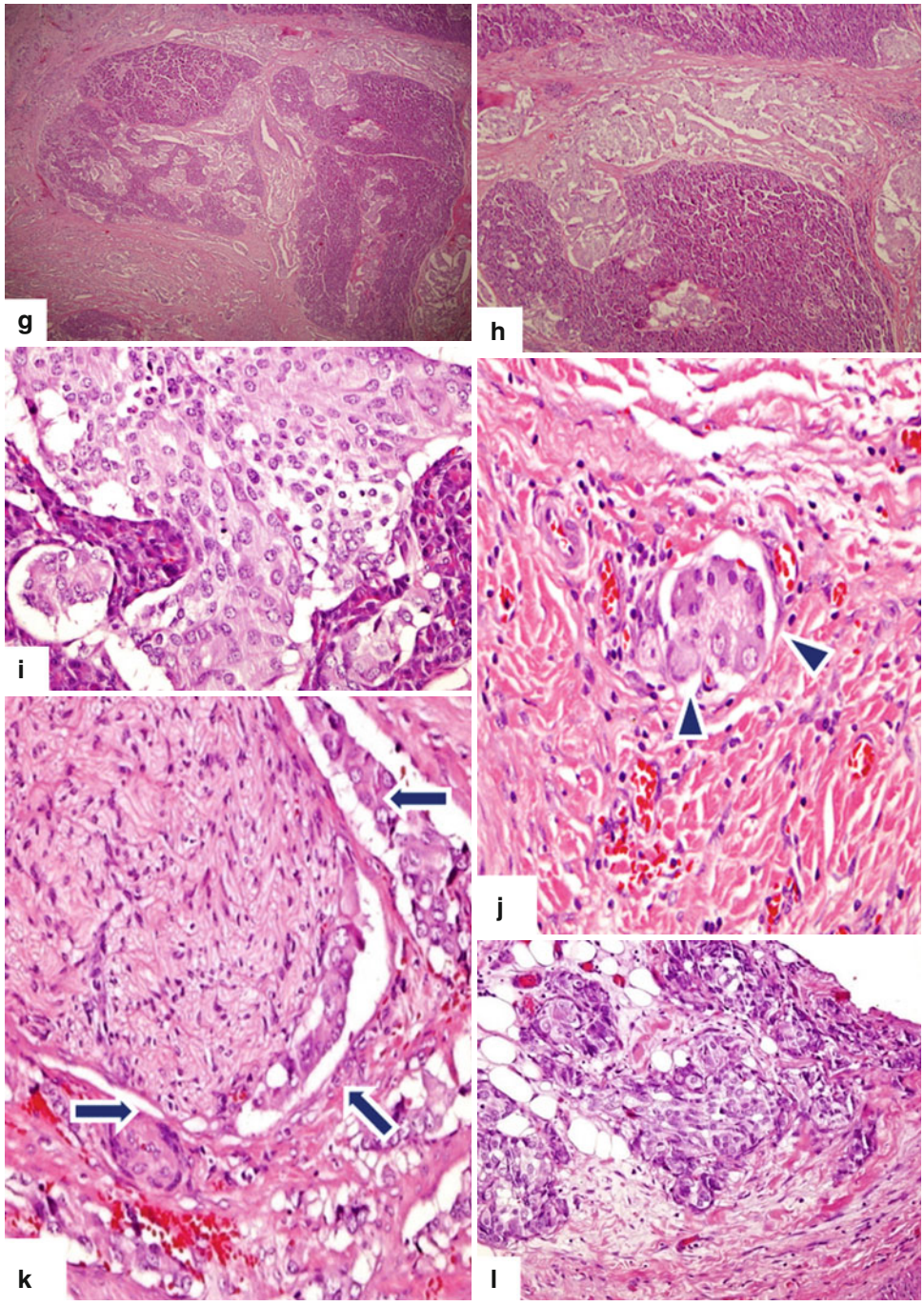

Fig. 10.40 (continued) Histological sections show a poorly differentiated neuroendocrine carcinoma, grade 3 (**g**) (H&E, 4x), with metastasis to multiple lymph nodes (**h**, **i**) (H&E 10x, 60x). Additionally, lymphovascular (**j**) (*arrowheads*), perineural (**k**) (*arrows*), and adipose tissue (**l**) invasion was present, (H&E, 60x, 40x)

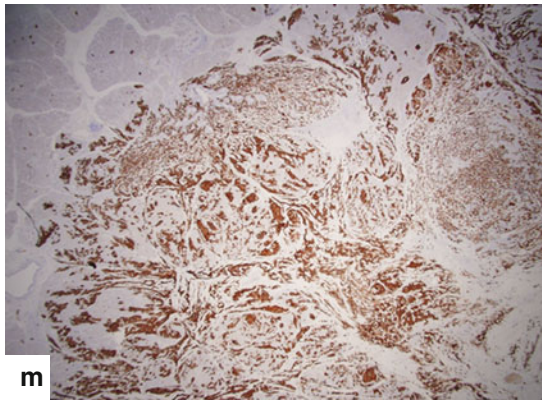

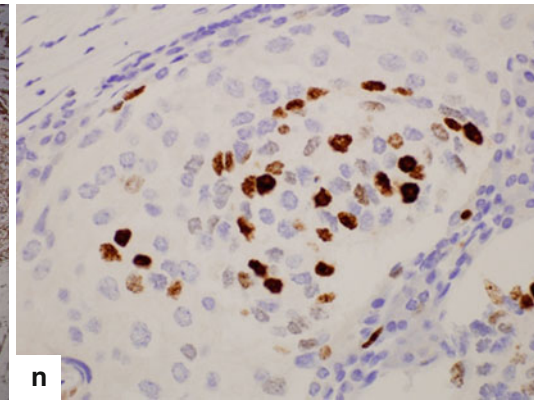

Fig. 10.40 (continued) Immunohistochemistry of the tumor cells reveals strong positivity for synaptophysin (**m**) and a Ki-67 proliferative rate > 20 %, grade 3 (**n**)

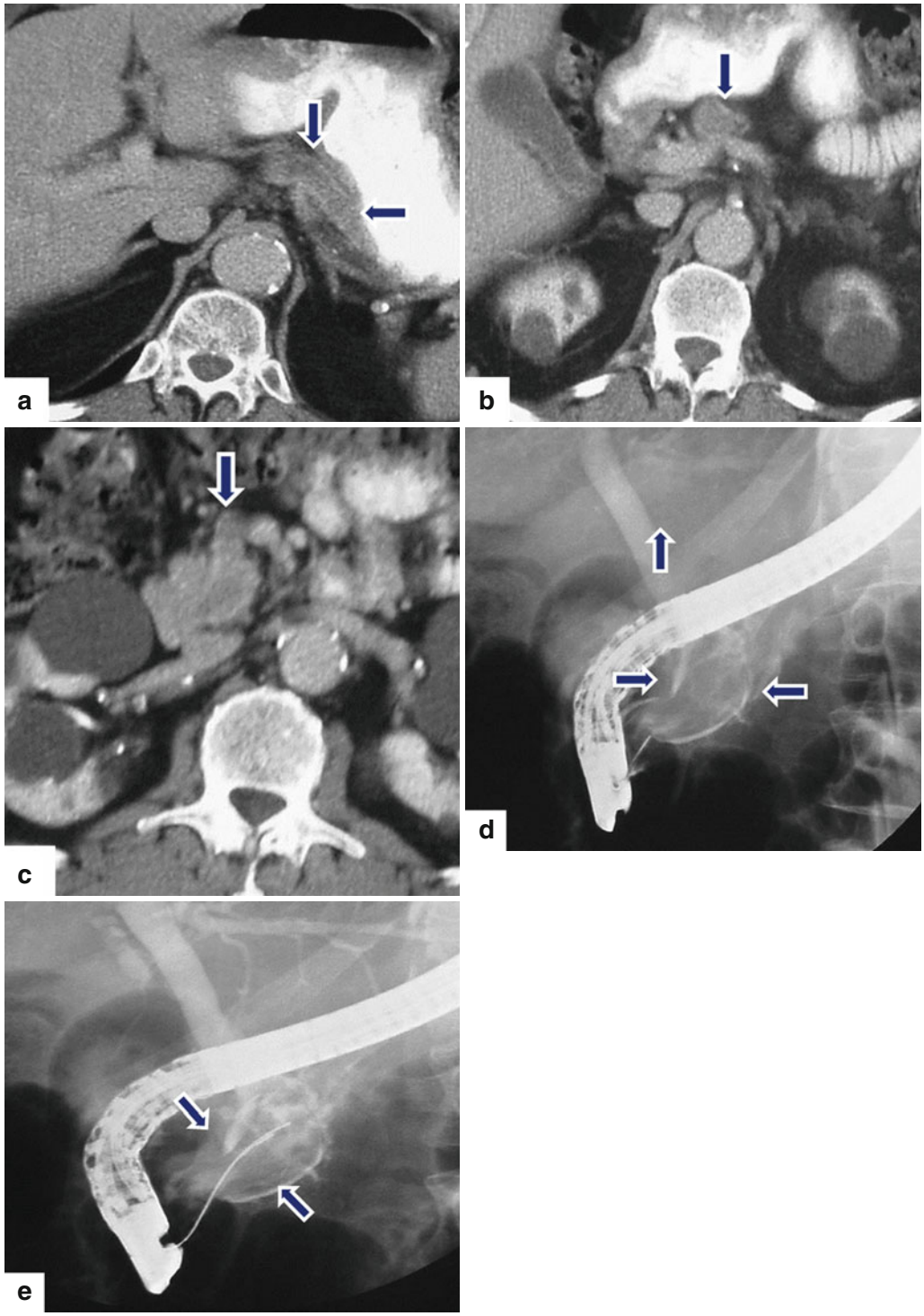

Fig. 10.41 Nonfunctional intraductal PNEN invading the pancreatic duct on CT and ERCP. A 77-year-old male with history of weight loss. CECT axial (**a–c**) images reveal severe dilatation of the entire pancreatic duct (*arrows*) up to the level of the major ampulla associated with atrophy of the entire pancreas. ERCP (**d**, **e**) images reveal a large filling defect within a dilated pancreatic duct (*arrows*). Initially, the patient was to undergo a pancreaticoduodenectomy. However, due to the positive surgical margins, a total pancreatectomy and splenectomy was performed

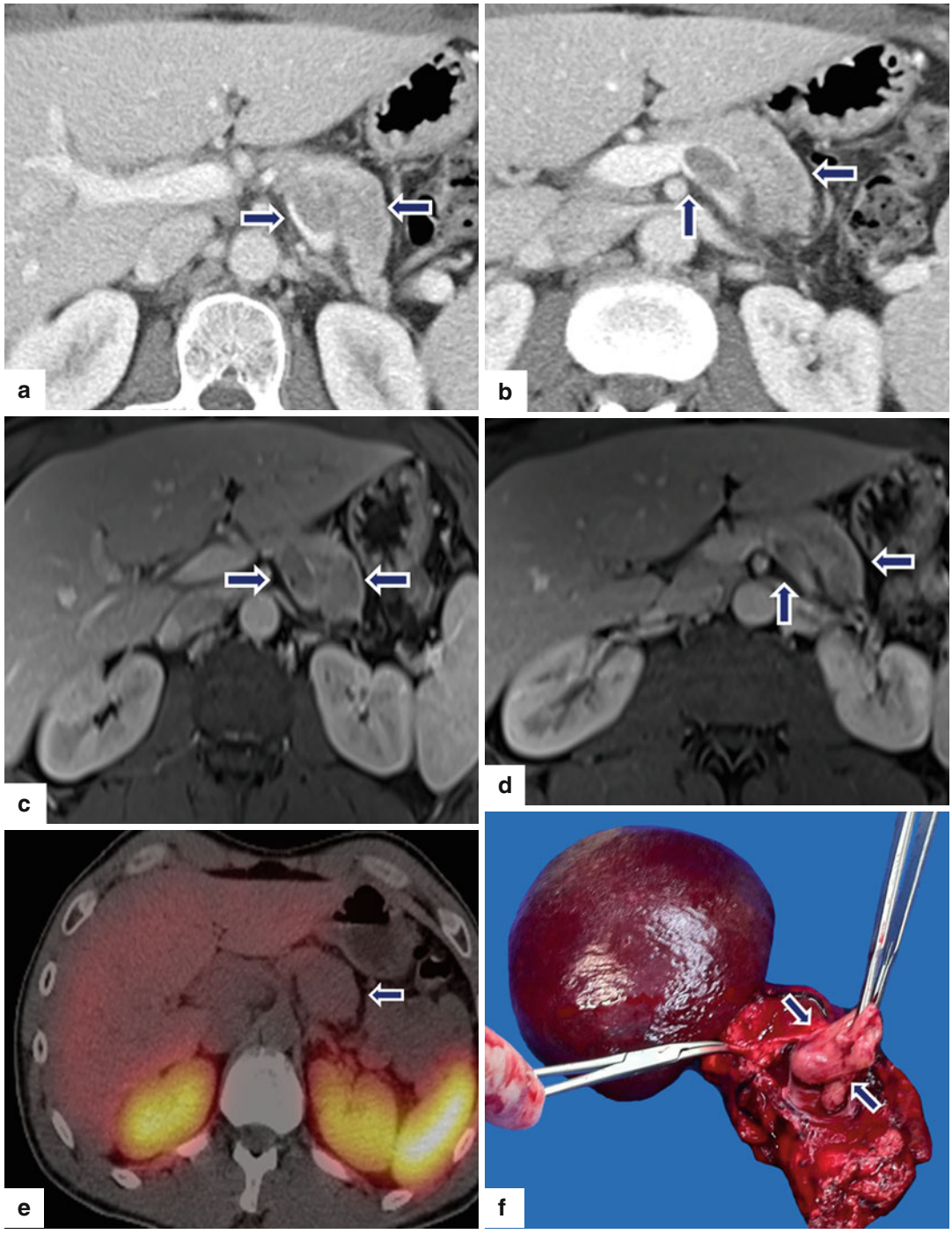

Fig. 10.42 Nonfunctional PNEN associated with vascular invasion on CT and MR. A 55-year-old male with epigastric pain. CECT axial (**a**, **b**) images show a low-attenuation mass in the pancreatic body extending into the splenic vein (*arrows*). Contrast-enhanced fat-suppressed gradient echo T1-weighted axial (**c**, **d**) images confirm the presence of a pancreatic mass with heterogeneous signal intensity extending into the splenic vein. Octreotide scan axial (**e**) image reveals poor radiotracer uptake by this pancreatic mass. The patient underwent a distal pancreatectomy and splenectomy. Photograph of the surgical specimen (**f**) reveals a white-tan, soft, lobulated, pancreatic mass invading the splenic vein (*arrows*)

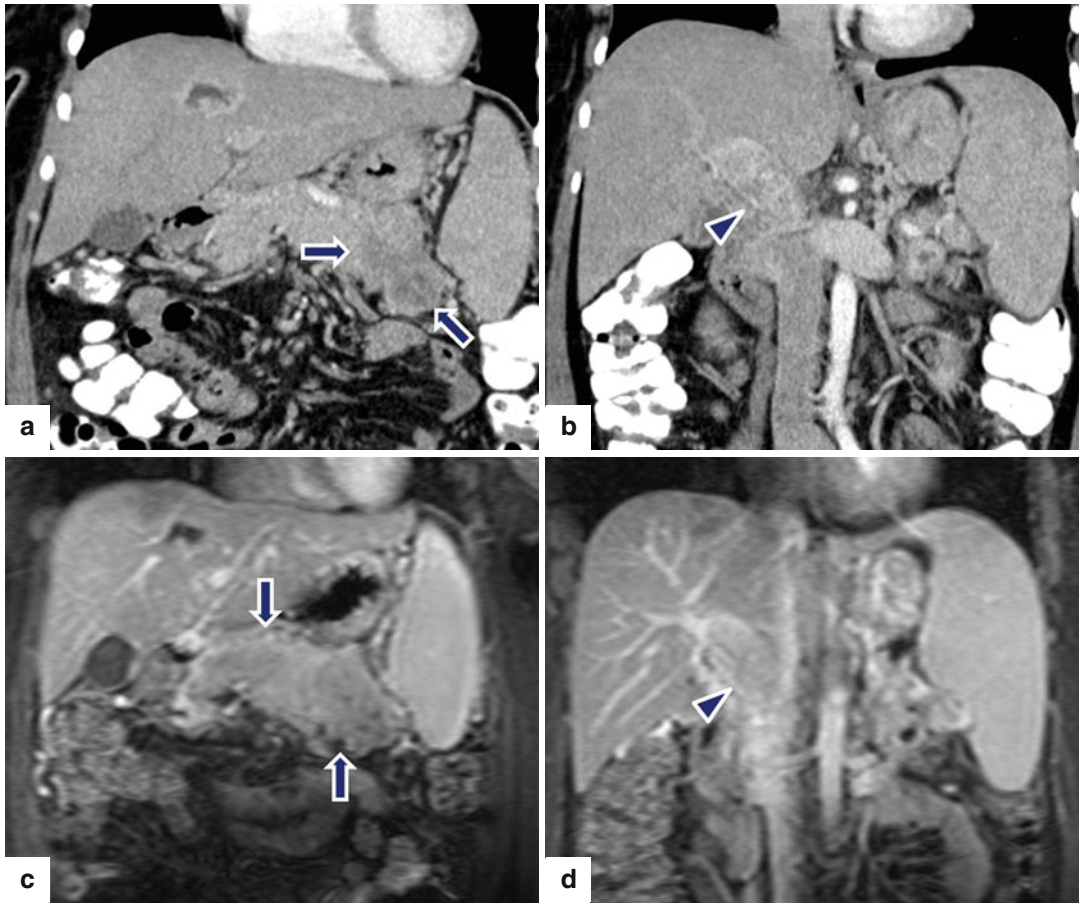

Fig. 10.43 Nonfunctional PNEN associated with vascular invasion on CT and MR. A 35-year-old female with abdominal pain and weight loss. CECT coronal (**a**, **b**) images demonstrate an amorphous, low-attenuation mass involving the body and tail of the pancreas (*arrows*) associated with a thrombus of heterogeneous density in the portal vein (*arrowheads*). On contrast-enhanced fat suppressed gradient echo T1-weighted coronal (**c**, **d**) images, the mass involving the body and tail of the pancreas appears more conspicuous (*arrows*) and the tumor thrombus in the portal vein was again demonstrated (*arrowheads*)

10.4.4.3 Magnetic Resonance Imaging (MRI) (Figs. 10.44–10.54)

MR Protocol

- T1-weighted (T1WI) and T2-weighted (T2WI) images, with and without fat suppression
- Diffusion weighted images (DWI)
- Contrast-enhanced fat-suppressed gradient echo T1-weighted images (arterial phase 20–25 s and portal phase 55–50 s after injection of intravenous gadolinium)

Findings

- **T1WI**: PNENs appear as round or oval, well-circumscribed masses with low signal intensity relative to the normal pancreatic signal intensity.
- **T2WI**: PNENs typically show a high or heterogeneous signal intensity.
- **T1WIFS with contrast**: small PNENs may have homogeneous, hyperintense signal relative to the normal pancreas. Large PNENs may have a heterogeneous signal intensity or ring-like peripheral signal intensity (central necrosis).

- **Hepatic metastases**: hypervascular, homogeneous, heterogeneous, or peripheral rim enhancing.
- **Lymph node metastases**: enlarged hyperintense nodes, homogeneous or heterogeneous signal intensity.

Practical Pearls

- Presence of numerous stromal blood vessels contributes to a hypervascular appearance of PNEN on contrast-enhanced CT or MR.
- Cystic PNENs may have a peripheral vascular rim which allows differentiation of PNENs from other cystic neoplasms.
- MR diffusion sequences have great sensitivity in the detection of hepatic metastases and lymph node enlargement.

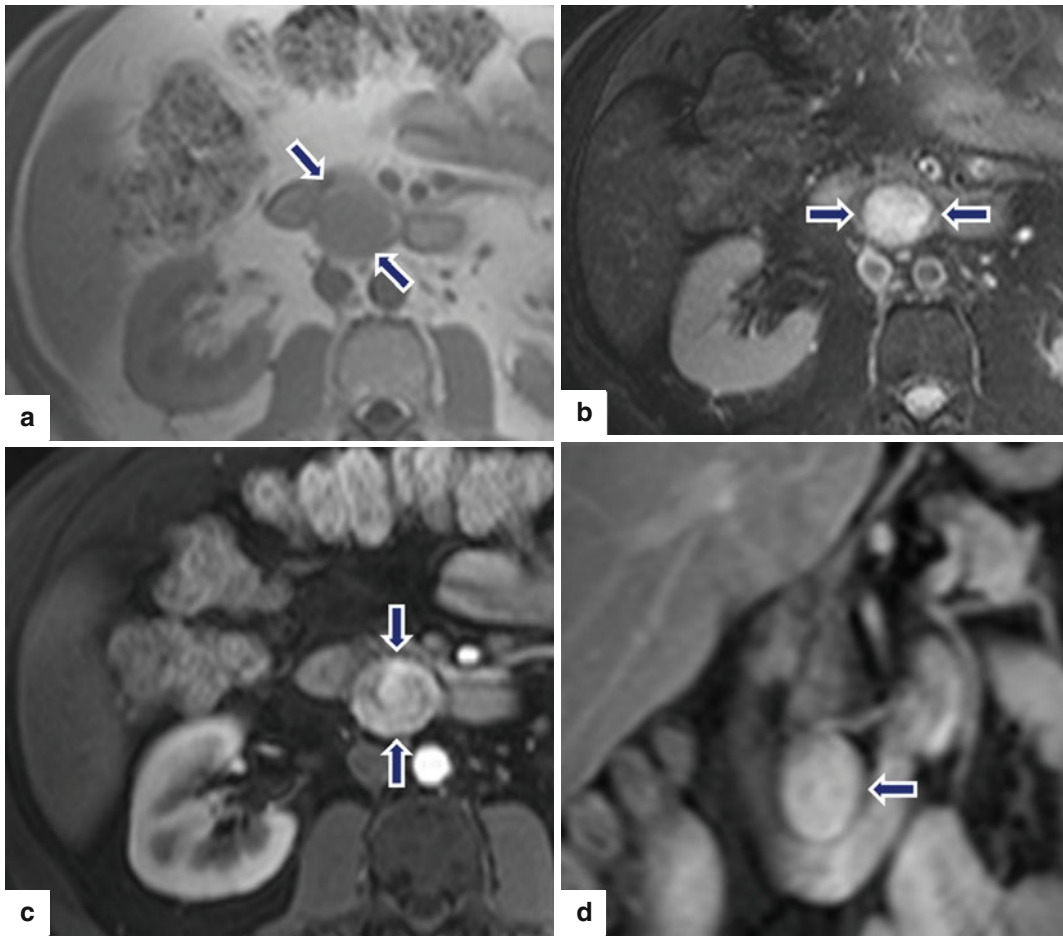

Fig. 10.44 Nonfunctional PNEN on MR. A 62-year-old female with vague abdominal pain. T1W axial (**a**) image shows an exophytic, round, low signal intensity mass arising from the pancreatic head (*arrows*). On fat-suppressed T2W axial (**b**) image, this mass shows a high signal intensity (*arrows*). On contrast-enhanced fat-suppressed gradient echo axial (**c**) and coronal images (**d**), this mass shows a heterogeneous, vascular enhancement (*arrows*)

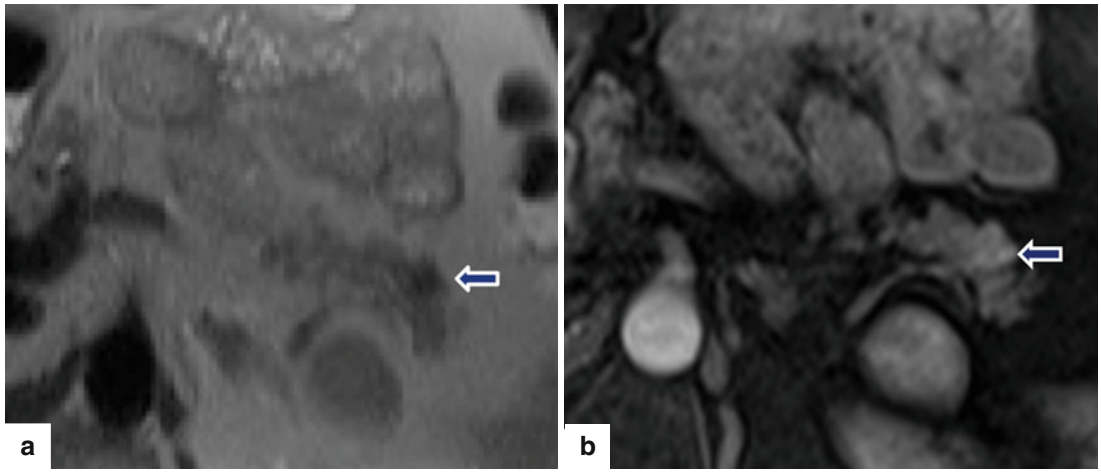

Fig. 10.45 Small, nonfunctional PNEN on MR. A 45-year-old male with an incidental finding. T1W axial (**a**) image demonstrates a small, lobulated, low signal intensity mass in the tail of the pancreas (*arrow*). Contrast-enhanced fat-suppressed gradient echo T1 weighted axial (**b**) image shows a heterogeneous, vascular enhancement by this mass (*arrow*)

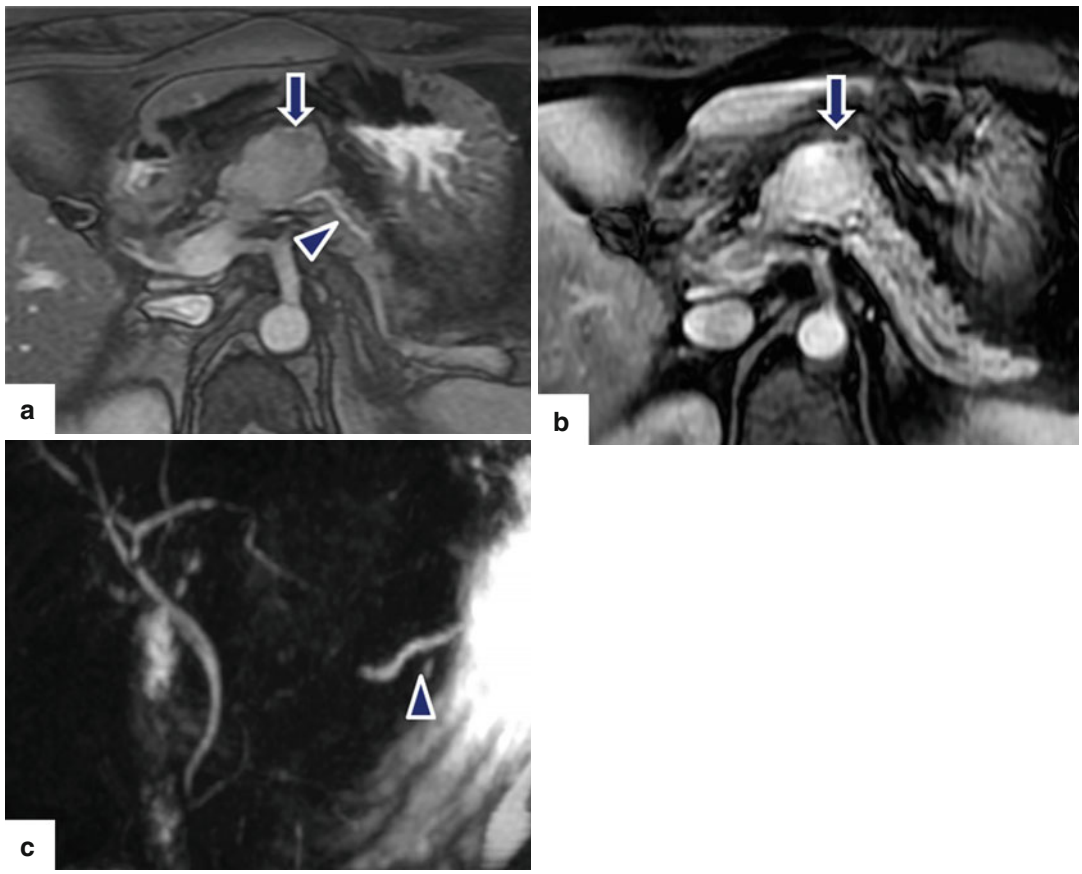

Fig. 10.46 Nonfunctional PNEN associated with obstruction of the pancreatic duct on MR. A 48-year-old female with history of abnormal liver function tests in which an abdominal MR was performed. Fat-suppressed T2W axial (**a**) image shows an ovoid, low signal intensity mass involving the pancreatic body (*arrow*) associated with mild dilatation of the distal pancreatic duct (*arrowhead*). Contrast-enhanced fat-suppressed gradient echo T1 weighted axial (**b**) image shows intense, homogeneous, contrast enhancement by this mass (*arrow*). MRCP thick slab (**c**) image shows abrupt obstruction of the pancreatic duct distal to the pancreatic mass (*arrowhead*).

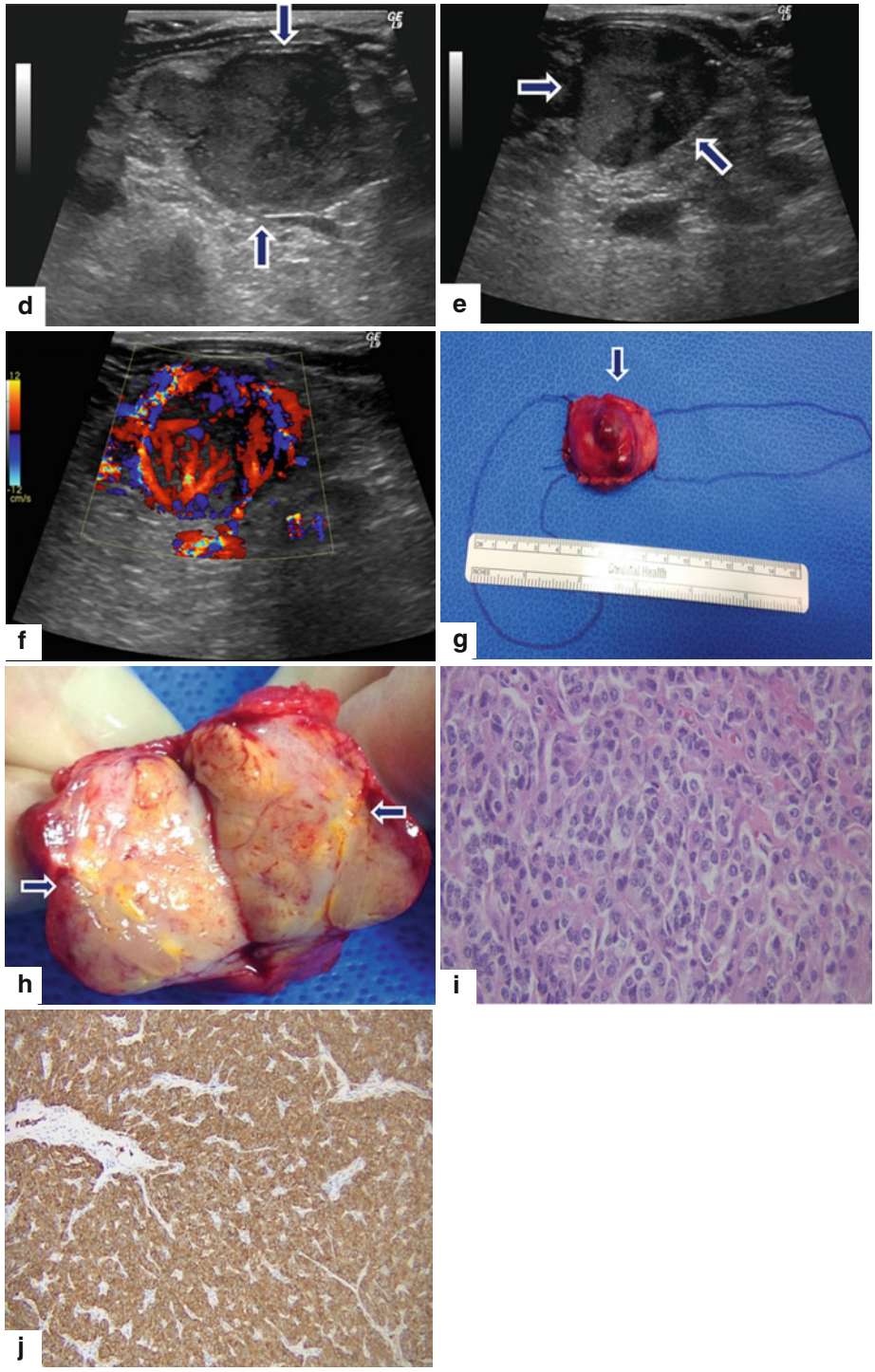

Fig. 10.46 (continued) IOUS gray scale (**d**, **e**) and color Doppler transverse (**f**) images show a lobulated hypoechoic, hypervascular mass (**d**, **e**) (*arrows*) with a coarse calcification. The patient underwent a central pancreatectomy. Photograph of the surgical specimen (**g**) shows a bilobulated pancreatic mass (*arrow*). Photograph of the bivalved gross specimen (**h**) shows a fleshy, tan, round, irregular mass with prominent white bands of fibrosis, residual yellow pancreatic tissue, and scattered, small hemorrhagic foci (*arrows*). Histological sections (**i**) show round cells with a "salt-and-pepper" appearance of the chromatin (H&E, 40×). Chromogranin immunostain (**j**) is strongly positive (immunohistochemistry, 10×)

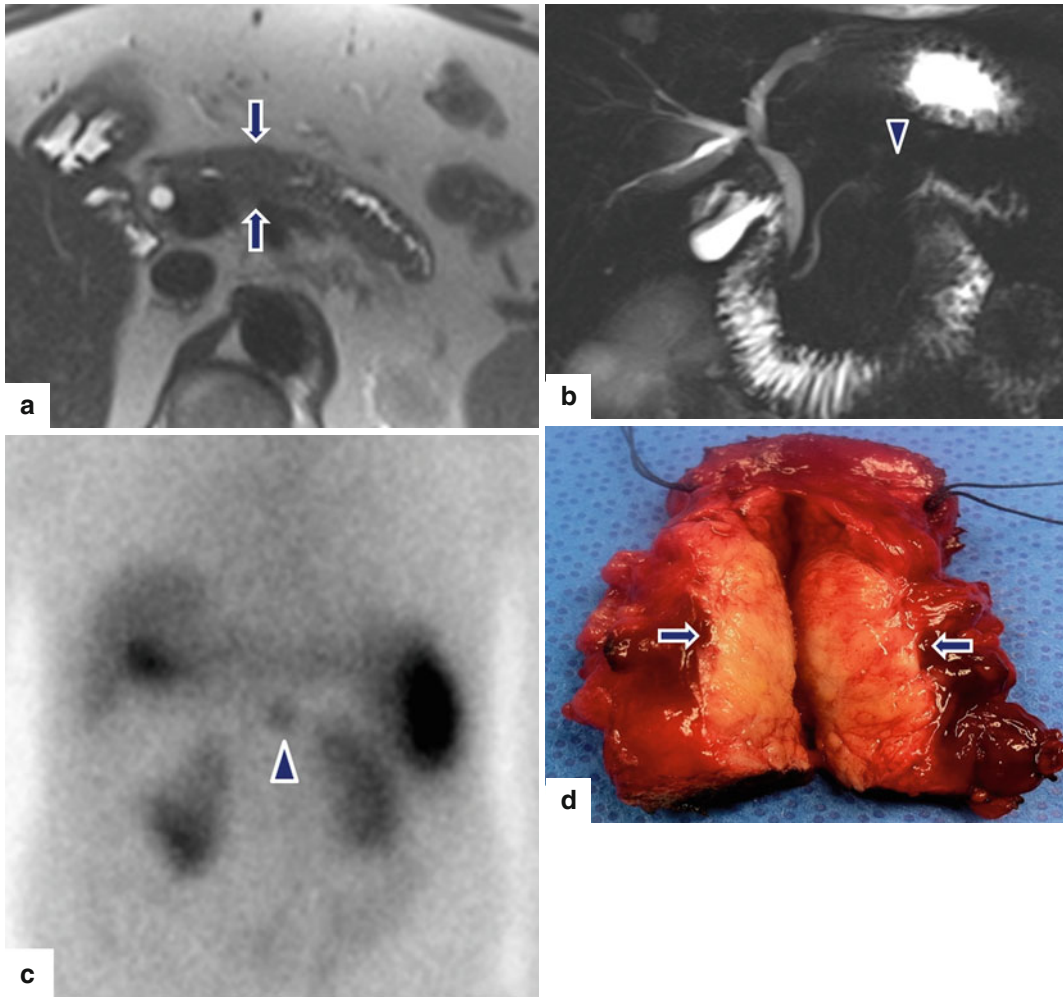

Fig. 10.47 Nonfunctional PNEN associated with obstruction of the pancreatic duct on MR. A 60-year-old male with history of thoracic aortic aneurysm. Follow-up CT showed an incidental pancreatic mass. T2W axial (**a**) image demonstrates an isointense mass in the pancreatic body (*arrows*) associated with dilatation of the distal pancreatic duct. MRCP thick slab (**b**) image confirms the dilatation of the distal pancreatic duct (*arrowhead*). (**c**) Octreotide scan demonstrates radiotracer uptake by this mass (*arrowhead*). The patient underwent a central pancreatectomy. Photograph of the resected specimen (**d**) demonstrates an irregular yellow/tan, firm mass (*arrows*).

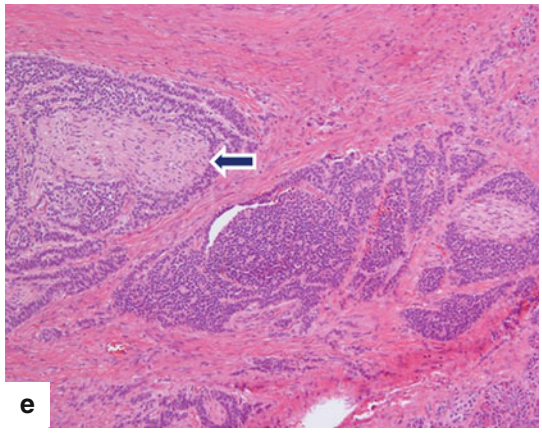

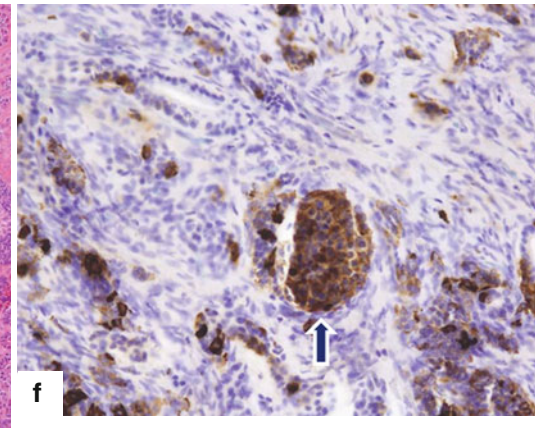

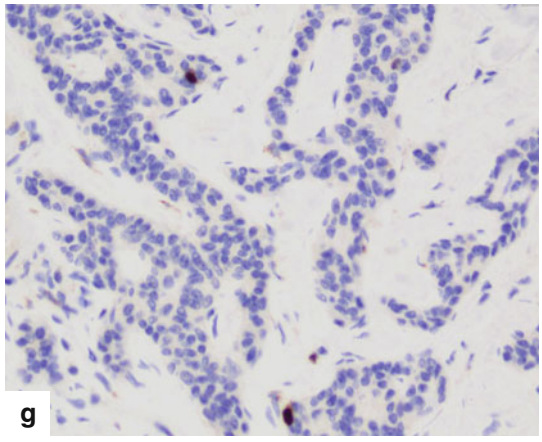

Fig. 10.47 (continued) Histological section (**e**) (H&E, 10×) shows a neuroendocrine neoplasm, grade 1, with extensive perineural invasion (*arrow*) and fibrosis. Chromogranin (**f**) (*arrow*) immunostain is positive. Ki-67 (**g**) immunostain is positive in a few cells revealing a low proliferative index < 2 (immunohistochemistry, 40×, 10×)

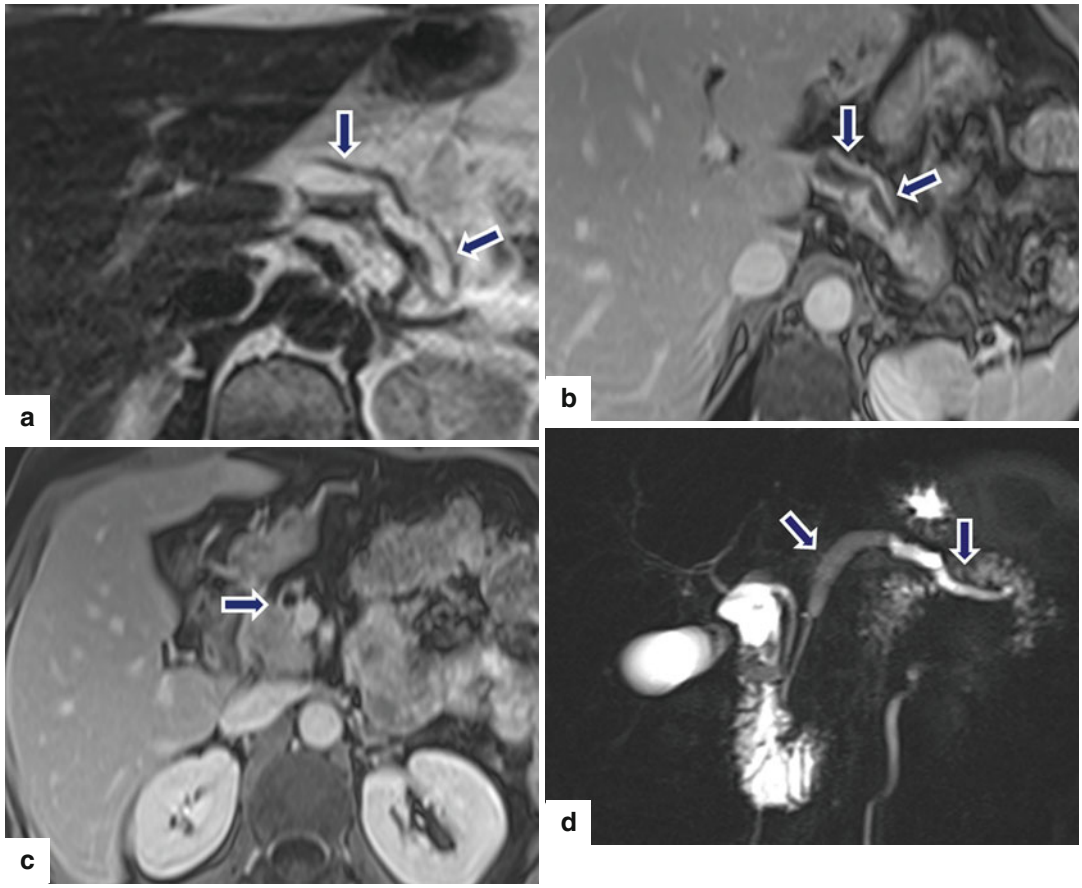

Fig. 10.48 Nonfunctional PNEN on MR. A 62-year-old female with left flank pain. T2W axial (**a**) image shows a dilated pancreatic duct in the body and tail of the pancreas (*arrows*). Contrast-enhanced fat-suppressed gradient echo T1 weighted axial (**b**, **c**) images confirm the dilatation of the pancreatic duct (*arrows*) with an abrupt cutoff in the neck (*arrows*). Note the absence of an obvious pancreatic mass. MRCP thick slab (**d**) image reconfirms the dilatation of the pancreatic duct in the body and tail of the pancreas (*arrows*). Patient underwent a central pancreatectomy.

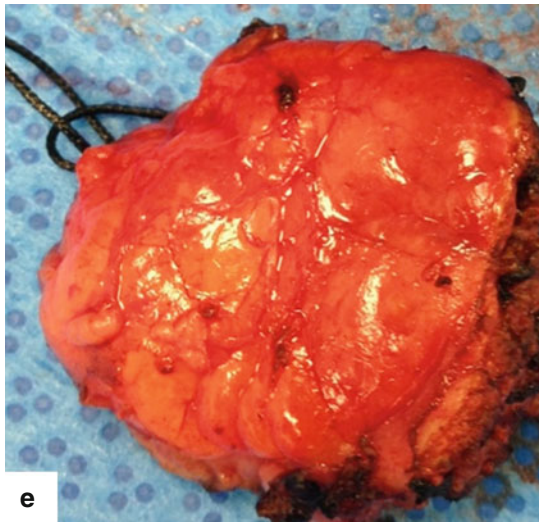

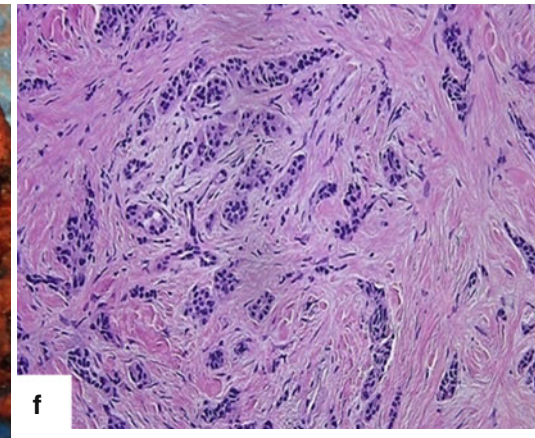

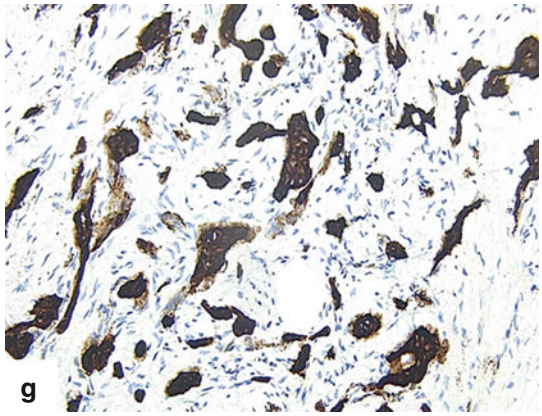

Fig. 10.48 (continued) Photograph of the resected pancreas (**e**). Histological section shows a well-differentiated neuroendocrine neoplasm, grade 2 (**f**) (H&E, 20×) with strong positivity for synaptophysin (**g**) (immunohistochemistry, 20×)

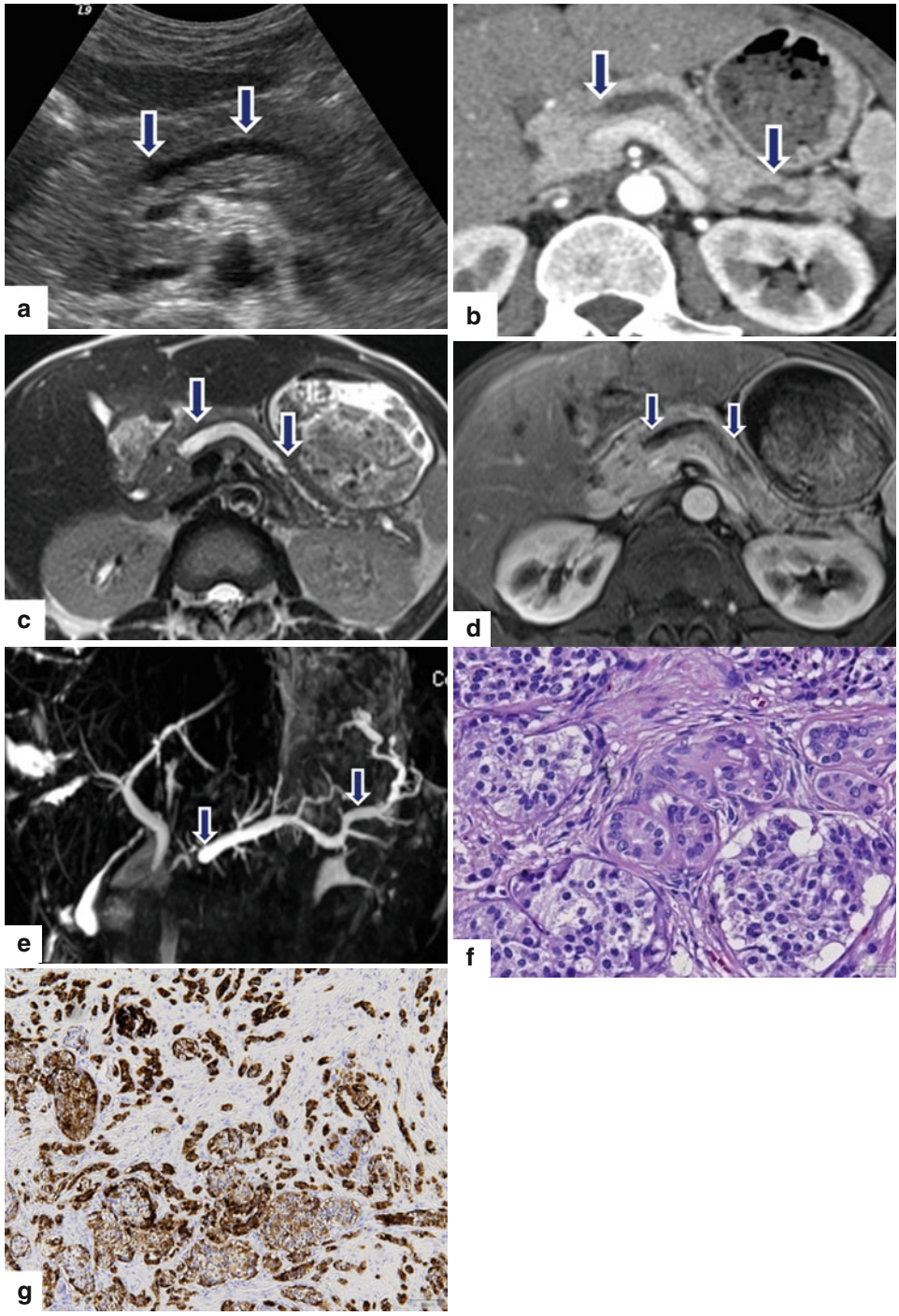

Fig. 10.49 Nonfunctional PNEN on US/CT/MR. A 50-year-old female with an incidental finding. US transverse (**a**) image shows dilatation of the pancreatic duct in the body and tail of the pancreas (*arrows*) with an abrupt cutoff at the neck. CECT axial (**b**), single-shot fast spin echo T2-weighted axial (**c**), contrast-enhanced fat-suppressed gradient echo T1-weighted axial (**d**), and MRCP coronal (**e**) images confirm the obstruction of the pancreatic duct with abrupt cutoff in the pancreatic neck (*arrows* point to the dilated pancreatic duct in all images). Note the absence of an obvious pancreatic mass in this location. The patient underwent an extended Whipple procedure. Histological section shows a well-differentiated neuroendocrine neoplasm (**f**) (H&E, 40×) with nesting pattern. The tumor cells are strongly positive for serotonin 5-HT by immunohistochemistry (**g**) (20×)

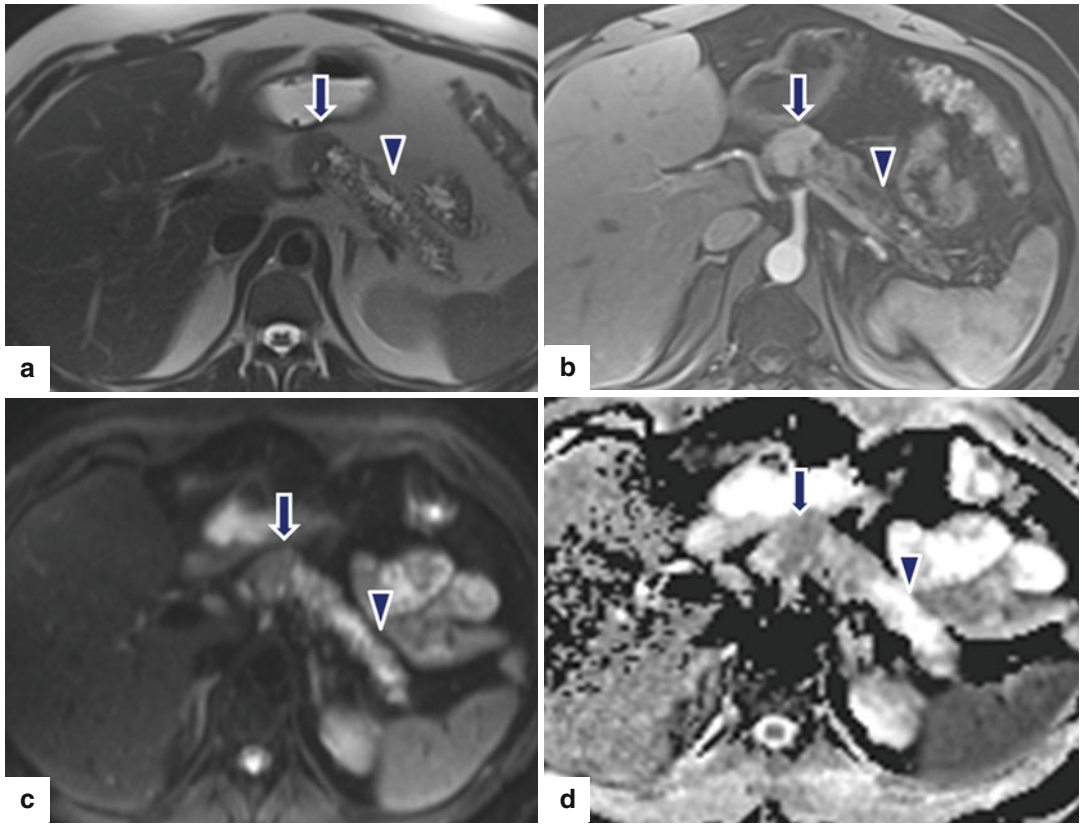

Fig. 10.50 Well-differentiated, nonfunctional PNEN on MR. A 36-year-old male with epigastric pain and weight loss. Single-shot fast spin echo T2-weighted (**a**) image demonstrates an isointense mass in the body of the pancreas (*arrows*) associated with dilatation of the distal pancreatic duct and parenchymal atrophy. Contrast-enhanced fat-suppressed gradient echo T1-weighted (**b**) image demonstrates homogeneous contrast enhancement by this mass (*arrows*). Diffusion axial (**c**) image demonstrates a low signal intensity mass (*arrows*). Note the signal restriction by this mass in the ADC map axial (**d**) image (*arrow*). (**a**–**d**) *Arrowheads* indicate dilatation of the distal pancreatic duct

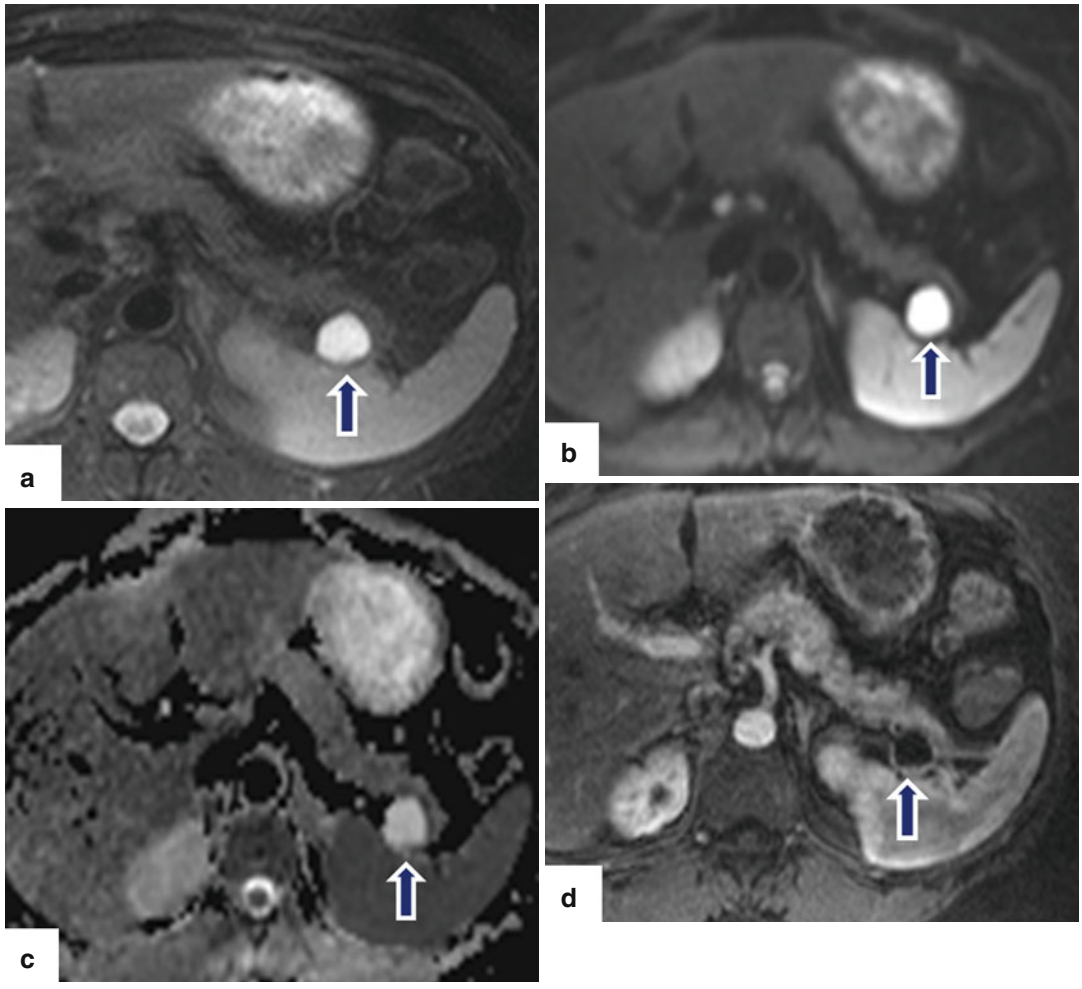

Fig. 10.51 Well-differentiated, nonfunctional PNEN with unusual appearance on MR and IOUS. A 46-year-old female with an incidental finding. Fat-suppressed T2W (**a**), diffusion (**b**), and ADC map, axial (**c**) images show a round, well-circumscribed, high signal intensity mass which does not restrict, located in the pancreatic tail (*arrows*). Contrast-enhanced fat-suppressed gradient echo T1-weighted axial (**d**) image shows poor contrast enhancement by this mass (*arrow*).

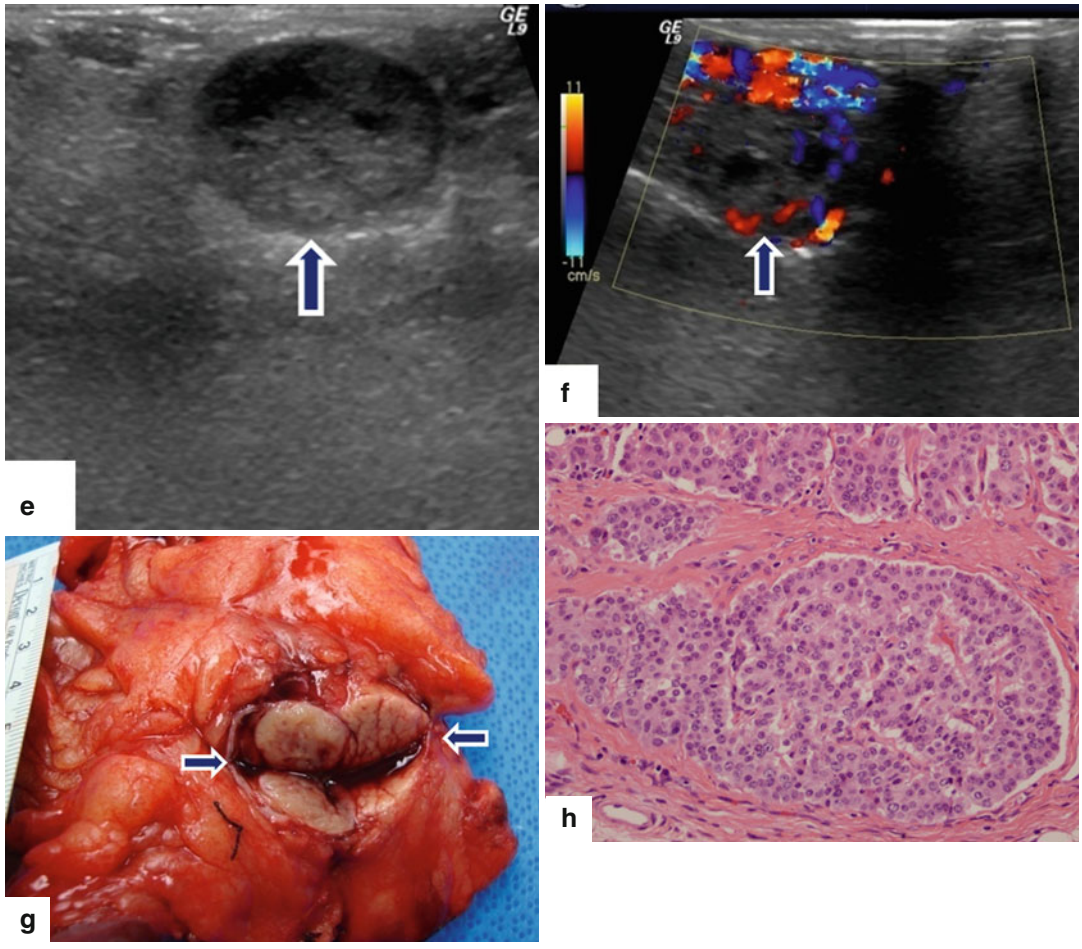

Fig. 10.51 (continued) Note the thick capsular wall thickening. IOUS gray scale transverse (**e**) and color Doppler (**f**) images show an ovoid complex mass with internal vascularity (*arrows*). Photograph of the bivalved specimen (**g**) shows a fleshy, gray-tan mass with well-defined borders (*arrows*). Histological section shows a neuroendocrine neoplasm with a nesting pattern of growth (**h**) (H&E, 40×)

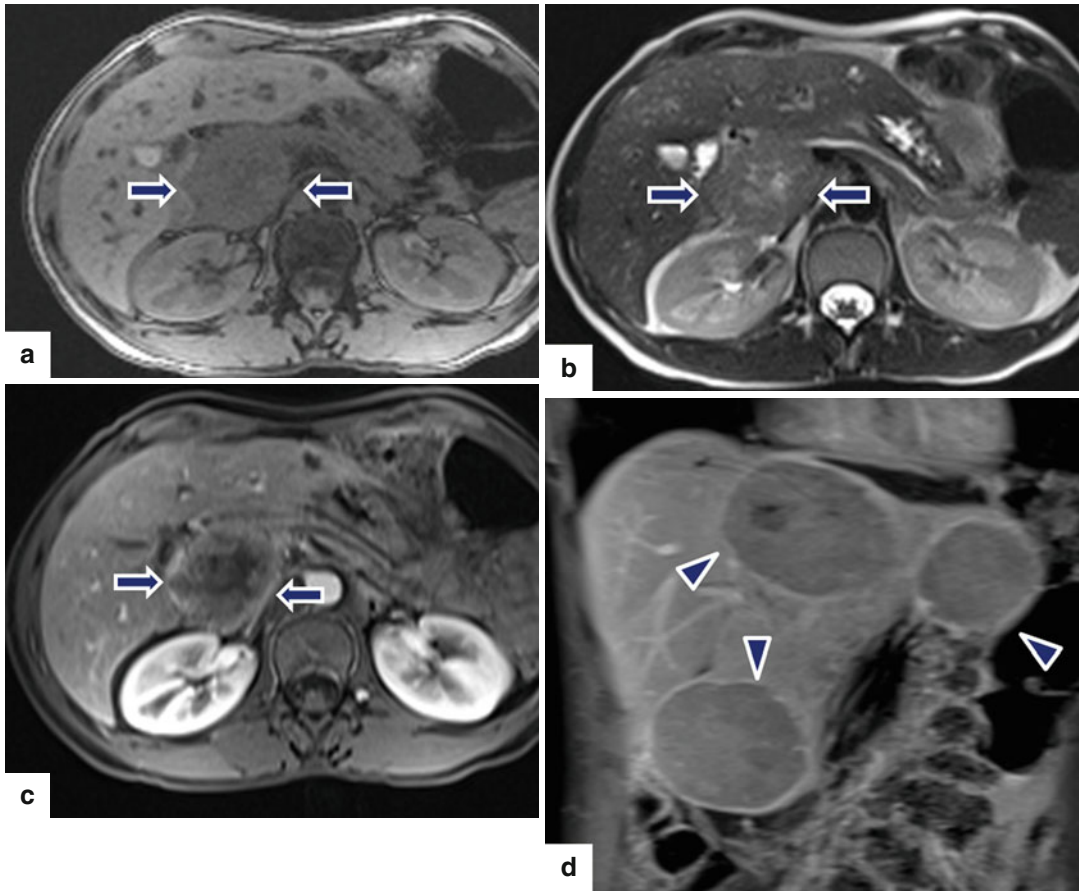

Fig. 10.52 Malignant nonfunctional PNEN on MR. A 47-year-old female with abdominal pain and weight loss. Fat-suppressed gradient echo T1-weighted image (**a**) demonstrates a mass in the pancreatic head with low signal intensity (*arrows*). T2-weighted axial (**b**) image of this mass demonstrates heterogeneous signal intensity (*arrows*). On fat-suppressed gradient echo T1-weighted axial (**c**) image, this mass demonstrates heterogeneous contrast enhancement (*arrows*). Contrast-enhanced fat-suppressed gradient echo T1-weighted coronal images (**d**) of the liver demonstrate three large metastases (*arrowheads*) with heterogeneous signal intensity and with an enhancing peripheral ring

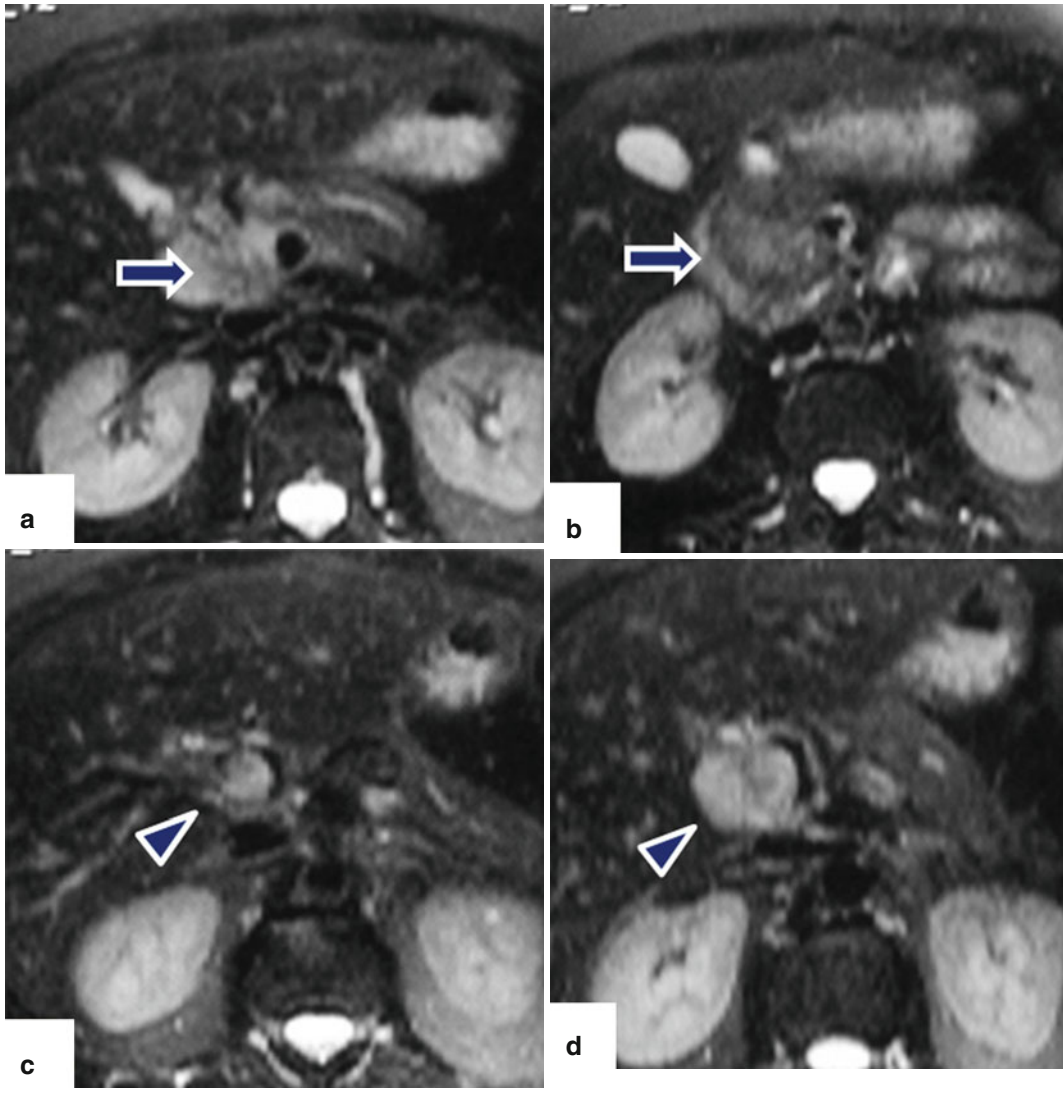

Fig. 10.53 Poorly differentiated PNEN associated with vascular invasion on MR. A 54-year-old female with history of painless jaundice. An ERCP was performed demonstrating an obstruction of the distal common bile duct (not shown). This duct was stented, relieving the patient's jaundice. Fat-suppressed T2W axial (**a–d**) images reveal a mass with heterogeneous signal intensity involving the pancreatic head (**a**, **b**) (*arrows*) and extending into the portal vein (**c**, **d**) (*arrowheads*).

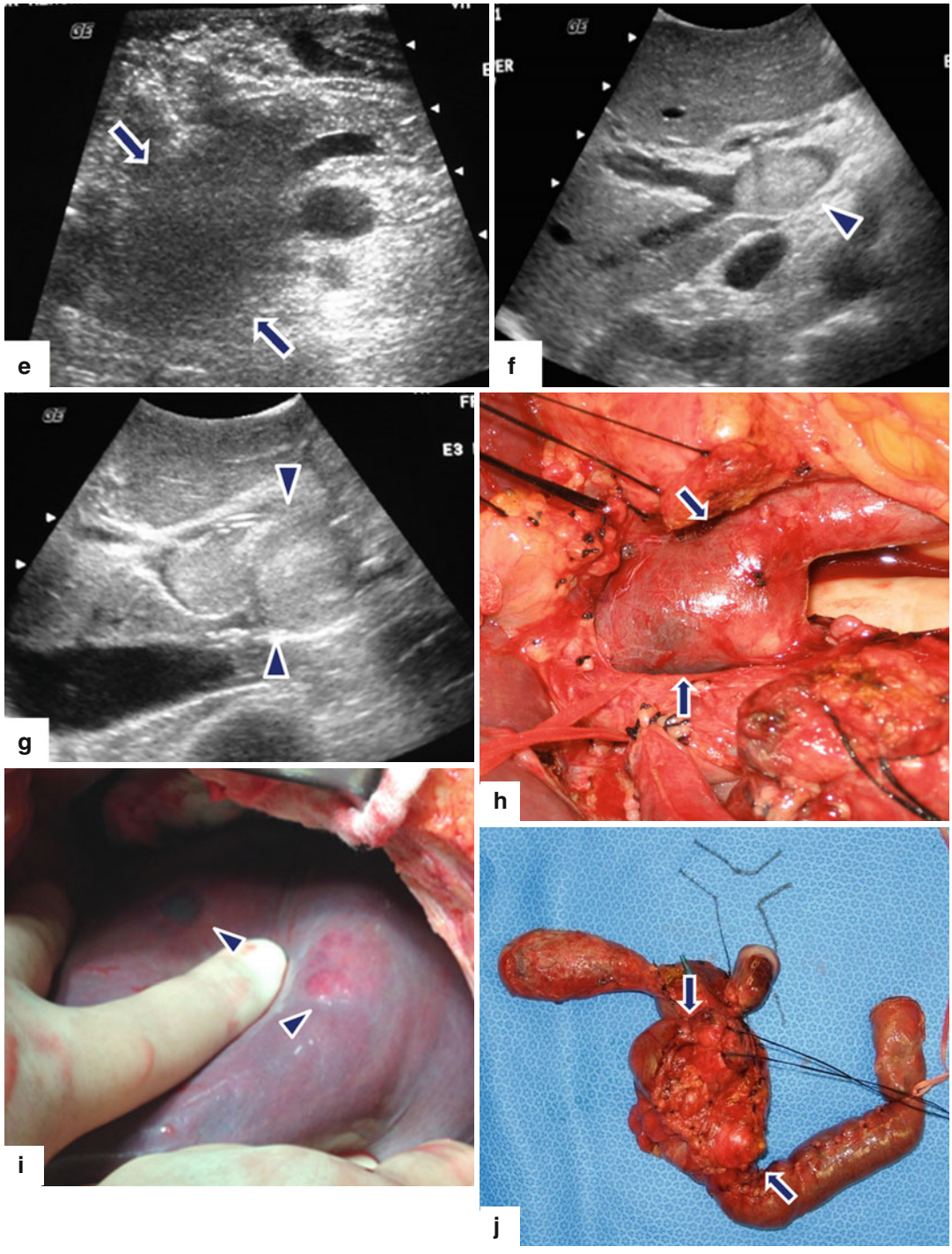

Fig. 10.53 (continued) IOUS transverse (**e**, **f**) and sagittal (**g**) images reveal a poorly defined hypoechoic mass involving the pancreatic head (**e**) (*arrows*) extending into the main portal vein (**f**, **g**) (*arrowheads*). Intraoperative photographs reveal a prominent main portal vein secondary to the intraluminal tumor (**h**) (*arrows*) and the presence of superficial hepatic metastases (**i**) (*arrowheads*). The patient underwent a pyloric-sparing Whipple procedure with reconstruction of the portal vein. Photograph of the surgical specimen (**j**) reveals the pancreatic mass with the portion of the portal vein resected (*arrows*).

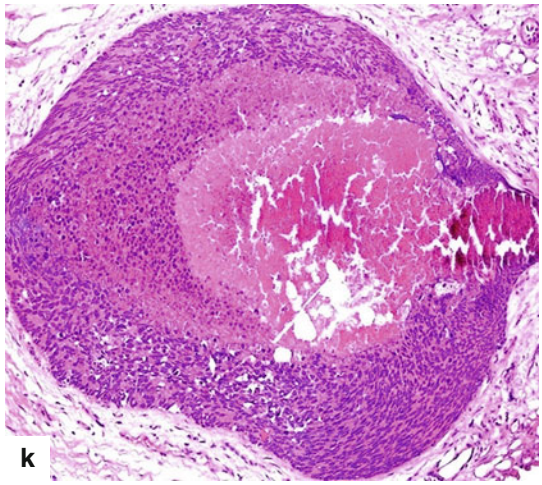

Fig. 10.53 (continued) Histological section shows a poorly differentiated neuroendocrine carcinoma, large cell type (**k**). The tumor had nests of necrotic cells with focal calcification as depicted in the image (H&E, 4×)

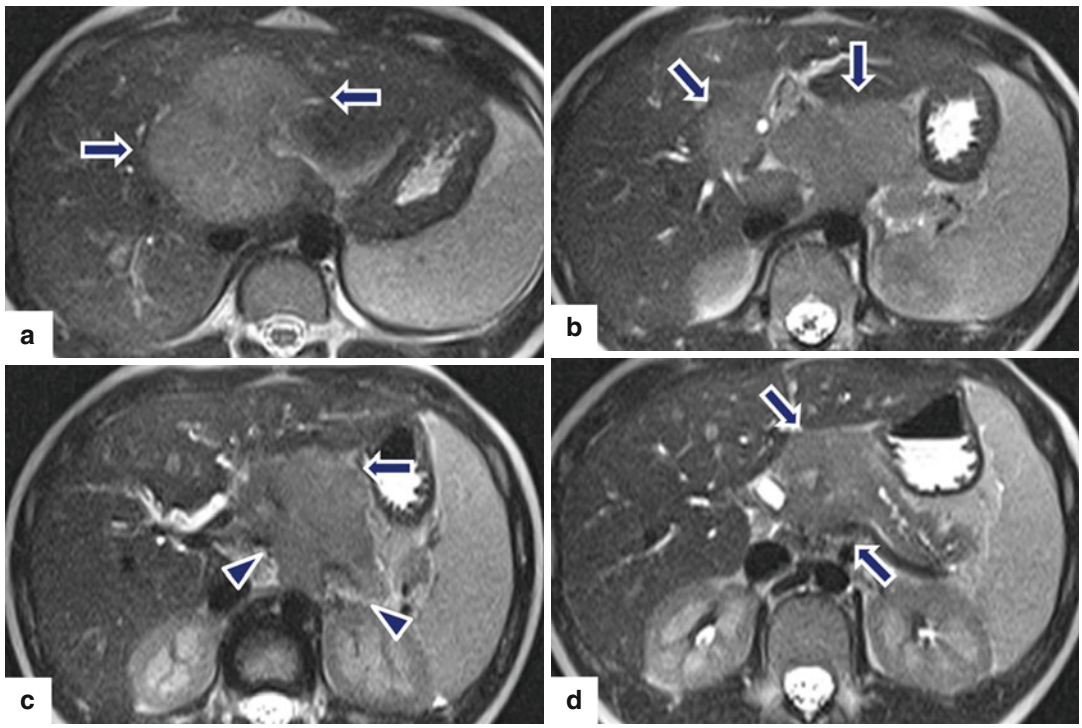

Fig. 10.54 Nonfunctional PNEN in a pediatric patient on MR. An 8-year-old male with history of acute painless jaundice. Single-shot fast spin echo T2-weighted (**a–d**) images show a lobulated mass of intermediate signal intensity, involving the pancreatic body (*arrows*) associated with mild dilatation of the distal pancreatic duct extending into the liver and obstructing the intrahepatic biliary system and encasing the celiac artery and its branches (*arrowheads*)

10.4.4.4 Differential Diagnosis (CT/MR)

- Pancreatic adenocarcinoma
- Pancreatic metastases
- Solid pseudopapillary tumor
- Intrapancreatic splenule
- Peripancreatic paraganglioma
- Pancreatic lymphoma

10.4.4.5 Nuclear Medicine Studies (Figs. 10.55 and 10.56)

^{111}In-Octreotide Scan (Octreoscan)

- Considered the gold standard for imaging PNEN.
- Overall sensitivity of this method is 80 % and varies depending on the hormone produced by the tumor.

Findings

- Accumulation of the radiotracer in the tumor

Positron Emission Tomography/ Computed Tomography (PET/CT)

- More precise in tumor localization than ^{111}In-octreotide studies.
- Increase 2-(fluorine-18) fluoro-2-deoxy-d-glucose (FDG) uptake is usually demonstrated in poorly differentiated PNEN.

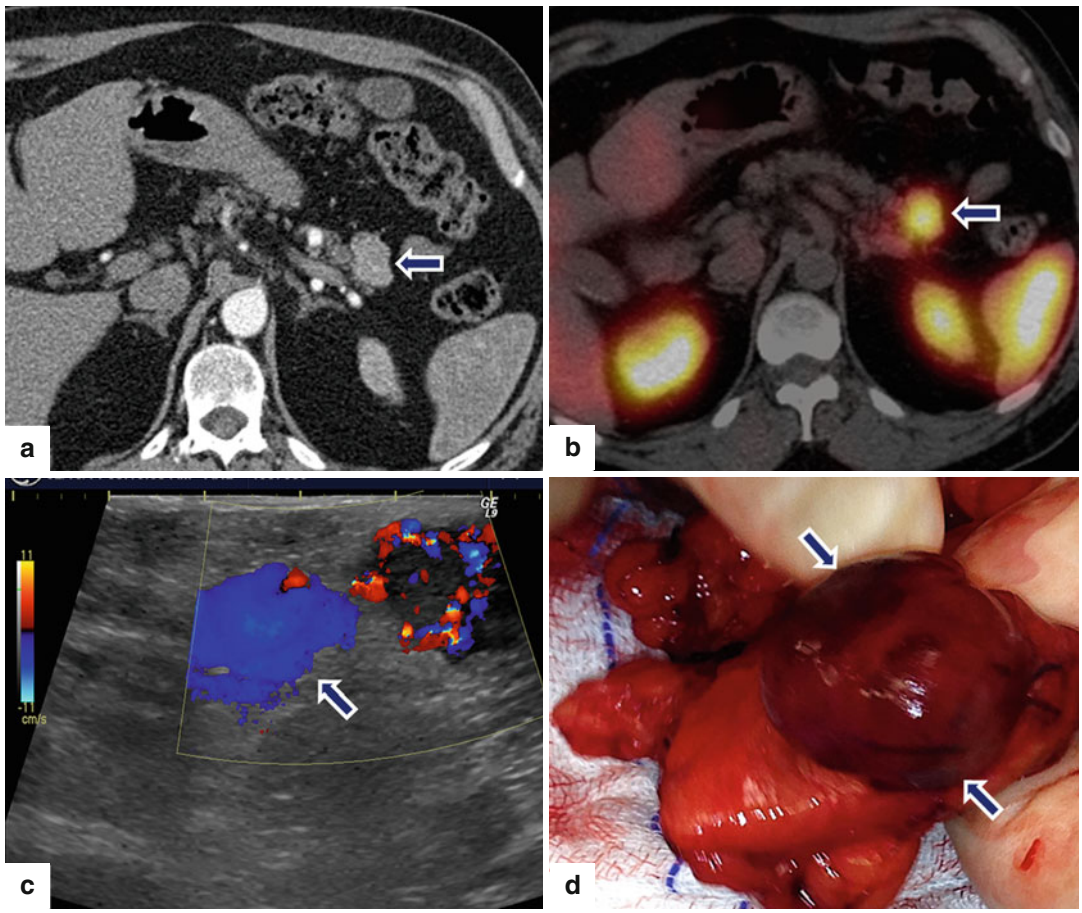

Fig. 10.55 Nonfunctional PNEN on CT on octreoscan SPECT/CT. A 57-year-old female with history of renal stones with an incidental pancreatic mass found on an abdominal CT. CECT axial (**a**) image shows a hypervascular, homogeneous mass in the pancreatic tail. Octreoscan SPECT/CT axial (**b**) image shows intense uptake of the radiotracer by this mass. Findings suggestive of a neuroendocrine tumor. IOUS transverse (**c**) image shows a hypervascular mass. The patient underwent a distal pancreatectomy and splenectomy. Photograph of the resected surgical specimen (**d**) shows an exophytic purple mass with smooth serosal surface (*arrows*). Final pathologic diagnosis: well-differentiated neuroendocrine neoplasm, grade 1

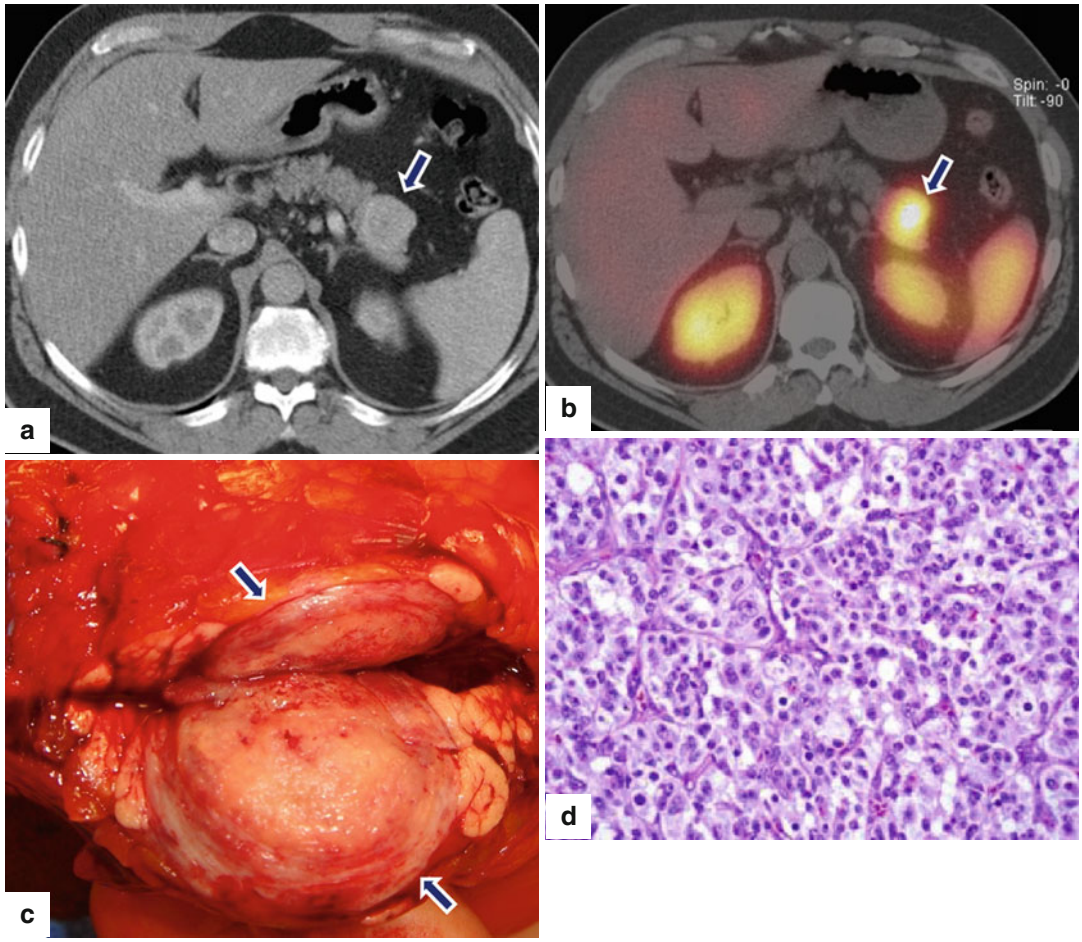

Fig. 10.56 Nonfunctional PNEN on octreoscan SEPCT/CT. A 45-year-old female with mild epigastric discomfort. CECT axial (**a**) image displays a round, homogeneous, hyperdense mass in the pancreatic tail (*arrow*). Octreoscan SPECT/CT axial (**b**) image displays accumulation of the radiotracer by this mass (*arrow*). Photograph of the bivalved, resected mass (**c**) displays a yellow, fleshy, well-circumscribed mass (*arrows*). Histological section (**d**) (H&E, 40×) shows a neuroendocrine neoplasm with cells arranged in an organoid pattern and "salt-and-pepper" chromatin

10.5 Functional Pancreatic Neuroendocrine Tumors (PNENs)

- Named after the predominant hormone secreted.
- Most common functional PNENs are insulinoma, gastrinoma, glucagonoma, VIPoma, and somatostatinoma.
- Related symptoms associated with functional PNEN are poorly specific.
- Proper diagnosis depends on physician awareness. It can be delayed for months or years after the first symptoms appear.
- With the exception of the insulinomas, functional PNEN are frequently malignant.
- Characterized by vascular invasion, gross infiltration of adjacent organs, and synchronous or metachronous nodal involvement or distant metastases.
- In some cases, the diagnosis of malignancy is made by the detection of metastases of a previously resected benign tumor.

10.5.1 Insulinomas

10.5.1.1 Epidemiology

- Most common functional PNEN.
- Arise from beta (β) cells of the pancreas.
- This tumor produces hypoglycemia due to insulin secretion.
- Incidence: 3 per million/year.
- Usually sporadic.
- Female to male predominance: 1.4:1.
- Peak age: 30–60 years (mean age 45 years).
- Malignant behavior: 10 %.
- May be seen in patients with neurofibromatosis type 1.
- Best prognosis among functional and nonfunctional PNEN.

10.5.1.2 Clinical Presentation

- These tumors tend to manifest earlier and have a smaller size than other nonfunctional or functional PNEN.
- Vast majority measure between 0.5 and 2 cm.
- **Patients present with classic triad (Whipple's triad)**:
  - Low glucose level (40md/dl or less).
  - Symptoms and signs of hypoglycemia: dizziness or weakness, associated with fasting or exercise. Diplopia, blurred vision, confusion, and personality changes.
  - Symptoms are relieved by glucose.

Symptoms Related to Catecholamine Release (Less Frequent)

- Tachycardia
- Chest pain
- Palpitations
- Diaphoresis

10.5.1.3 Laboratory Evaluation

Biochemical Diagnosis

- Monitored 72 h fasting with serial measurements of blood glucose and insulin levels

Parameters

- Serum insulin levels of 10 μU/ml or more (normal <6 μU/ml)
- Glucose levels of less than 40 mg/dl
- C-peptide level exceeding 2.5 μ/ml (normal <6 μ/ml)
- Proinsulin levels greater than 25 % (or up to 90 %) that of immunoreactive insulin
- Screening for sulfonylurea negative

10.5.1.4 Imaging (Figs. 10.57–10.66)

- Tumor size: 90 % is <2 cm; 40 % is <1 cm
- Location: intrapancreatic, even distribution throughout the pancreatic head, body, and tail
- Usually solitary lesion
- Multiple in MEN-1 syndrome, 2–10 % of patients

Ultrasound: (US, EUS, and IOUS)

Findings

- Well-circumscribed, hypoechoic, hypervascular mass

Computed Tomography (CT)

Findings

- Small intrapancreatic or partially exophytic, well-circumscribed, hypervascular mass (arterial and venous phase)
- Rare: cystic changes or calcifications

Malignant Insulinoma

- Enlarged hypervascular nodes
- Hypervascular hepatic metastases

Magnetic Resonance (MR)

Findings

- **T1WI**: low signal intensity mass
- **T2WI**: hyperintense to normal pancreas
- **T1WI post gadolinium**: hyperintense to normal pancreas

Octreotide Scan

Finding

- Poor radiotracer uptake (few somatostatin receptors)

Practical Pearls

- Surgical exploration and intraoperative ultrasound are the gold standards for detecting pancreatic insulinomas.
- CT and MR imaging, with multiple reformatted planes (sagittal, coronal, and oblique), are very useful techniques for detecting small, exophytic, pedunculated, or perivascular insulinomas.
- Calcium stimulated angiography, portal venous sampling, and selective arterial secretagogue infusion are best used for insulinomas that are undetectable by all other imaging modalities.
- With transhepatic portal venous sampling (THPVS), small peripancreatic veins can be accessed and tested for insulin levels.

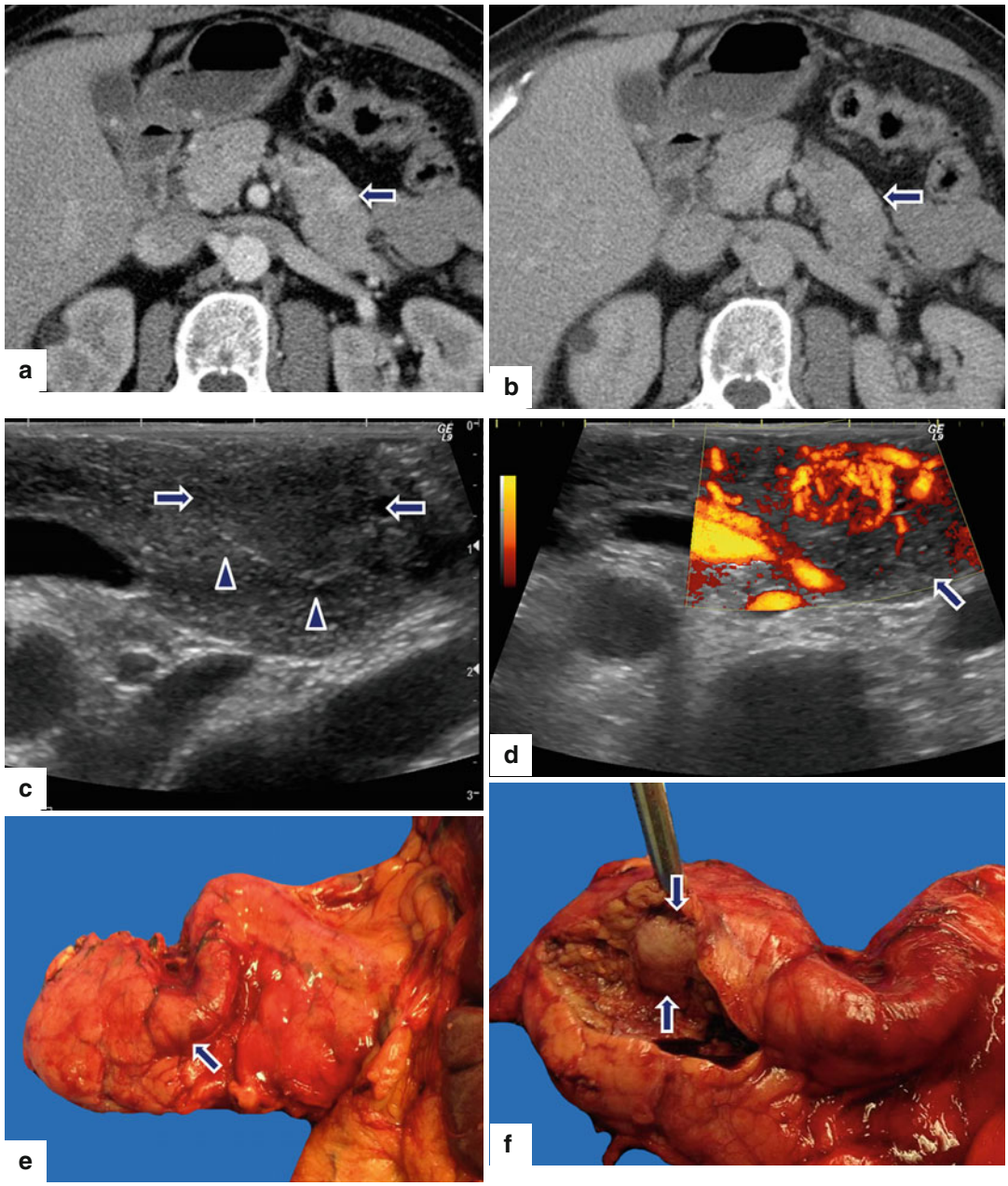

Fig. 10.57 Pancreatic insulinoma on CT and IOUS. A 71-year-old male with history of episodes of confusion and unresponsiveness while driving. Blood glucose of 38 mg/dl. Symptoms resolved upon administration of IV glucose. CECT axial (**a**, **b**) images demonstrate an 8 mm hypervascular mass in the body of the pancreas (*arrows*). IOUS gray scale (**c**) and power Doppler (**d**) images show a hypoechoic, hypervascular mass (*arrows*) abutting the pancreatic duct (*arrowheads*). Due to this last finding, a distal pancreatectomy and splenectomy was performed instead of a tumor enucleation. Photograph of the resected surgical specimen (**e**) shows the small firm mass (*arrow*). Photograph of the bivalved surgical specimen (**f**) demonstrates a round, yellow mass (*arrows*).

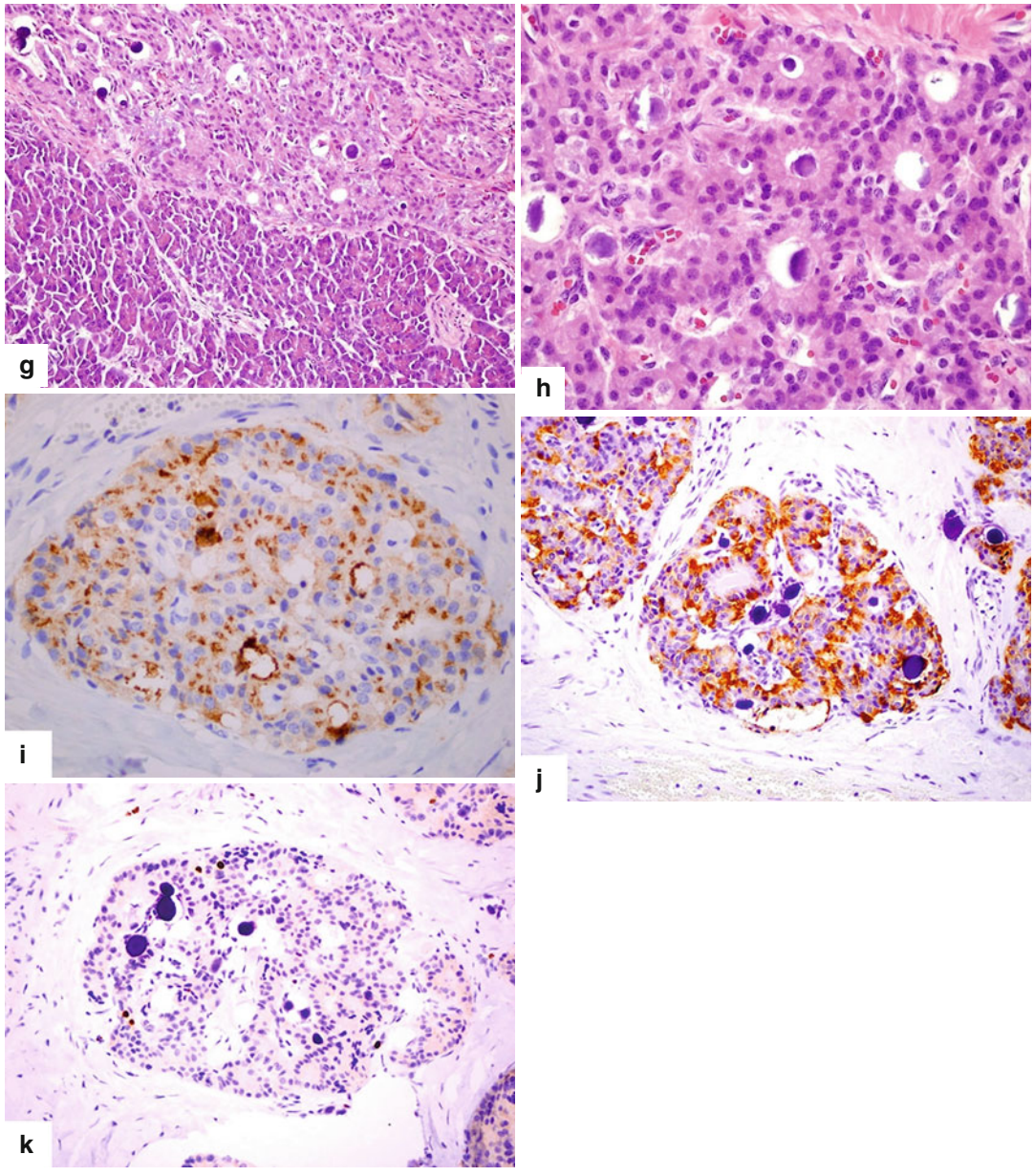

Fig. 10.57 (continued) Microscopic examination (**g**, **h**) revealed a well-differentiated neuroendocrine neoplasm, grade 1, with a pseudo-glandular arrangement and scattered psammomatous calcifications (H&E, 20×, 40×). Tumor cells were positive for chromogranin (**i**) and insulin (**j**). Ki-67 proliferative index was low (**k**) (Immunohistochemistry, 60x, 20x)

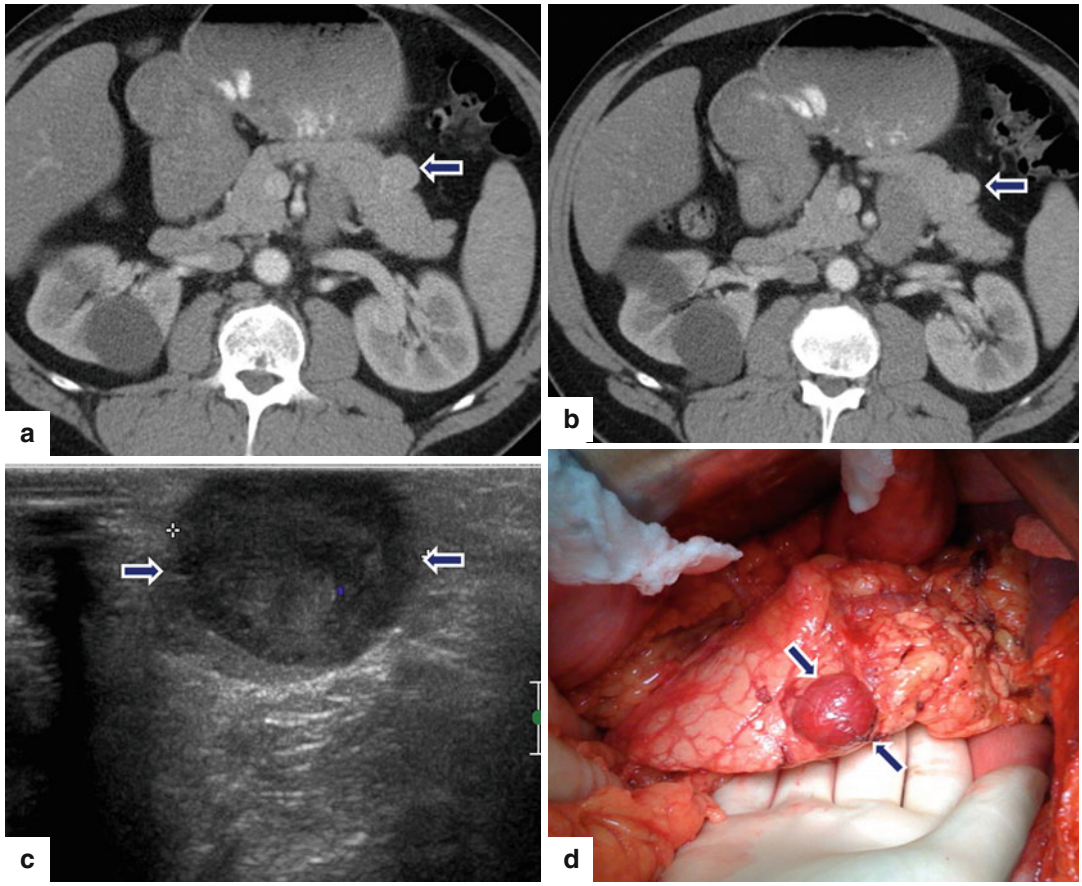

Fig. 10.58 Pancreatic insulinoma on CT and IOUS. A 50-year-old male with a 2-year history of recurrent hypoglycemia, with episodes of flushing, jitteriness, tremors, and lethargy resolved with eating. CECT axial (**a**, **b**) images demonstrate a partially exophytic, round, hypervascular, homogeneous mass in the pancreatic body (*arrows*). IOUS transverse (**c**) image shows a well-circumscribed hypoechoic mass. Intraoperative photograph (**d**) demonstrates a partially exophytic purple mass with smooth serosal surface (*arrows*)

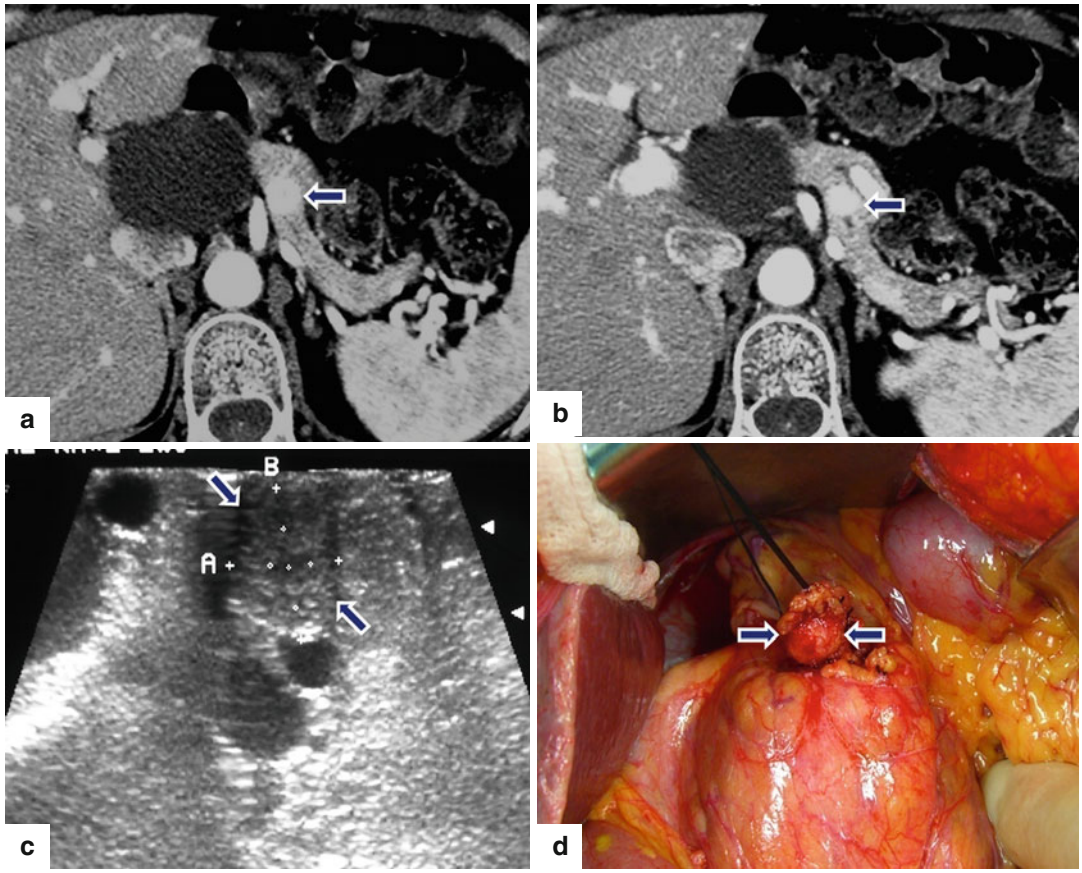

Fig. 10.59 Pancreatic insulinoma on CT and IOUS. A 66-year-old female with history of episodic syncope and memory loss. Laboratory workup revealed hypoglycemia with levels as low as 24 mg/dl. CECT axial (**a**, **b**) images display a small hypervascular mass in the pancreatic body (*arrows*) and a large cystic mass in segment one of the liver. IOUS transverse (**c**) image displays a hypoechoic mass (*arrows*). Intraoperative photograph (**d**) displays the tumor being enucleated from the pancreas (*arrows*)

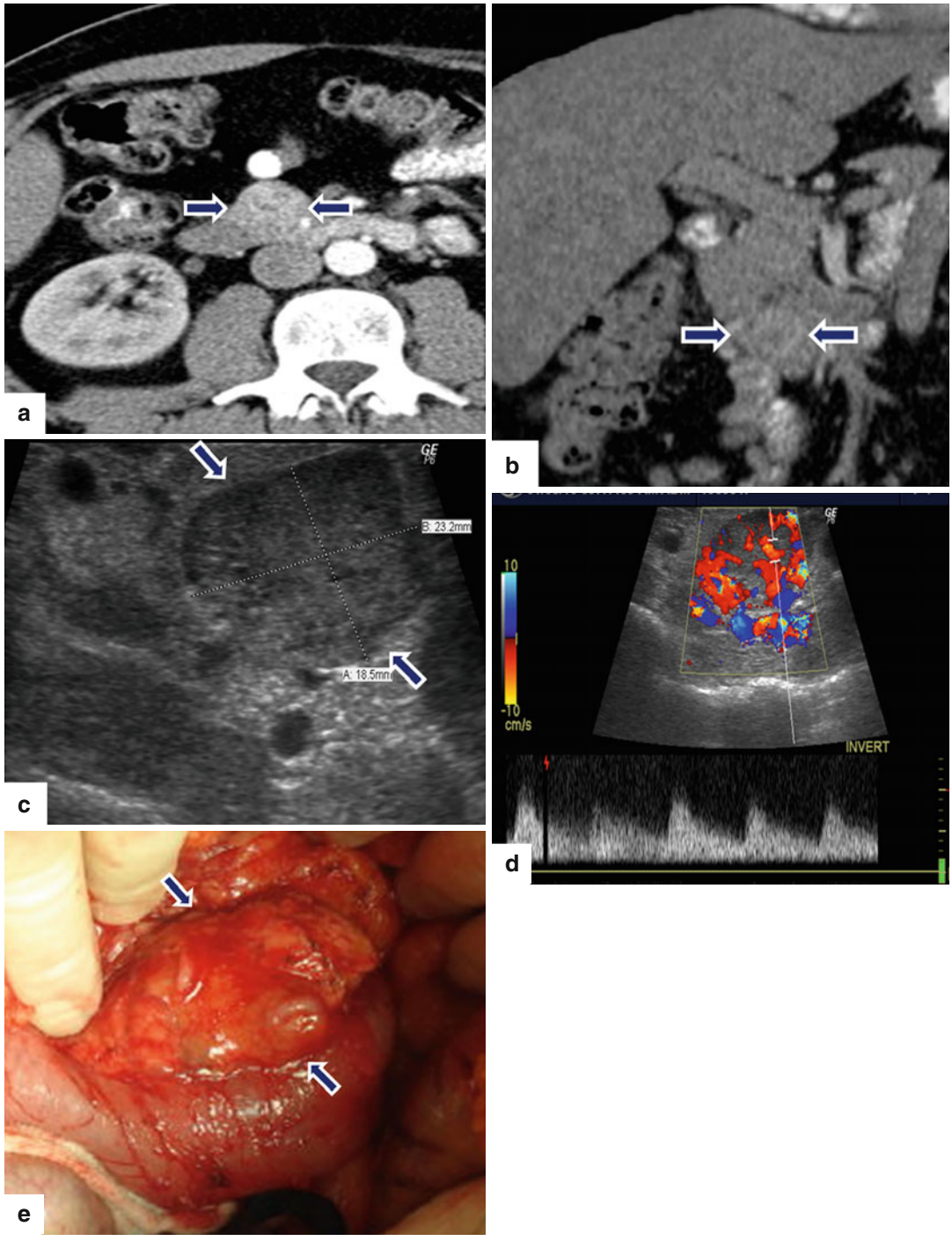

Fig. 10.60 Pancreatic insulinoma on CT and IOUS. A 49-year-old male with a 2-year history of subtle and recently more profound episodes of hypoglycemia. CECT axial (**a**) and coronal (**b**) images demonstrate a round, heterogeneous, vascular mass involving the pancreatic head (*arrows*). IOUS gray scale (**c**) and color Doppler (**d**) images demonstrate a well-circumscribed, 2 cm, hypoechoic, hypervascular mass (*arrows*). Intraoperative photograph (**e**) shows a small, hypoechoic, hypervascular, lobulated mass located in the head of the pancreas (*arrows*)

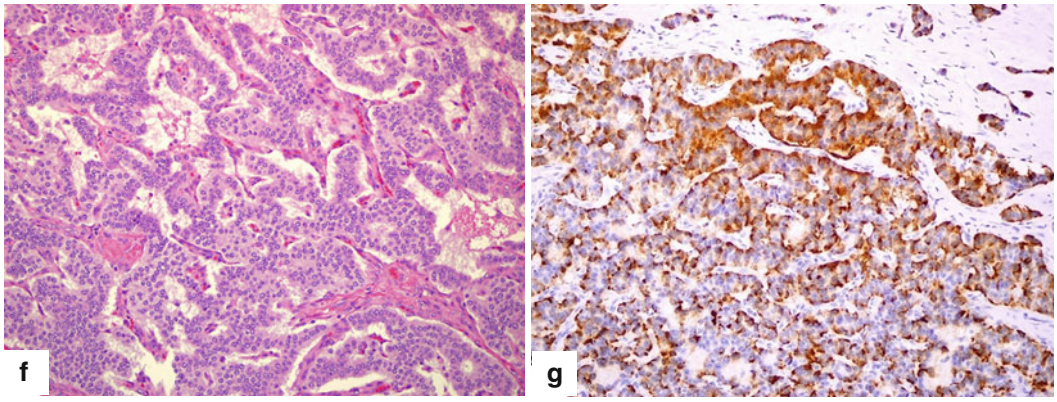

Fig. 10.60 (continued) Histologic section (**f**) shows the characteristic gyriform pattern seen in insulinomas, as well as the "salt-and-pepper" chromatin pattern (H&E, 20×). Tumor cells were positive for insulin immunostain (**g**) (immunohistochemistry, 20×)

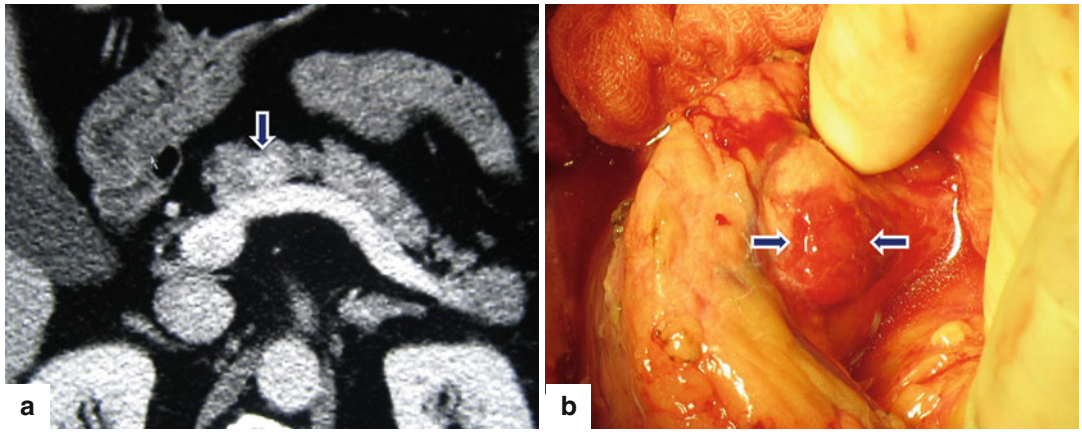

Fig. 10.61 Pancreatic insulinoma on CT. A 56-year-old male with history of episodes of dizziness. The patient became aware of increased hunger and weight gain. CECT axial (**a**) image demonstrates a 1 cm homogeneous, hypervascular mass in the body of the pancreas (*arrow*). Intraoperative photograph (**b**) demonstrates a circumscribed purple mass (*arrows*)

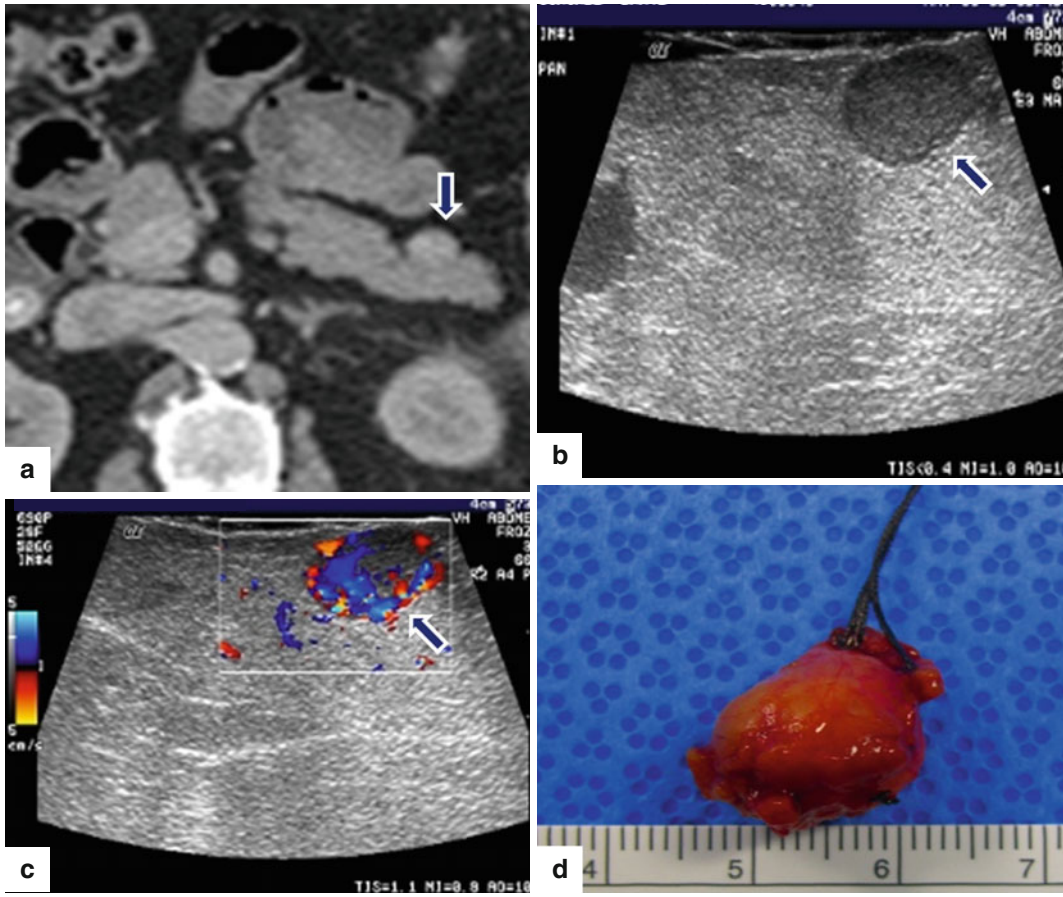

Fig. 10.62 Pancreatic insulinoma on CT. A 48-year-old male with history of episodes of mental confusion and weakness. CECT axial (**a**) image shows a partially exophytic, hypervascular mass in the pancreatic tail (*arrow*). IOUS gray scale and color Doppler transverse images (**b**, **c**) show a small hypoechoic, hypervascular mass (*arrows*). This mass was surgically excised. Photograph (**d**) shows the enucleated insulinoma

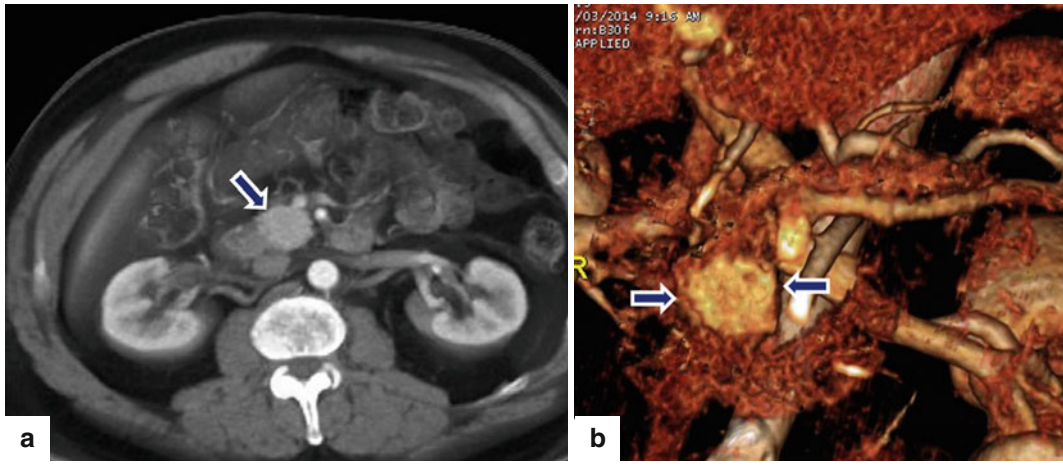

Fig. 10.63 Pancreatic insulinoma on CT. A 68-year-old male with history of episodes of diaphoresis, tachycardia, and altered mental status. CECT axial (**a**) and coronal (**b**) volume-rendered images show a round, hypervascular, homogeneous pancreatic mass in the pancreatic head (*arrows*)

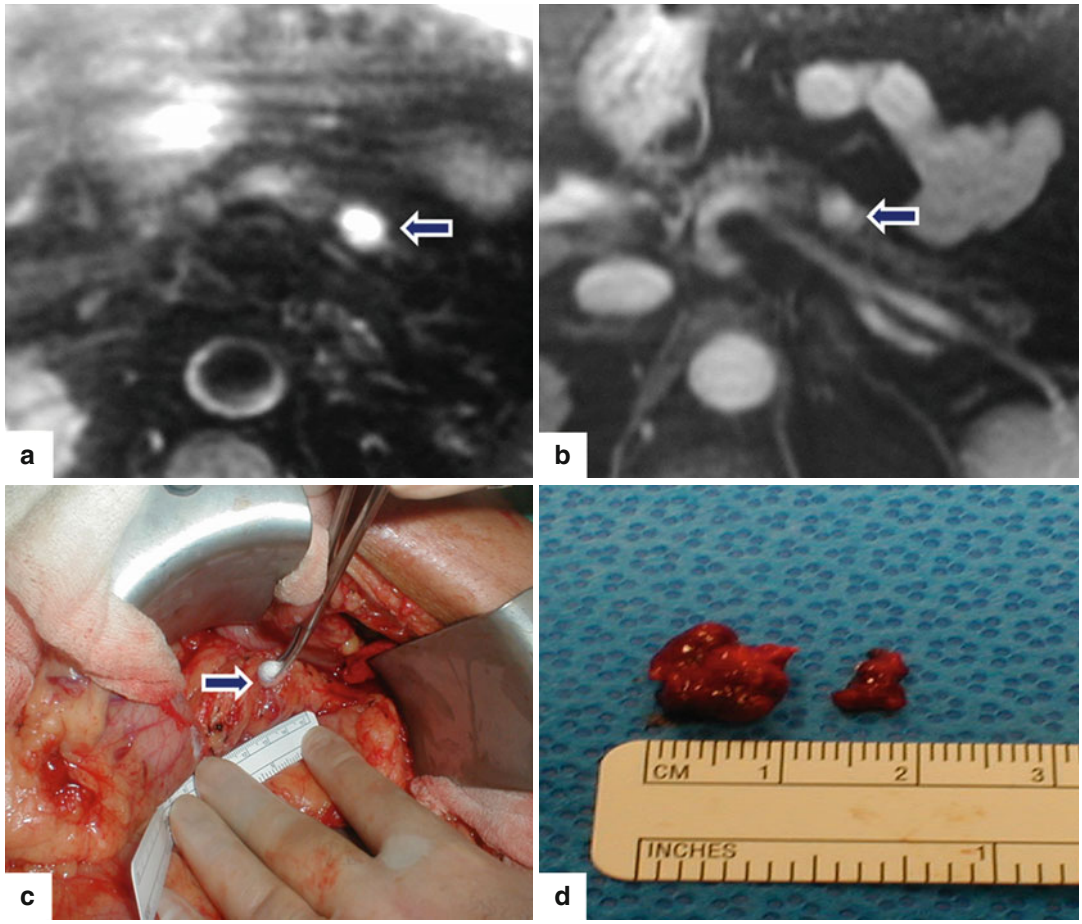

Fig. 10.64 Pancreatic insulinoma on MR. A 52-year-old female with history of multiple episodes of hypoglycemia. Fat-suppressed T2-weighted axial (**a**) image reveals a small mass with high signal intensity in the pancreatic body (*arrow*). Contrast-enhanced fat-suppressed gradient echo T1-weighted axial (**b**) image reveals intense contrast enhancement by the mass (*arrow*). Intraoperative photograph (**c**) shows a small, round mass being resected (*arrow*). Small gross specimen is depicted in picture (**d**)

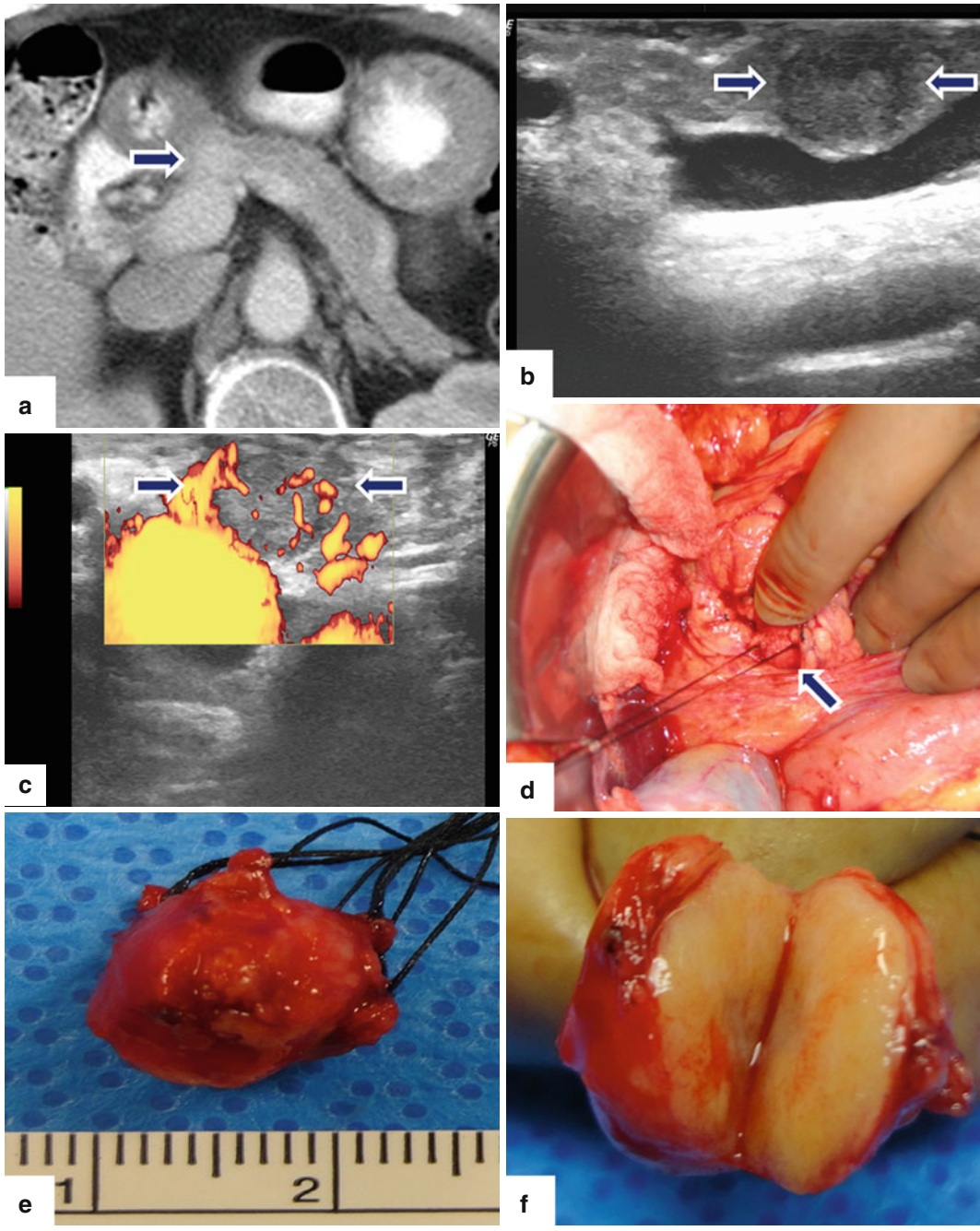

Fig. 10.65 Pancreatic insulinoma difficult to identify on CT. A 79-year-old male with history of daily episodes of feeling unwell, tremors, fatigue, disorientation, and 40 lb weight gain. Laboratory workup reveals 78.4 pg/ml proinsulin, 8.76 μU/ml fasting insulin, 41 mg/dl fasting glucose, and 2.64 ng/ml fasting C-peptide (normal 1.10–4.4 ng/ml). CECT (**a**) image shows a questionable, small, hypervascular mass in the pancreatic body (*arrow*). IOUS gray scale (**b**) and color power Doppler (**c**) confirmed the presence of a well-defined hypoechoic, hypervascular mass in the proximal pancreatic body (*arrows*). Intraoperative photograph (**d**) displays the tumor being enucleated from the pancreas (*arrows*). Photograph shows the small enucleated tumor (**e**). Photograph of the bivalved specimen demonstrates a well-defined, round, white-tan, fleshy mass (**f**)

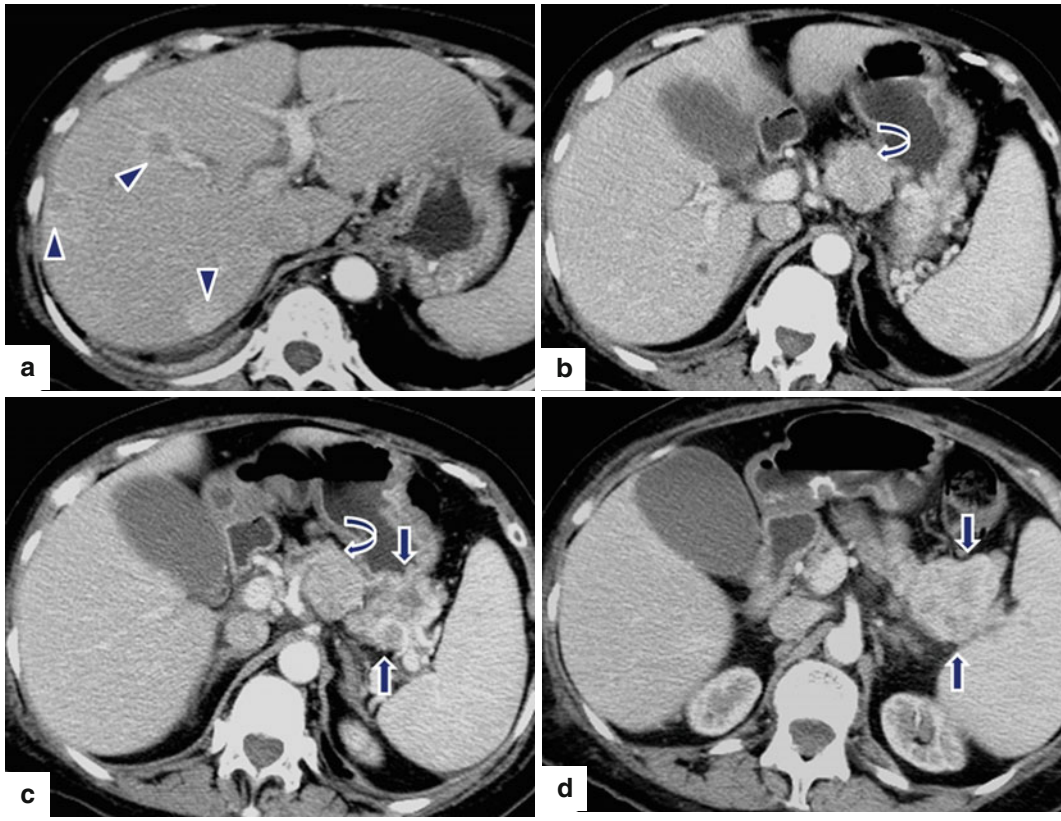

Fig. 10.66 Malignant insulinoma on CT. A 67-year-old female patient with history of uncontrollable hypoglycemia. CECT axial (**a–d**) images demonstrate a lobulated, heterogeneous, hypervascular mass involving the tail of the pancreas (*arrows*) associated with large periceliac nodes (*curved arrows*) and multiple hyperdense and target-like hepatic metastases (*arrowheads*)

10.5.2 Gastrinoma (Zollinger-Ellison Syndrome)

10.5.2.1 Epidemiology

- Second most common functional PNEN
- Arise from pancreatic islets stem cells
- Associated with excessive amounts of gastrin which results in an overproduction of gastric acid
- Peak of incidence: fifth decade of life
- Male: 60 %
- Most are sporadic
- 20–25 % associated with MEN-1 syndrome
- Size: average diameter of pancreatic gastrinomas: 1–4 cm
- Malignant behavior: 60–90 %

10.5.2.2 Clinical Presentation

Related to elevation of gastrin levels: hypersecretion of gastric acid

- **Intractable epigastric pain due to**:
  - Atypical gastroduodenal ulcer disease is generally the hallmark to diagnose this condition
  - Solitary ulcer: 90 % of cases
  - Peptic ulcers in atypical location: 25 % (distal duodenum, proximal jejunum)
- **Diarrhea due to**:
  - Malabsorption secondary to breakdown of lipase from excessive gastric acid
- **Dysphagia due to**:
  - Esophagitis

Zollinger-Ellison Syndrome (Described in 1955)

- Atypical peptic ulceration
- Gastric hypersecretion/acidity
- Non-insulin-producing islet cell tumor of the pancreas

Practical Pearls

- Diarrhea is generally the first symptom to appear; frequently lasting several years before diagnosis becomes recognized.
- Due to the overflow of gastropancreatic secretions, diarrhea is generally watery.
- Zollinger-Ellison syndrome is responsible for approximately 0.1 % of peptic ulcer disease.

Clinical Situations Requiring Further Investigation for Gastrinoma

- Multiple GI ulcers or ulcers in atypical locations
- Recurrent peptic ulcers after appropriate medical or surgical therapy
- Failure of peptic ulcer to heal on appropriate medical therapy
- Peptic ulcer or GERD with diarrhea
- Peptic ulcer in absence of *H. pylori*
- Persistent diarrhea without clear etiology
- Family history of peptic ulcer disease
- Peptic ulcer disease (PUD) resulting in complication (bleeding, perforation, obstruction)
- Personal or family history of MEN-1 tumors or endocrinopathies
- Prominent gastric rugae with PUD

10.5.2.3 Laboratory Evaluation

- **Fasting serum gastrin level**: elevation of serum gastrin levels over 1,000 pg/ml (normal level <100 pg/ml); 30 % of patients
- Most patients present with gastrin levels between 200 and 1,000 pg/ml
- A secretin stimulation test is recommended for patients with normal or mildly elevated serum gastrin levels

10.5.2.4 Imaging (Figs. 10.67–10.75)

- Most gastrinomas are found in the gastrinoma triangle, limited by:
  - Superiorly: junction of the cystic duct and common bile duct
  - Inferiorly: second and third portions of the duodenum
  - Medially: neck and body of the pancreas
- 55 % of gastrinomas arise in the duodenum
- Other sites: pancreas, peripancreatic nodes

Practical Pearls

- Although most gastrinomas are located in the gastrinoma triangle, 10 % occur in very unusual locations, such as the kidney (Fig. 10.73), liver, ovary, mesentery, lungs, or heart.
- In a small percentage of patients, the gastrinomas may be found only in peripancreatic lymph nodes harboring the primary tumor.

Ultrasound (US, EUS, IOUS)

EUS is the best imaging modality for identifying gastrinomas that arise in the duodenal wall and peripancreatic node.

Findings

- Well-circumscribed, hypoechoic, hypervascular mass

Computed Tomography (CT)

Findings

- Solid, well-circumscribed, hypervascular mass
- Central necrosis and peripheral enhancement may be identified

Magnetic Resonance (MR)

Findings

- **T1WI**: low signal intensity mass
- **T2WI**: hyperintense to normal pancreas
- **T1WI post gadolinium**: hyperintense to normal pancreas

Octreotide Scan

Finding

- Uptake of the radiotracer by the tumors and metastases (high concentration of somatostatin receptors)

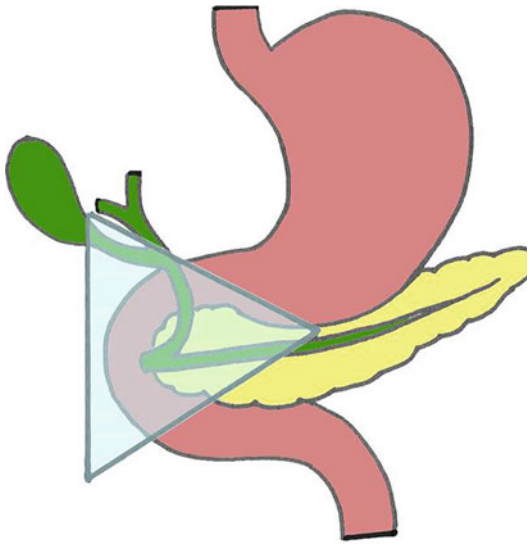

Fig. 10.67 Gastrinoma triangle diagram

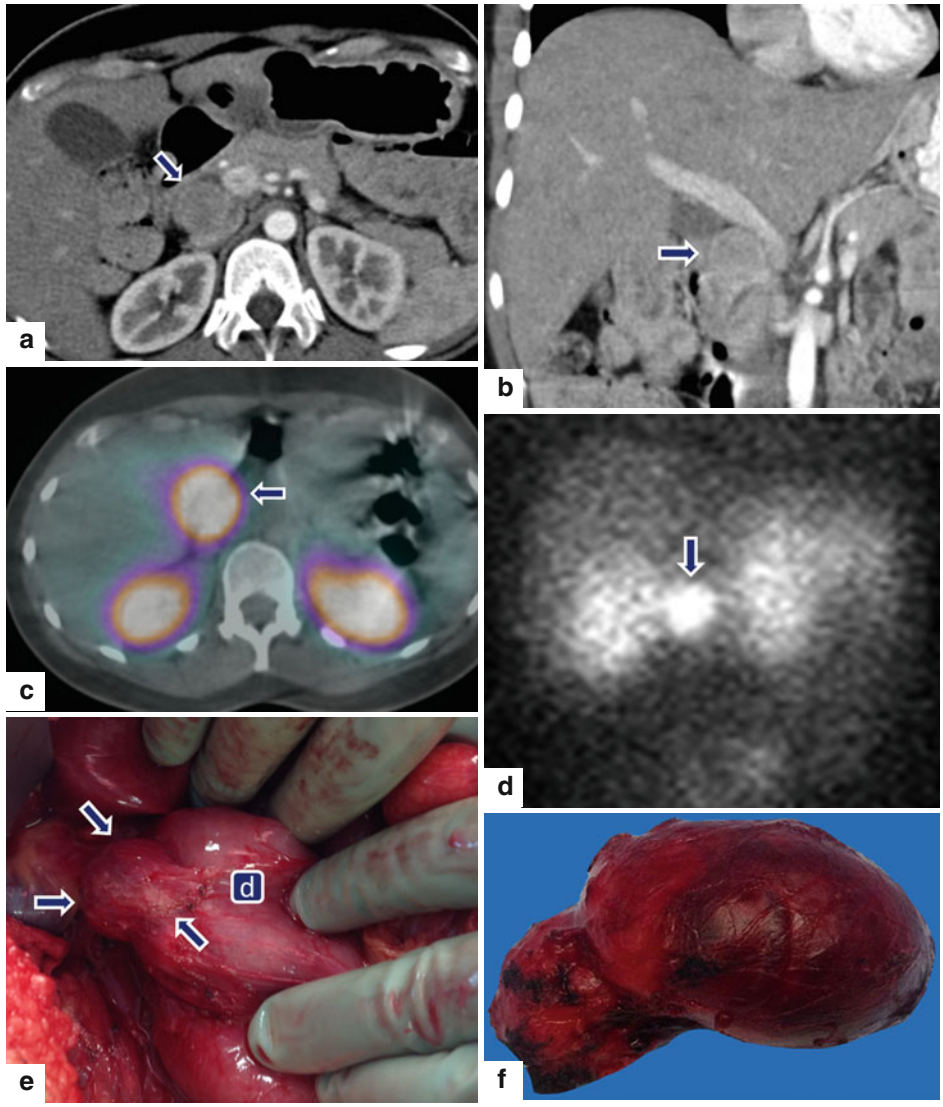

Fig. 10.68 Gastrinoma on CT and octreotide scan. A 36-year-old female with history of chronic daily diarrhea for 2 years. Laboratory results revealed a serum gastrin of 800 pg/ml and chromogranin of 118 ng/ml. CECT axial (**a**) and coronal (**b**) images show a round, well-defined, heterogeneous mass (*arrows*) posterior to the portal vein, anterior to the inferior vena cava, and abutting the first and second portions of the duodenum. Octreotide scan axial (**c**) and coronal (**d**) images show a focal area of high-intensity activity close to the pancreas (*arrows*). Intraoperative photograph (**e**) shows a reddish mass with smooth serosal surface (*arrows*) abutting the duodenum (*boxed d*). This mass was resected (**f**) and a highly selective vagotomy was performed.

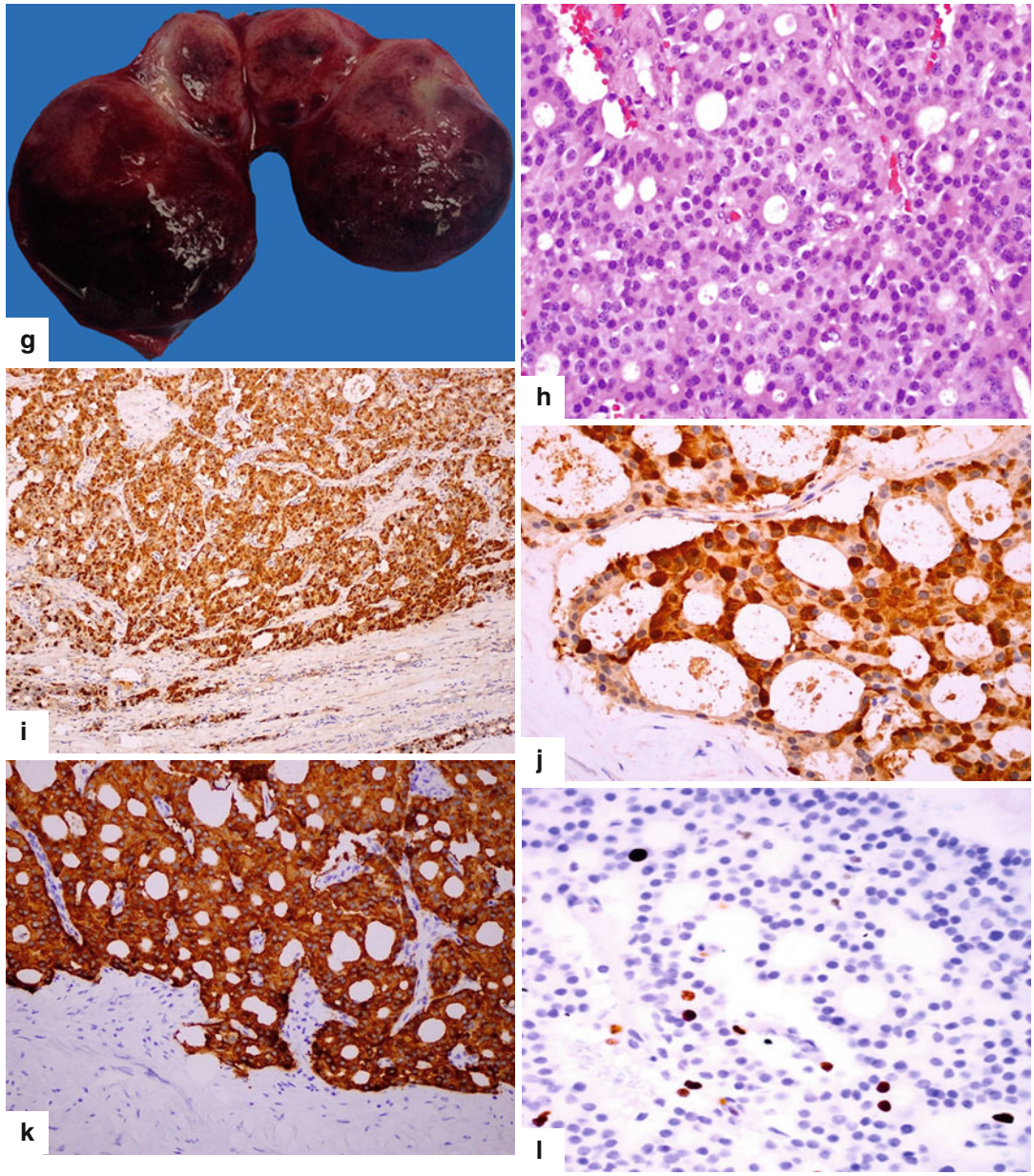

Fig. 10.68 (continued) Photograph of the bivalved specimen (**g**) shows a lobulated, fleshy mass with hemorrhagic areas. Histological section (**h**) shows a neoplasm with small uniform cells with pseudoacinar pattern (H&E, 40×). Immunohistochemical stains demonstrate that the cells are positive for synaptophysin (**i**), chromogranin (**j**), and gastrin (**k**), and show a Ki67 proliferative index of about 4% (**l**), consistent with a grade 2 PNEN (Immunostains, 10×, 60×, 40×)

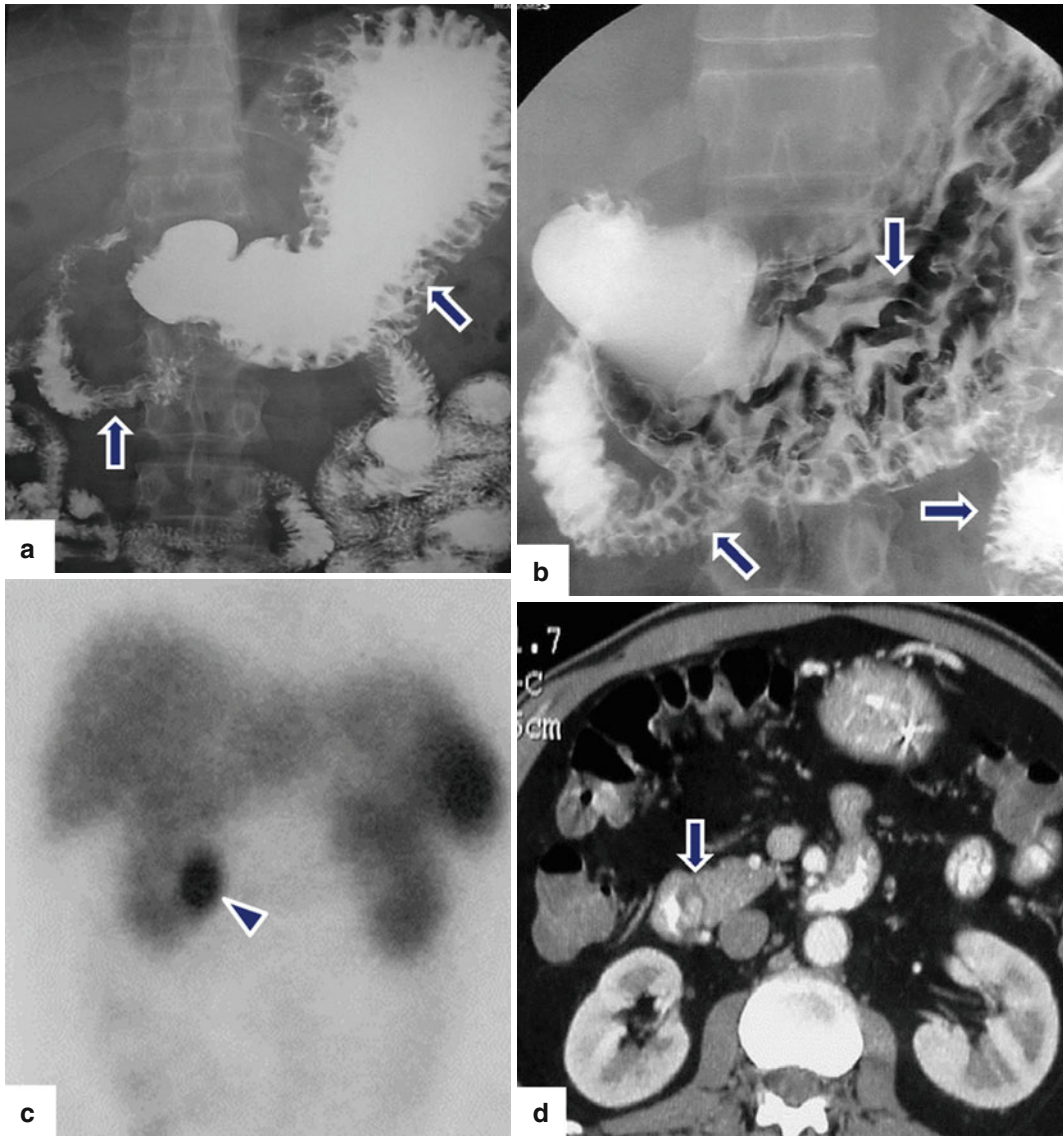

Fig. 10.69 Gastrinoma on multimodality imaging. A 40-year-old male with history of chronic diarrhea and epigastric pain. Laboratory results show a serum gastrin of 920 pg/ml. UGI films (**a**, **b**) demonstrate diffuse thickening of the gastric, duodenal, and proximal jejunum folds (*arrows*). Octreotide scan (**c**) demonstrates a focal area of increased activity around the pancreatic head (*arrowhead*). CECT axial (**d**) image demonstrates a well-circumscribed, hypervascular intramural mass in the second portion of the duodenum (*arrows*).

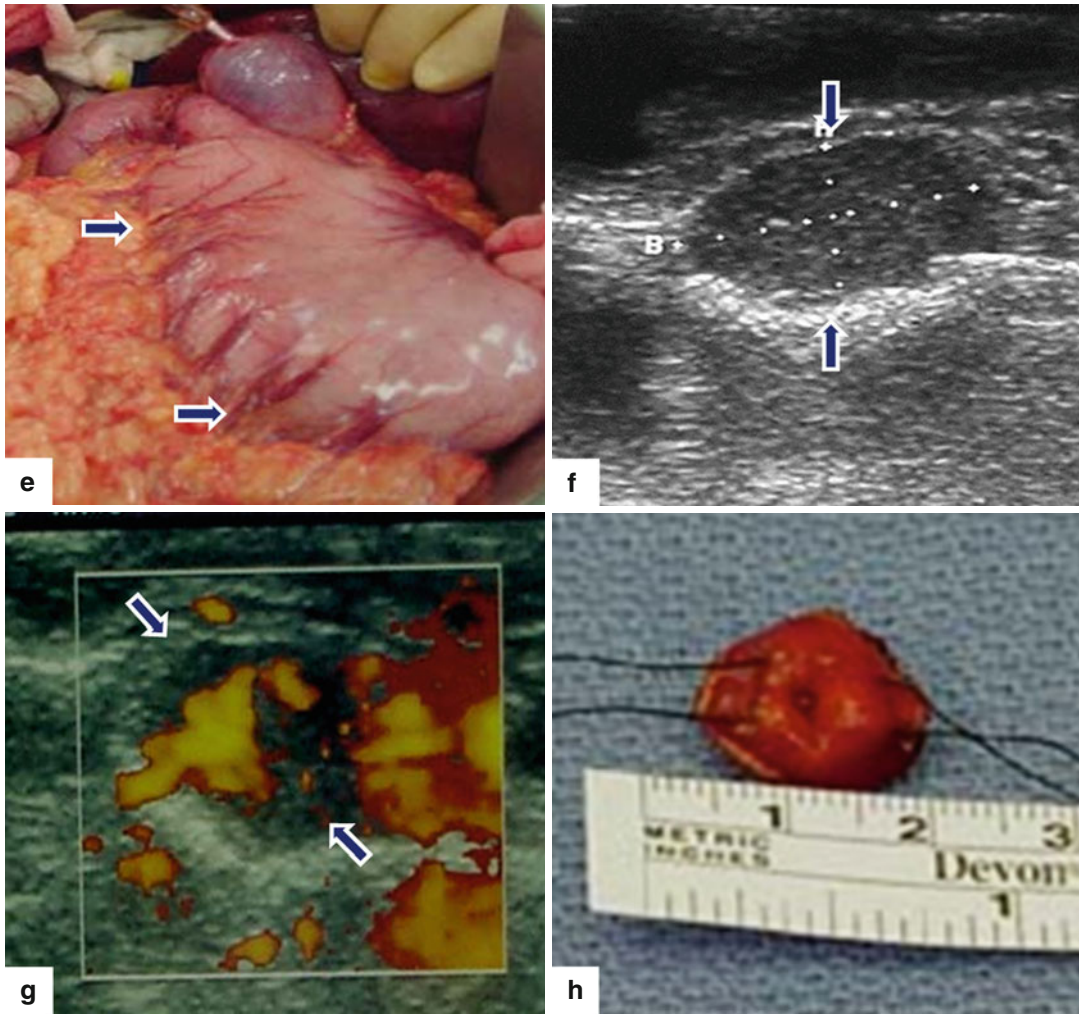

Fig. 10.69 (continued) Intraoperative photograph (**e**) confirms the presence of gastric fold thickening (*arrows*). IOUS gray scale (**f**) and power Doppler (**g**) images demonstrate an intramural hypoechoic, hypervascular mass with smooth margins in the second portion of the duodenum (*arrows*). This mass was surgically enucleated. Photograph (**h**) of the enucleated mass

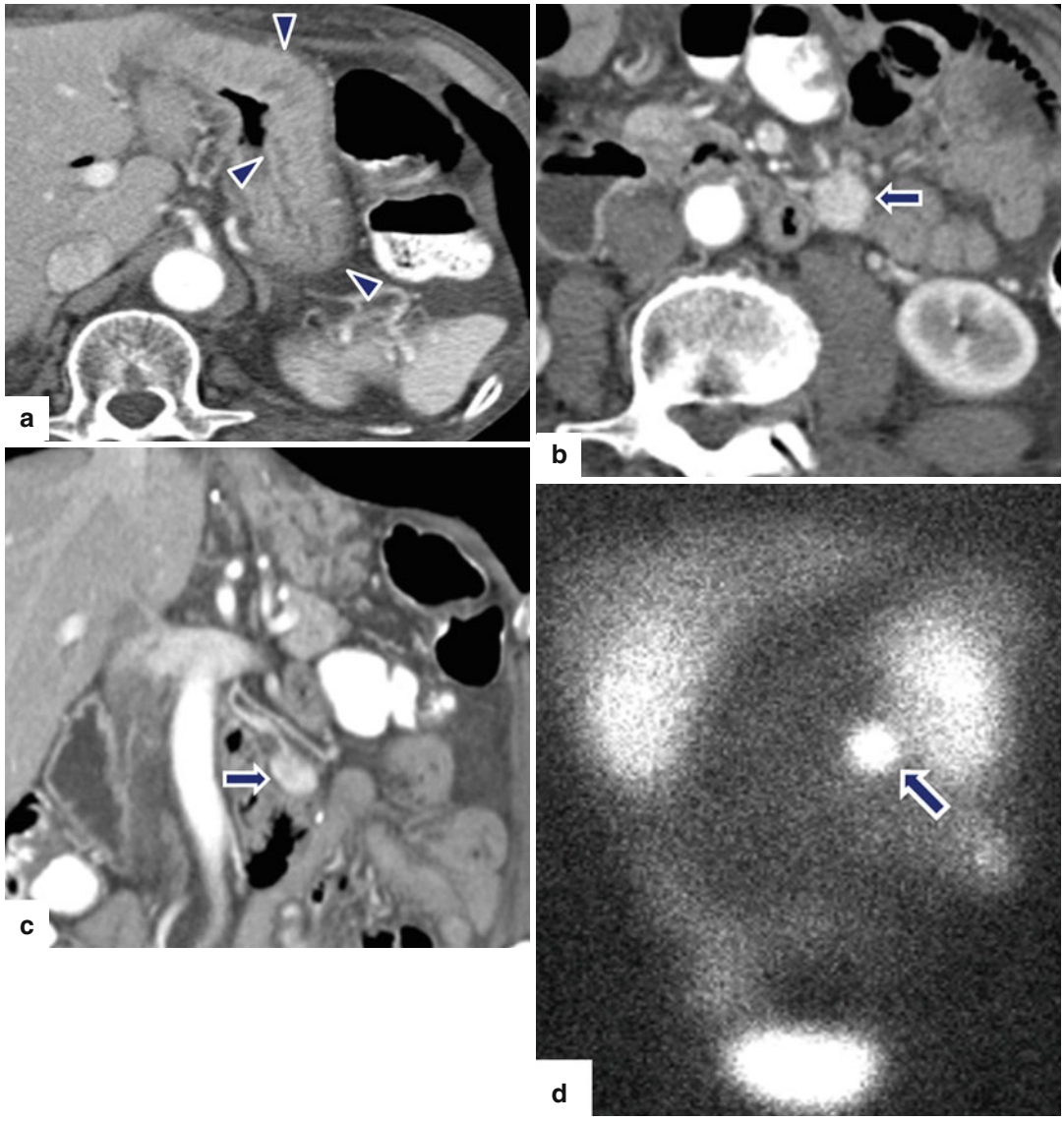

Fig. 10.70 Gastrinoma associated with multiple endocrine neoplasia type 1 (MEN-1) on multimodality imaging. A 70-year-old male with history of Zollinger-Ellison syndrome, hyperprolactinemia, and hyperparathyroidism. CECT axial (**a**, **b**) and coronal (**c**) images reveal an ovoid, left retroperitoneal infrapancreatic hypervascular mass (**b**, **c**) (*arrows*). Note the associated gastric fold thickening (**a**) (*arrowheads*). Octreotide SPECT (**d**) reveals avid uptake of radiotracer by the mass (*arrow*)

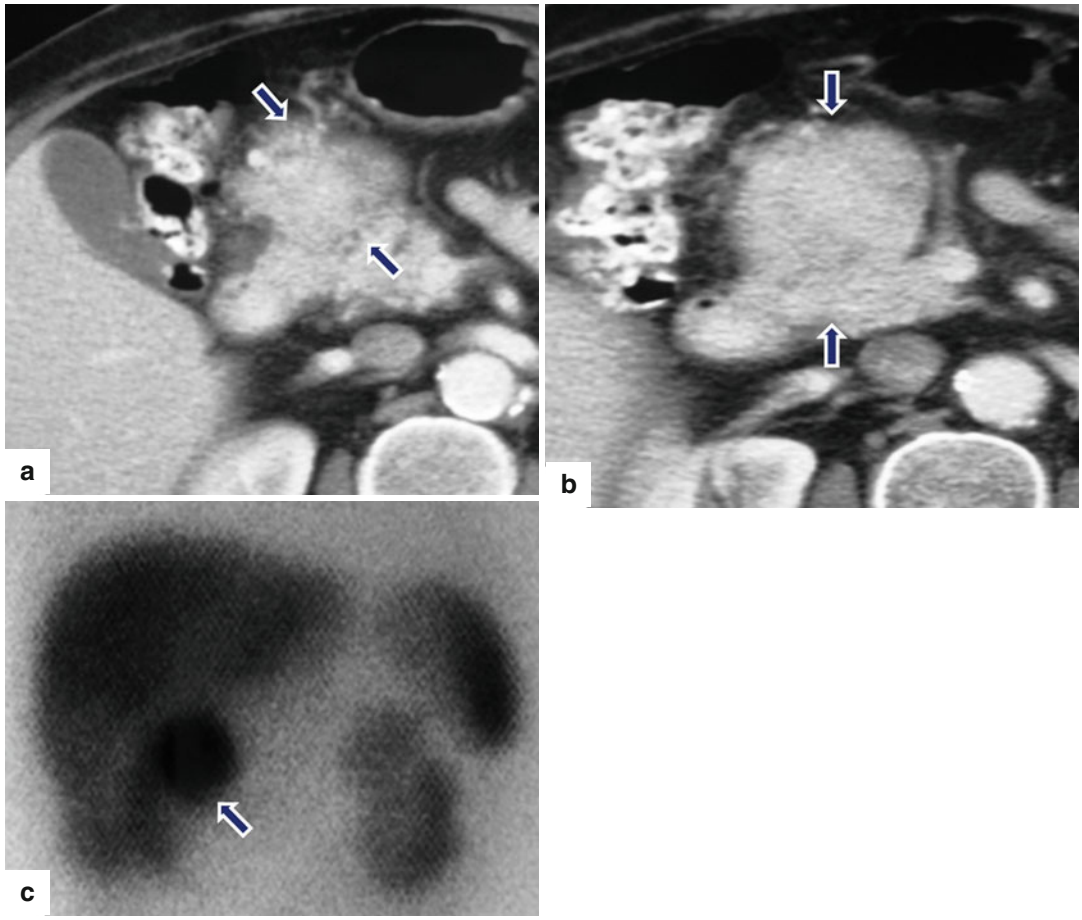

Fig. 10.71 Gastrinoma on multimodality imaging. A 55-year-old female with history of Zollinger-Ellison syndrome. CECT axial (**a**, **b**) images display a large exophytic, heterogeneous, hypervascular mass difficult to separate from the pancreatic head and duodenum (*arrows*). Octreotide scan (**c**) displays intense radiotracer activity within this tumor (*arrow*)

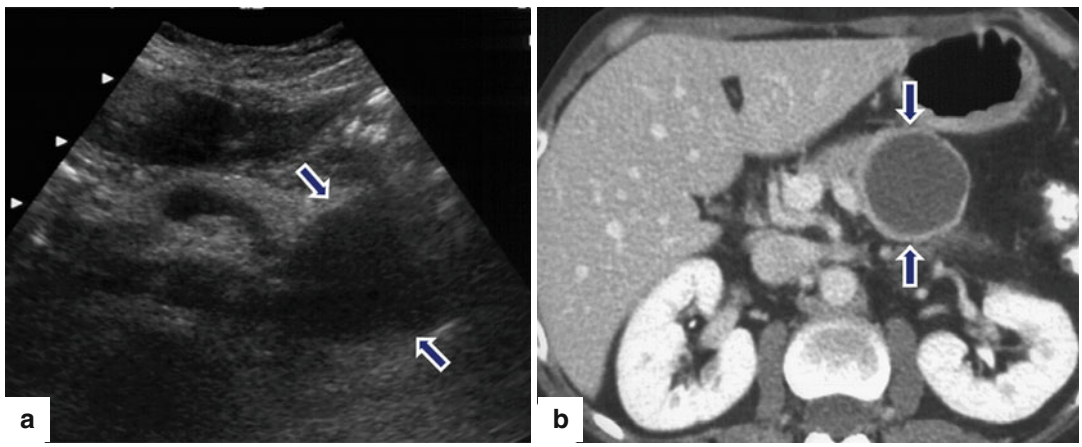

Fig. 10.72 Cystic gastrinoma on multimodality imaging. A 47-year-old female with history of Zollinger-Ellison syndrome. Ultrasound transverse (**a**) image shows a cystic mass with thick walls involving the pancreatic body (*arrows*). CECT axial (**b**) image confirms the presence of a cystic mass with a thick hypervascular wall (*arrows*). Final pathology: cystic gastrinoma (Courtesy of Pablo Clickman, MD)

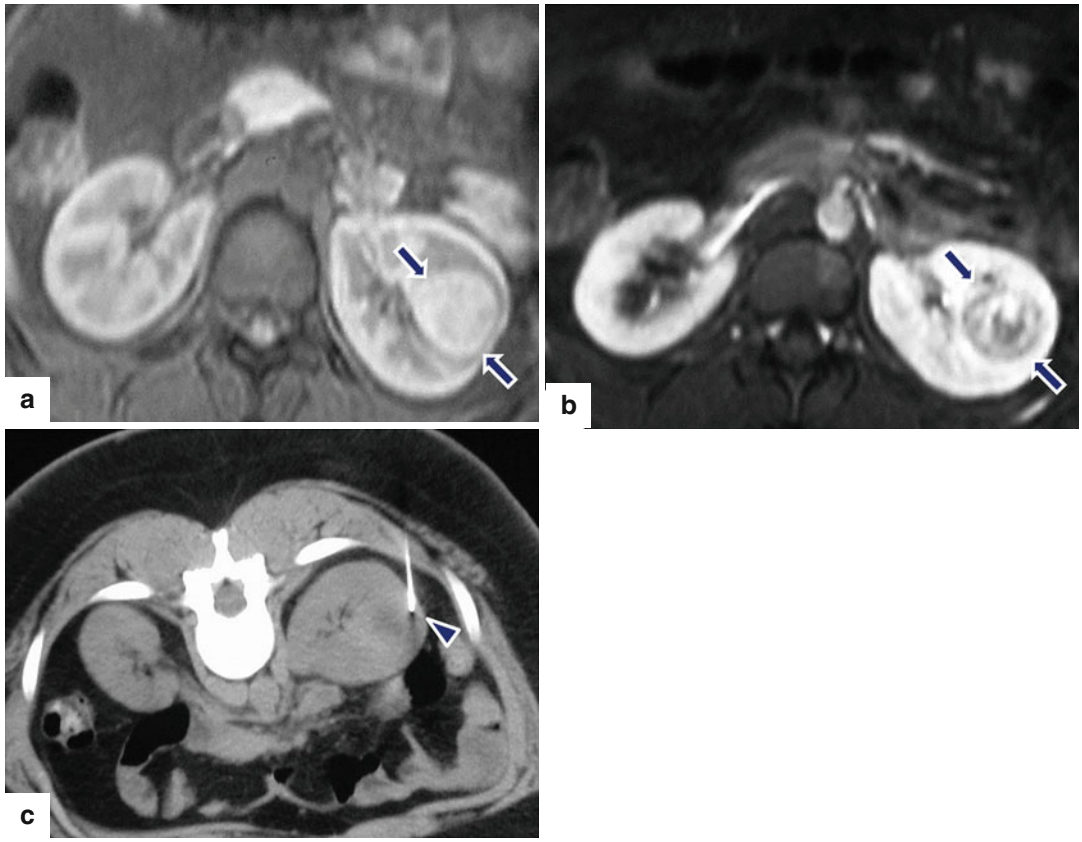

Fig. 10.73 Gastrinoma in unusual location on MR. A 19-year-old male with duodenal ulcers refractory to treatment and elevated serum gastrin levels. EUS of the pancreas and peripancreatic areas were negative. Fat-suppressed T2-weighted (**a**) image shows a round, hyperintense mass in the left kidney (*arrows*). Contrast-enhanced fat-suppressed gradient echo T1-weighted axial (**b**) image shows a complex, hypervascular mass in the left kidney (*arrows*). This lesion was biopsied percutaneously with CT guidance (**c**) (*arrowhead*). Biopsy results revealed a neuroendocrine tumor. Patient underwent a left nephrectomy. Final pathology: renal gastrinoma

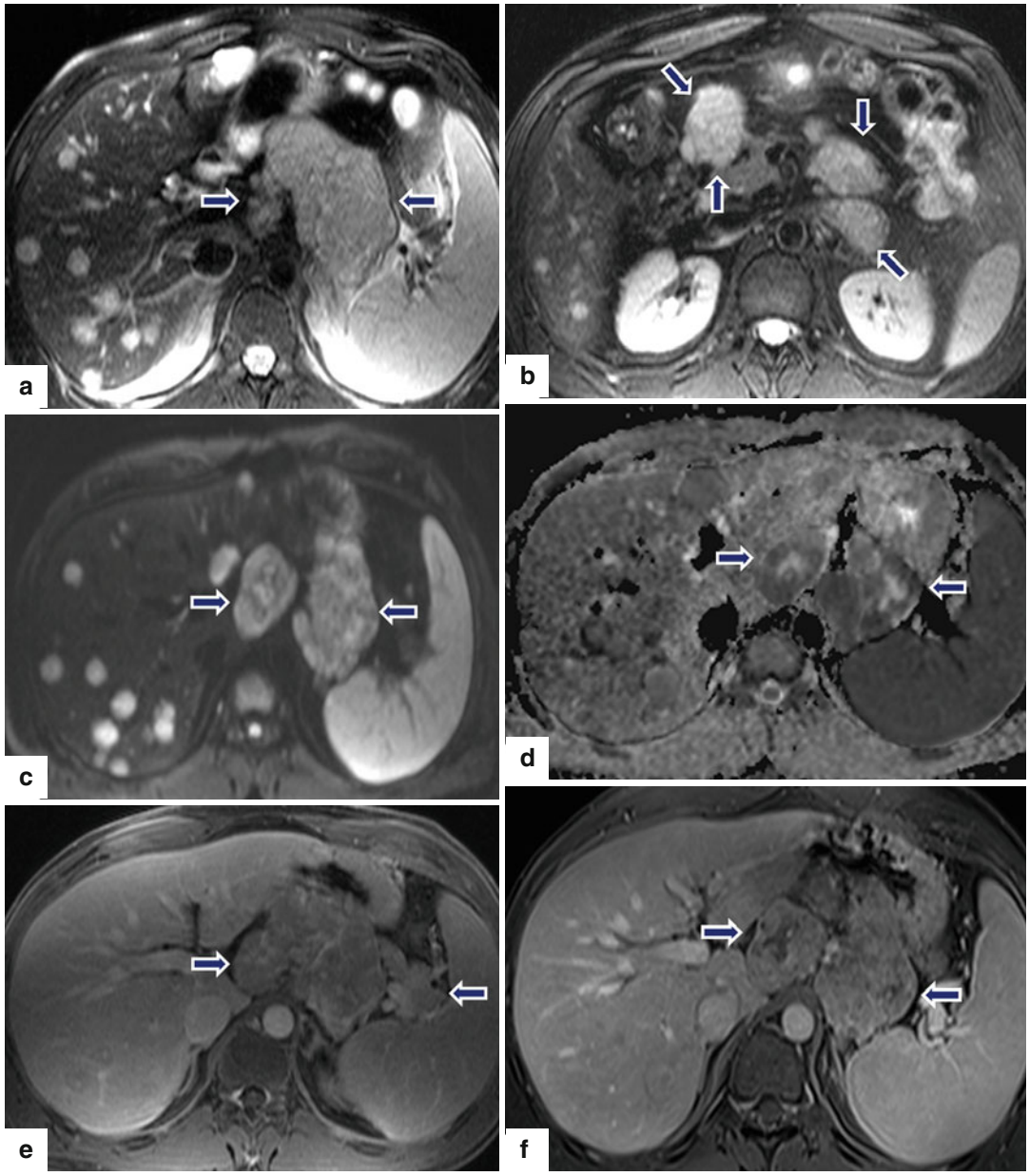

Fig. 10.74 Metastatic gastrinoma on imaging. A 24-year-old male with history of Zollinger-Ellison syndrome. Fat-suppressed T2-weighted axial (**a**, **b**) images show multiple large peripancreatic and right-sided mesenteric masses of intermediate signal intensity (*arrows*) and multiple hepatic lesions of high signal intensity. On diffusion axial (**c**) image, the liver metastases and peripancreatic nodes appear more conspicuous (*arrows*). Note the restriction of these masses on the ADC map (**d**).

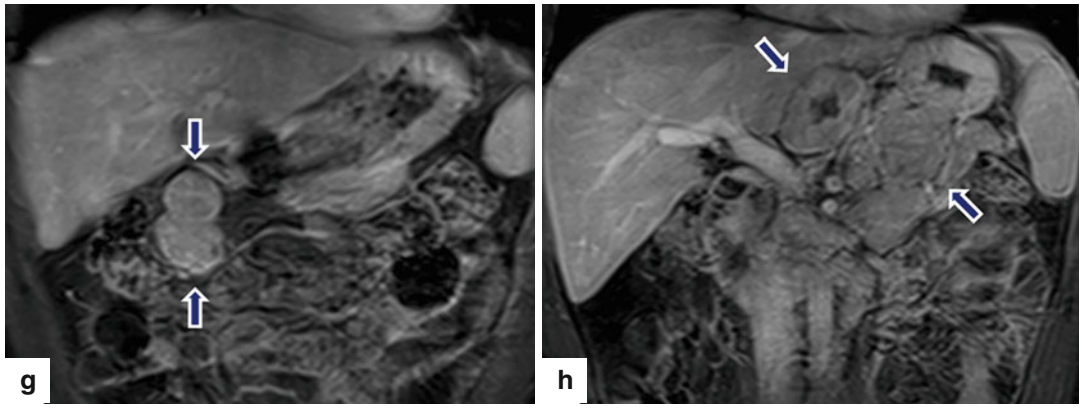

Fig. 10.74 (continued) Contrast-enhanced fat-suppressed gradient echo T1-weighted axial (**e**, **f**) and coronal (**g**, **h**) images show heterogeneous enhancement of the peripancreatic nodes (**e**–**h**) (*arrows*). Note the poor visualization of the hepatic metastases in this phase

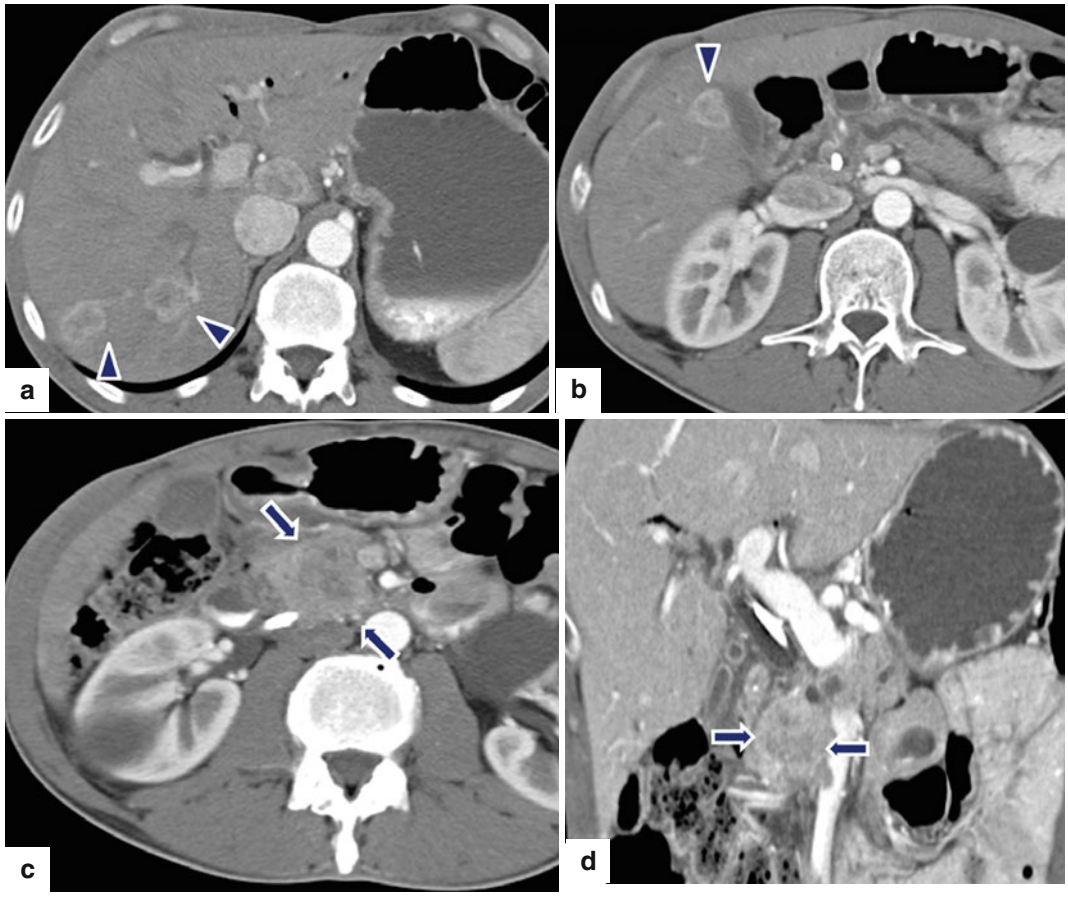

Fig. 10.75 Metastatic gastrinoma on imaging. A 54-year-old male with history of painless jaundice, chronic diarrhea, and ulcerogenic syndrome. Laboratory workup showed an elevated serum gastrin level. CECT axial (**a–c**) and coronal (**d**) images reveal multiple heterogeneous, hepatic metastases in the right lobe of the liver (*arrowheads*) associated with a heterogeneous mass in the pancreatic head (*arrows*). Note the obstruction of the pancreatic duct distal to this mass (**b**) and the presence of a biliary stent decompressing the biliary system (**b**–**d**).

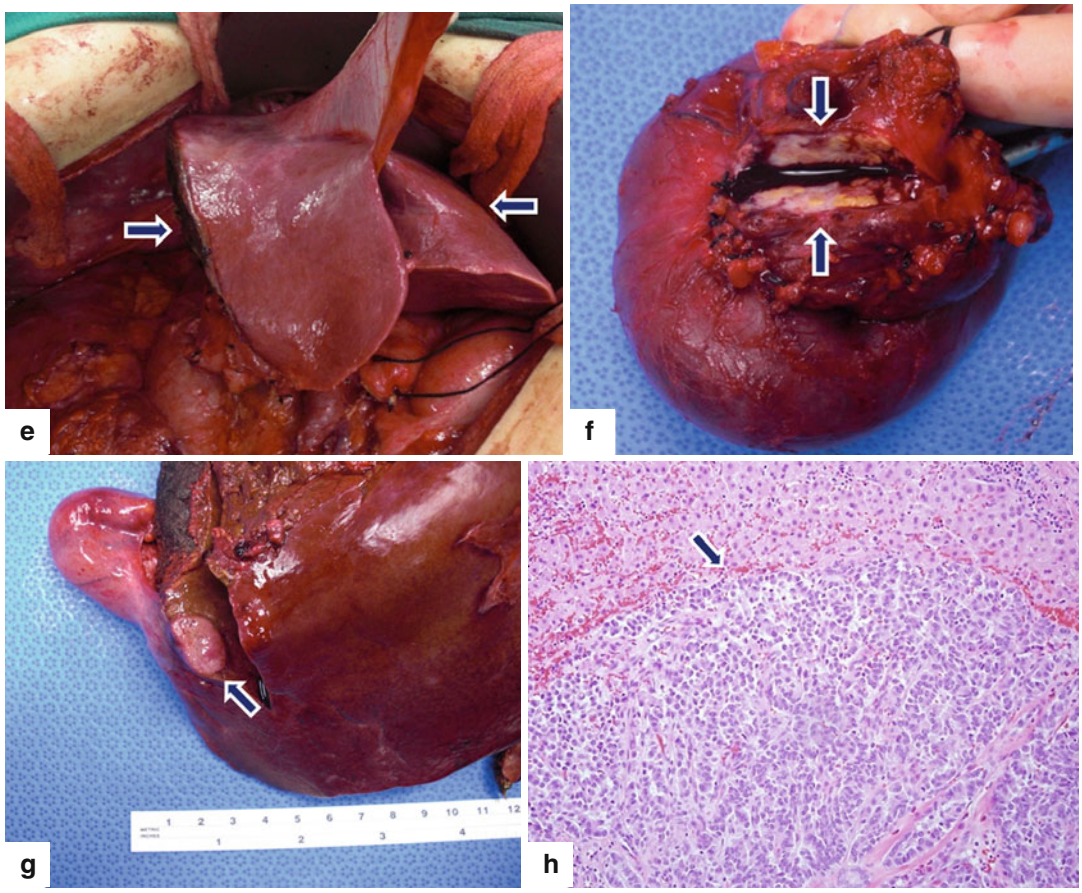

Fig. 10.75 (continued) Patient underwent a pyloric-sparing pancreaticoduodenectomy and a right hepatectomy. Intraoperative photograph (**e**) shows the remaining liver after partial hepatectomy (*arrows*). Photograph of the bivalved surgical specimen (**f**) reveals a firm, white pancreatic mass with hemorrhage (*arrows*). Photograph of the resected liver (**g**) reveals a small, round, well-defined liver mass (*arrow*). Histological section (**h**) demonstrates a well-differentiated PNEN invading the congested liver parenchyma (*arrow*) (H&E, 20×)

10.5.3 Glucagonoma

10.5.3.1 Epidemiology

- Third most common functioning PNEN
- Arise from pancreatic alpha (α) cells of the pancreatic islets
- These tumors produce glucagon. Glucagon counteracts the effects of insulin on glucose metabolism resulting in glucose intolerance
- Incidence: 1 in 20 million people per year
- Age: 40–60 years of age
- Equal gender distribution
- Usually sporadic
- Most are malignant (50 %)

10.5.3.2 Clinical Symptoms

- **Glucagonoma syndrome is referred to as the 4D syndrome** (**dermatitis**, **diabetes**, **deep vein thrombosis**, **and depression**).
  - **Dermatitis** (necrolytic migratory erythema) in 2/3 of the patients, painful pruritic plaques that start in the abdomen and groin and spread to the trunk and extremities (pathognomonic sign)
  - **Diabetes** present in most of the patients (mild or severe)
  - **Deep vein thrombosis** (lower extremities and subsequent pulmonary embolism)
  - **Depression**

Other symptoms: diarrhea, glossitis, weight loss, and various neurologic and psychiatric symptoms.

Practical Pearl

- Skin lesions are indirectly caused by hyperglucagonemia and may be due to zinc or amino acid deficiency.

10.5.3.3 Laboratory Findings

- **Elevated serum glucagon**, usually 10–20 times above normal **(normal: 0–150 pg/ml)**

10.5.3.4 Imaging (Fig. 10.76)

- Most glucagonomas originate in the body and tail of the pancreas
- Size: average diameter is 5–6 cm
- Most times, the diagnosis is delayed

Ultrasound (US, EUS, IOUS)

Findings

- Hypoechoic, vascular mass
- Hypoechoic, target-like liver lesions (metastases)

Computed Tomography (CT)

Findings

- Small or large bulky mass, with homogeneous or heterogeneous enhancement
- Hypervascular metastases (liver and/or lymph nodes)

Magnetic Resonance (MR)

Findings

- **T1WI**: low signal intensity mass
- **T2WI**: hyperintense to the pancreas
- **T1WIFS with gadolinium**: homogeneous or heterogeneous enhancement

Octreotide Scan

Finding

- Uptake of the radiotracer by the tumor/s and metastases

Practical Pearl

- The diagnosis of glucagonoma may be suggested by the clinical presentation and biopsy of skin lesions but is confirmed by elevated levels of fasting serum glucagon and the presence of a pancreatic mass on CT.

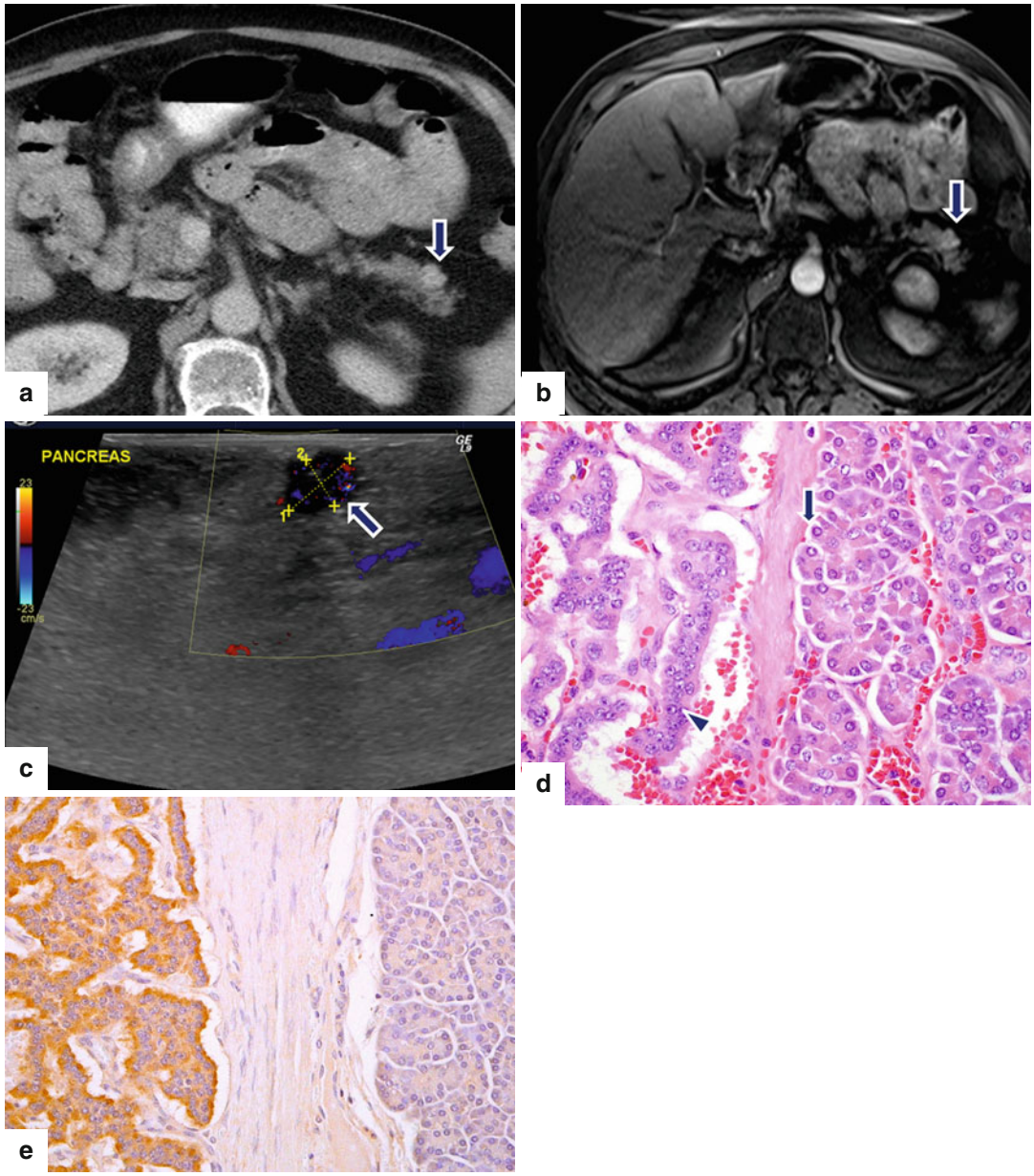

Fig. 10.76 Glucagonoma on imaging. A 67-year-old male with history of diarrhea and weight loss. Incidental pancreatic mass found on abdominal CT. CECT axial (**a**) and contrast-enhanced fat-suppressed T1-weighted axial (**b**) images demonstrate a small, hypervascular mass in the pancreatic tail (*arrows*). IUOS transverse image (**c**) demonstrates a small, hypervascular mass involving the pancreatic tail (*arrow*). Histological section (**d**) (H&E, 60×) shows a PNEN. Note the interphase between normal pancreas (*arrow*) and tumor (*arrowhead*). The tumor cells showed positivity for glucagon (**e**) by immunohistochemistry (40×)

10.5.4 Vasoactive Intestinal Peptide-Secreting Tumor (VIPoma)

10.5.4.1 Epidemiology

- Very rare
- Secretes vasoactive intestinal polypeptide (VIP)
- VIP acts on cyclic adenosine monophosphate within the bowel epithelium to inhibit the absorption of and stimulate the secretion of water and electrolytes into the bowel lumen
- Peak incidence: fifth and sixth decades
- Equal gender distribution
- Rarely associated with MEN-1 syndrome
- Most present with malignant behavior

10.5.4.2 Clinical Syndrome (Verner-Morrison Syndrome)

- Severe, intermittent, watery diarrhea (6–8 L per day)
- Hypokalemia
- Achlorhydria

Practical Pearl

- The secretory-type diarrhea is secondary to a massive jejunal net secretion of water and electrolytes.

10.5.4.3 Laboratory Findings

- Elevated fasting serum VIP level
- Usually more than 200 pg/ml
- Hypokalemia/achlorhydria
- Elevated calcium levels during episodes of diarrhea

10.5.4.4 Imaging (Fig. 10.77)

- Most frequently occur in the pancreatic tail
- 20 % extrapancreatic (sympathetic ganglia of retroperitoneum or mediastinum)
- Other unusual locations: esophagus, small bowel, colon, liver, and kidney
- Size: mean of 5 cm at diagnosis
- 60–80 % metastases at time of presentation

Ultrasound (US, EUS, IOUS)

Finding

- Hypoechoic, hypervascular mass

Computed Tomography (CT)

Findings

- Small masses: homogeneous enhancement.
- Larger lesions: heterogeneous, hyperenhancing masses; cystic changes and/or calcifications may be present.

Magnetic Resonance (MR)

Findings

- **T1WI**: low signal intensity mass
- **T2WI**: hyperintense to the pancreas
- **T1WIFS with Gad**: homogeneous or heterogeneous enhancement

Octreotide Scan

Findings

- Uptake of the radiotracer by the tumor and metastases

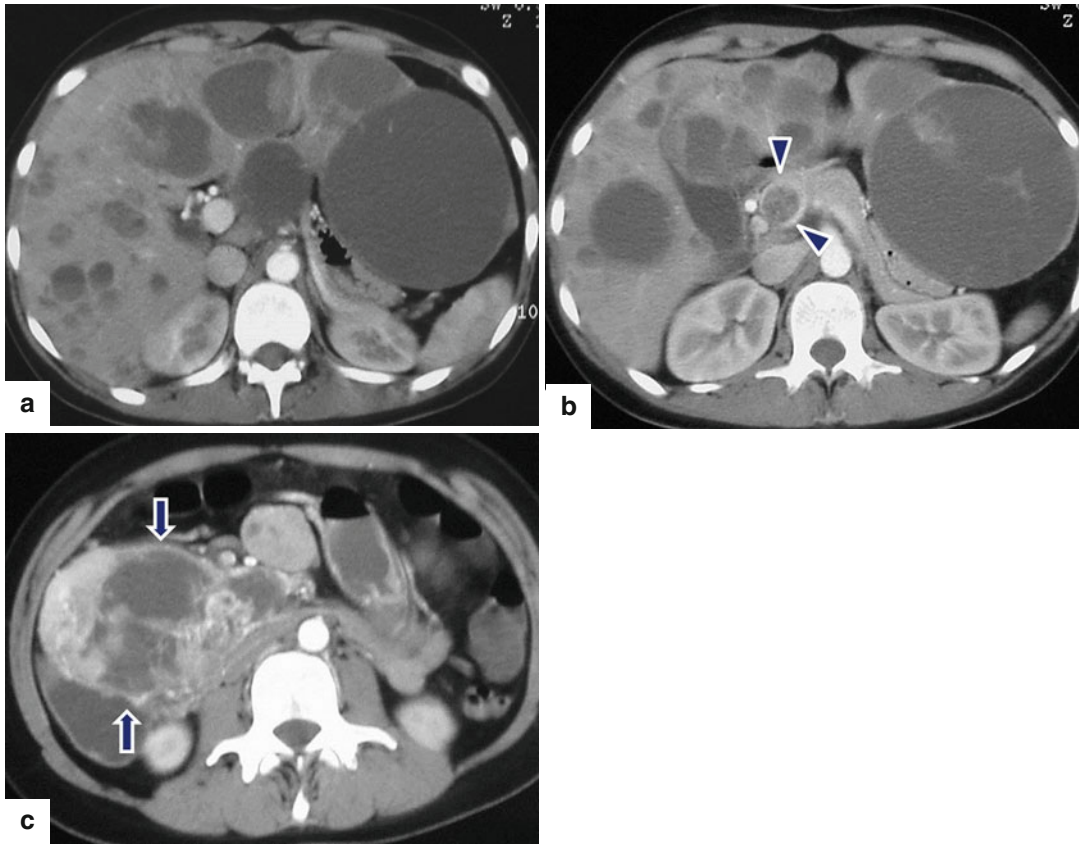

Fig. 10.77 Vasoactive intestinal peptide-secreting tumor (VIPoma) on CT. **A** 53-year-old female with history of intermittent diarrhea and elevated serum VIP level. CECT axial (**a–c**) images show a complex, large, hypervascular mass (**c**) (*arrows*) in the pancreatic head extending into the portal vein (**b**) (*arrowheads*), associated with multiple necrotic hepatic metastases (**a, b**)

10.5.5 Somatostatinoma

10.5.5.1 Epidemiology

- Accounts for less than 2 % of all well-differentiated PNENs
- Arise from delta (δ) cells of the pancreatic islet cells
- These tumors produce somatostatin. Somatostatin inhibits the intestinal absorption and gut motility and release of insulin, glucagon, gastrin, and pancreatic enzymes
- Mean age of presentation: 50 years
- Equal sex distribution
- Most are malignant (90 %)

Associated with

- **Neurofibromatosis type 1 (von Recklinghausen's disease)**
- **MEN-1 syndrome**

10.5.5.2 Clinical Symptoms

- Nonspecific
- Occur in 20 % of patients
- **Diabetes mellitus**, **steatorrhea**, **diarrhea**, **cholelitiasis**, **hypochlorhydria**, **and weight loss**

Practical Pearl

- Somatostatinomas detected in neurofibromatosis type 1 are usually asymptomatic and less frequently associated with metastases.

10.5.5.3 Laboratory Evaluation

- Fasting serum somatostatin levels are 50-fold higher than normal

10.5.5.4 Imaging

(Figs. 10.78 and 10.79)

- The majority occur in the pancreatic head or duodenum (ampullary and periampullary regions).
- Duodenal somatostatinomas are most likely related to neurofibromatosis, type 1.
- Rare primary sites: small bowel and colon.
- Metastases (liver, lymph nodes) are common at presentation.

Ultrasound (US, EUS, IOUS)

Findings

- Hypoechoic or heterogeneous, hypervascular mass

Computed Tomography (CT)

Findings

- Heterogeneous, hyperenhancing mass
- Hypervascular metastases (liver and/or lymph nodes), homogeneous or with ring-like enhancement

Magnetic Resonance (MR)

Findings

- **T1WI**: low signal intensity mass in relation to the pancreas
- **T2WI**: high signal intensity
- **T1WIFS with Gad**: homogeneous or heterogeneous enhancement

Octreotide Scan

Findings

- Uptake of the radiotracer by the tumor and metastases

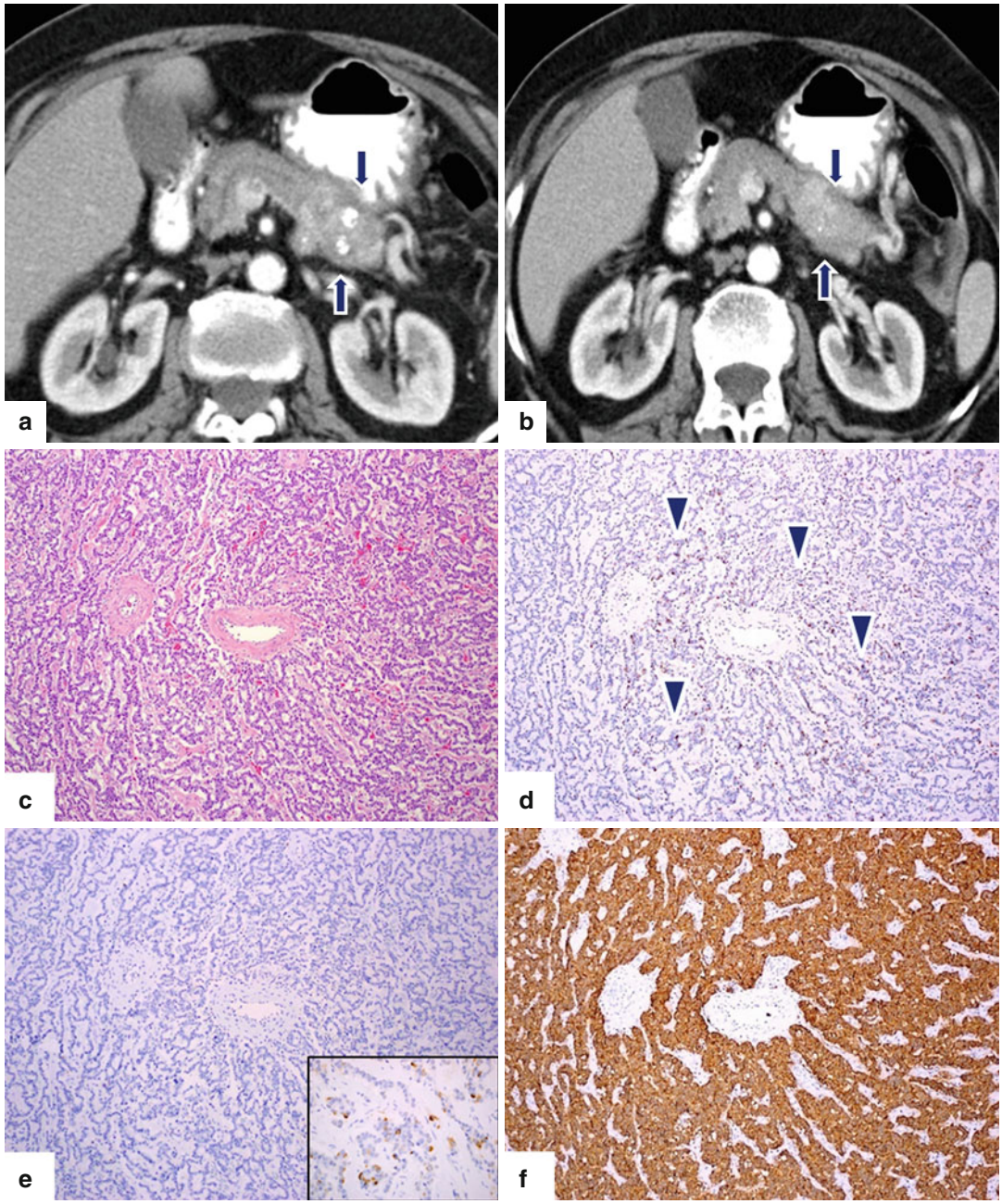

Fig. 10.78 Somatostatinoma on CT. A 78-year-old female with history of episodes of diarrhea, steatorrhea, and weight loss. CECT axial (**a**, **b**) images reveal a poorly defined hypervascular mass with coarse calcifications involving the pancreatic body and tail (*arrows*). Microscopic examination revealed a well-differentiated neuroendocrine neoplasm, grade 1, with a trabecular pattern (**c**) (H&E, 10×). Tumor cells were focally positive for glucagon (**d**) (*arrowheads*) and somatostatin (**e**) (*inset*).

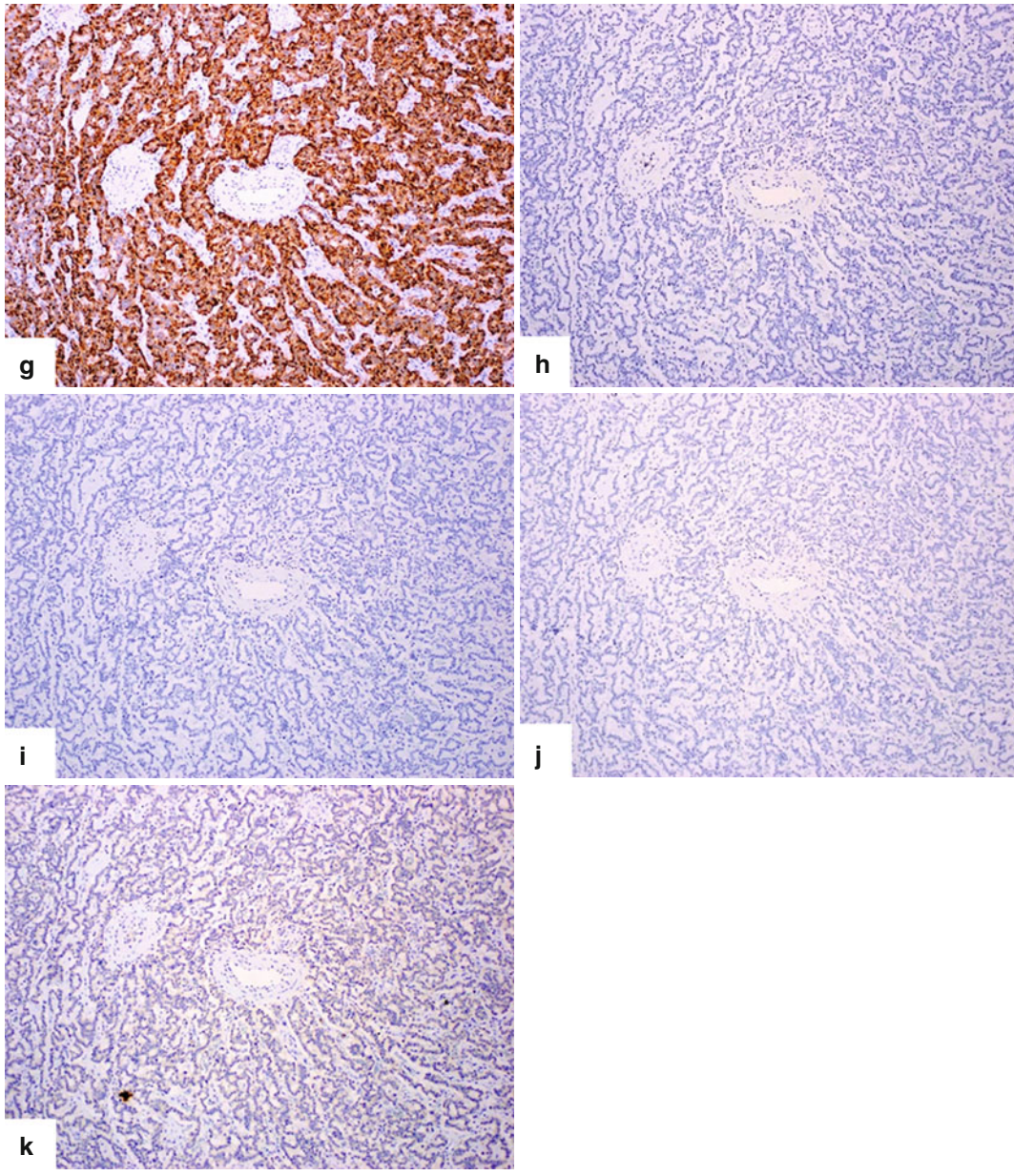

Fig. 10.78 (continued) Tumor cells were also strongly positive for synaptophysin (**f**) and chromogranin (**g**), and negative for insulin (**h**), pancreatic polypeptide (**i**), and VIP (**j**). Ki-67 proliferative index was <3 % (**k**) (immunohistochemistry, 10×)

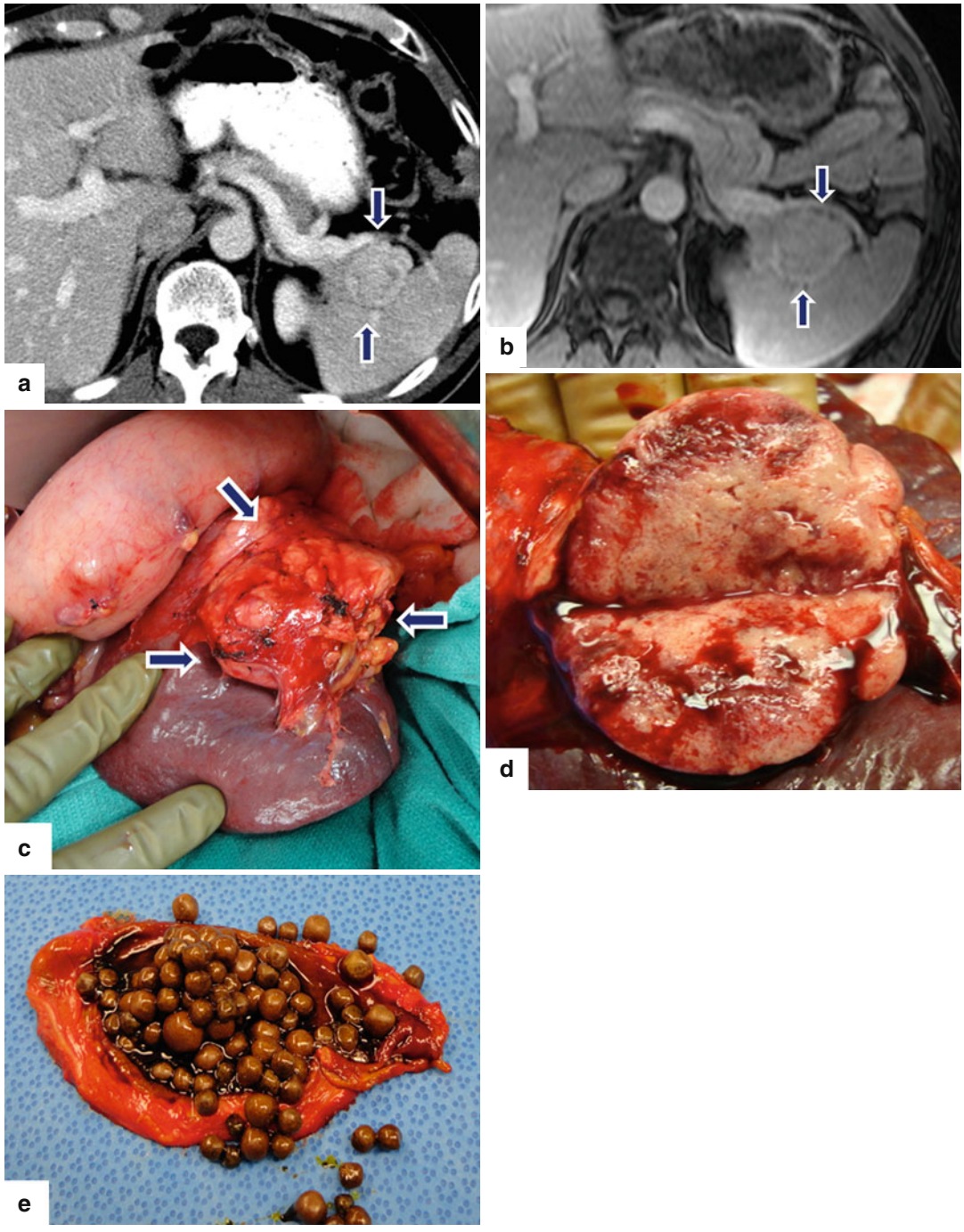

Fig. 10.79 Somatostatinoma on CT/MR. A 53-year-old male with history of acute onset of diabetes, cholelithiasis, and weight loss. CECT axial (**a**) and contrast-enhanced fat-suppressed gradient echo T1-weighted (**b**) images demonstrate a hypervascular, heterogeneous mass (*arrows*) in the pancreatic tail. Intraoperative photograph (**c**) demonstrates a large, lobulated mass in the pancreas extending into the splenic hilum (*arrows*). Photograph of the bivalved gross specimen (**d**) demonstrates a large, fleshy, partially hemorrhagic mass. Photograph of the open gallbladder (**e**) demonstrates multiple, small, round brown gallstones

10.6 Other Functioning PNENs

- Many other types of functioning PNEN have been described
- Extremely rare
- **May secrete**:
  - Adrenocorticotropic hormone (Figs. 10.80–10.82)
  - Serotonin
  - Parathyroid hormone
  - Growth hormone
  - Calcitonin

Practical Pearl

- PNEN may cause symptoms related to more than one hormone. These symptoms may occur either synchronously or sequentially during treatment.

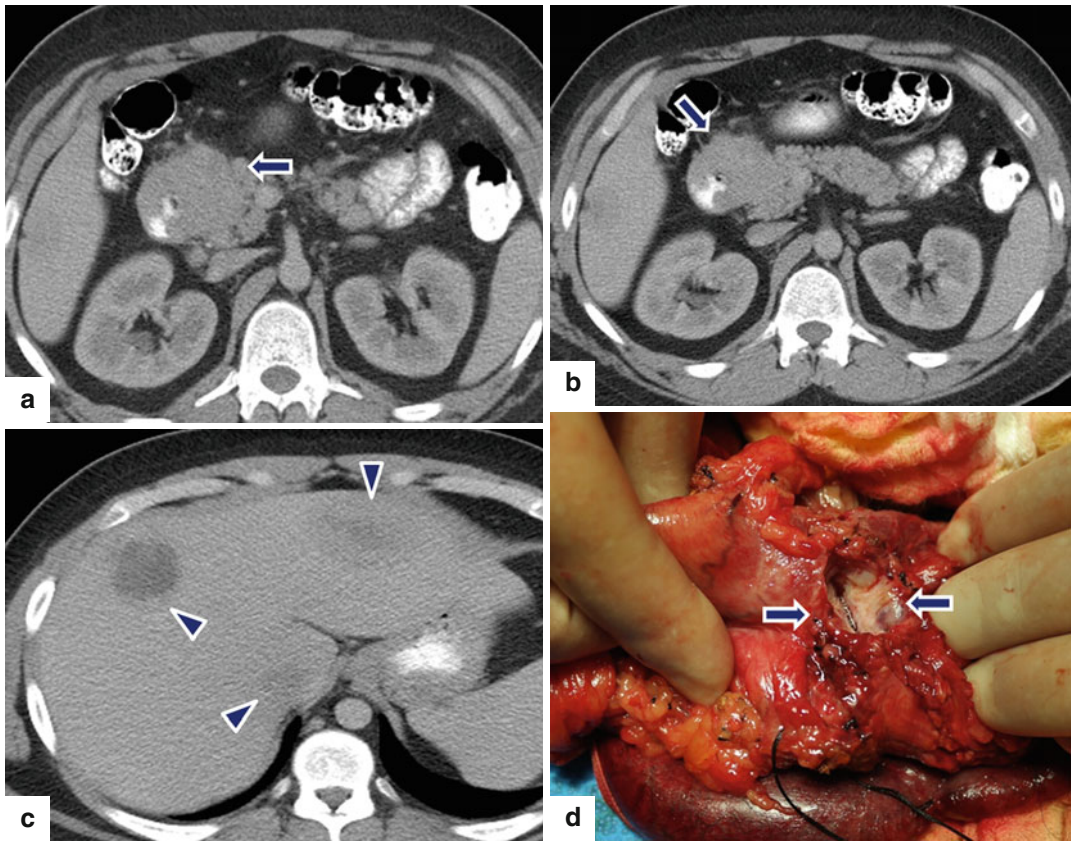

Fig. 10.80 ACTHoma on imaging. A 26-year-old male with history of exogenous obesity, diabetes mellitus, Cushing syndrome, and a serum chromogranin of 60 ng/ml. Endoscopic ultrasound showed a pancreatic head mass, which was percutaneously biopsied. Pathology report showed a neuroendocrine tumor. CECT axial (**a–c**) images show a pancreatic head mass with poorly defined margins involving the second portion of the duodenum (*arrows*) and the presence of hepatic metastases (*arrowheads*). The pancreatic tumor and the hepatic metastases were treated successfully with chemotherapy, somatostatin, and Y-90 therapy with the eventual surgical removal of the pancreatic head mass. Patient underwent a pancreaticoduodenectomy. Photograph of the bivalved specimen (**d**) shows a white-tan tumor (*arrows*).

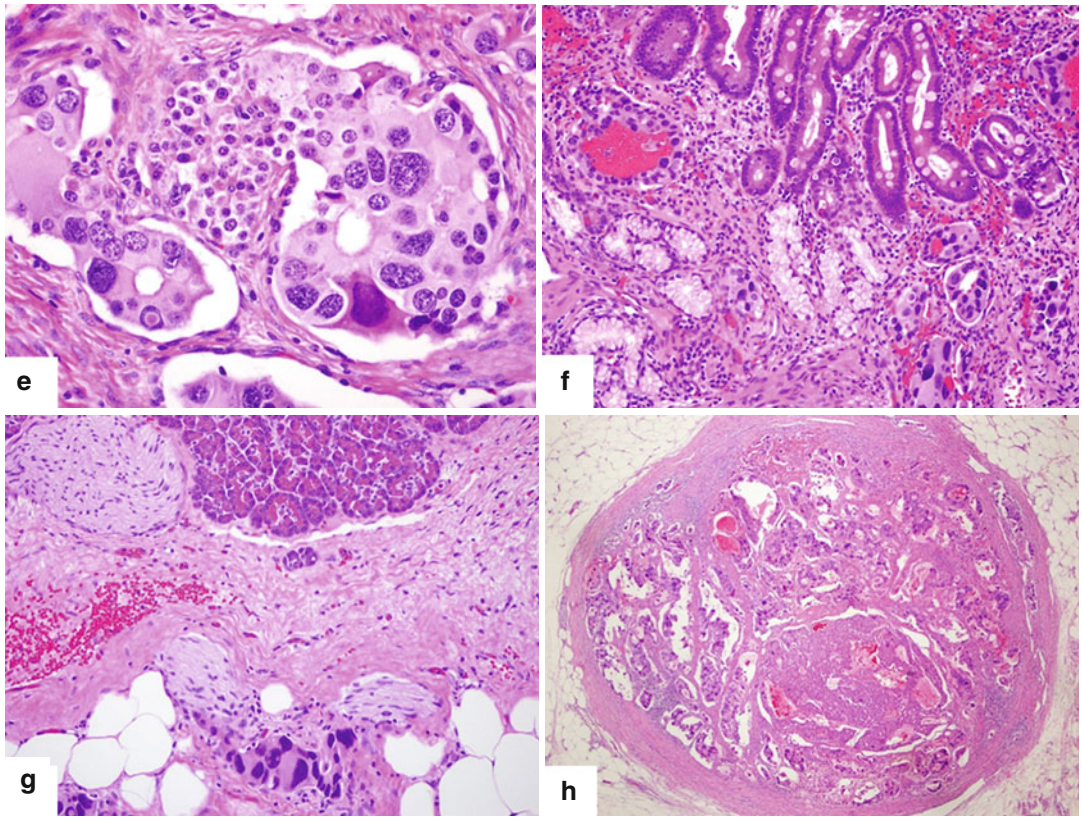

Fig. 10.80 (continued) Microscopic examination revealed a well-differentiated neuroendocrine neoplasm, grade 2, with cellular atypia (**e**), infiltrating the duodenum (**f**), and displaying diffuse perineural invasion (**g**) and node metastasis. A small peripancreatic lymph node (**h**) was completely replaced by the tumor (H&E, 60×, 10×, 4×).

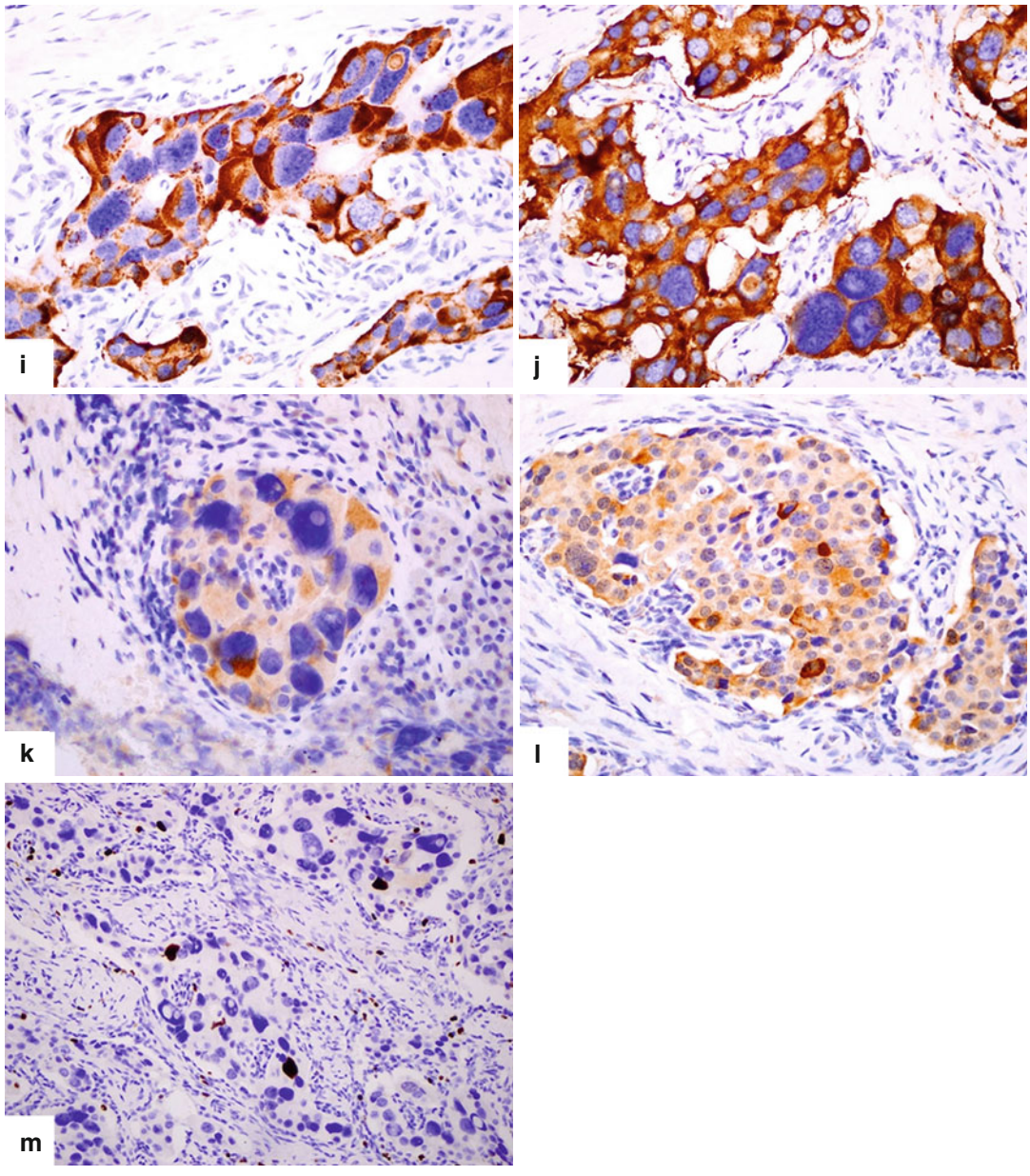

Fig. 10.80 (continued) Pleomorphic tumor cells were strongly positive for chromogranin (**i**) and synaptophysin (**j**) and were mildly positive for ACTH (**k**) and serotonin (**l**). Ki-67 proliferation index was approximately 4 % (**m**) (immunohistochemistry, 60×)

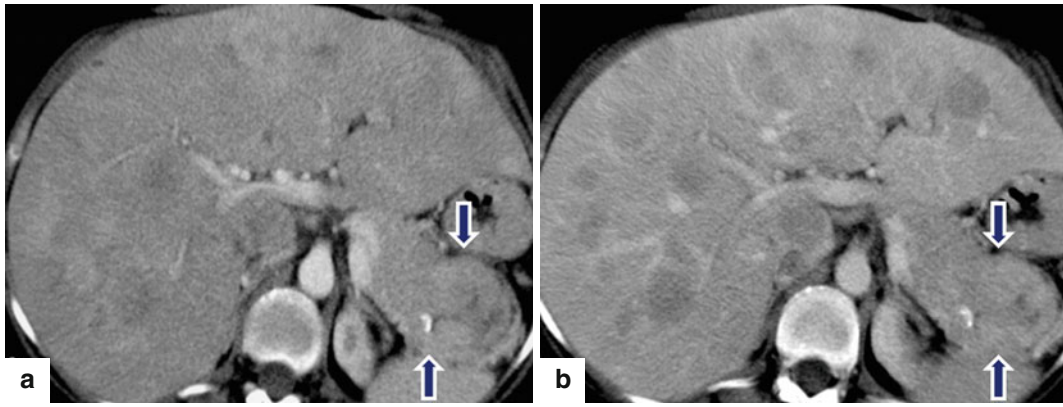

Fig. 10.81 ACTHoma on imaging. A 24-year-old female with history of hirsutism, central abdominal obesity, striae, weight gain, acne, and elevated serum ACTH levels. CECT axial (**a**, **b**) images demonstrate a large hypervascular, heterogeneous mass with coarse calcifications involving the body and tail of the pancreas (*arrows*) and the presence of multiple hypovascular, hepatic metastases. The patient underwent a multivisceral transplant as treatment

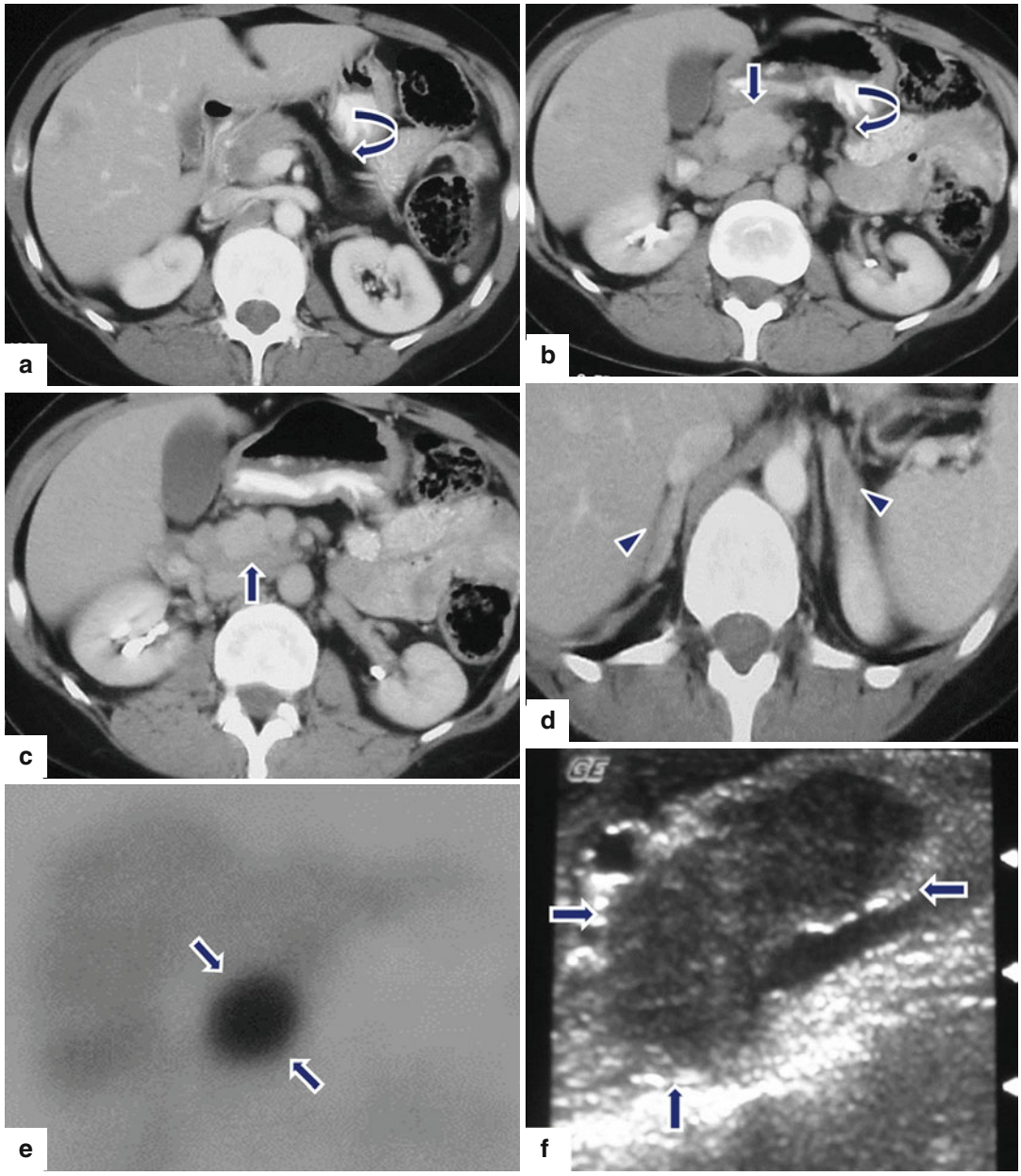

Fig. 10.82 ACTHoma on imaging. A 44-year-old female patient with Cushing syndrome. CECT axial **(a–d)** images demonstrate a homogeneous mass in the pancreatic head (*arrows*) associated with lipodystrophy of the body and tail of the pancreas (*curved arrows*) and diffuse enlargement of the adrenal glands (*arrowheads*). Octreotide scan (**e**) demonstrates radiotracer uptake by this mass (*arrows*). IOUS transverse (**f**) image confirms the presence of a large mass in the pancreatic head (*arrows*)

10.7 Syndromes Associated with PNEN

10.7.1 Multiple Endocrine Neoplasia Type I (Werner Syndrome) (Figs. 10.9, 10.14, 10.70, and 10.83)

- Genetic disorder characterized by two or more endocrine tumors resulting in malignancy or increased glandular function
- Most often associated with parathyroid, pancreatic, and pituitary tumors
- Autosomal dominant condition
- Prevalence: one person in every 30,000 people
- Equal gender distribution
- MEN-1 tumor suppressor gene is located on chromosome 11q13 encoding the protein menin, which suppresses cell proliferation
- MEN-1 mutation present in 21 % of patients with sporadic PNEN

PNEN in MEN-1 Syndrome

- Mean age of presentation: mid-30s
- Gastrinomas: 60 % of patients (more common in duodenum)
- Insulinomas: 20–30 % of patients
- May have multiple microadenomas and nonfunctioning PNEN throughout the pancreas

Practical Pearl

- MEN-1 is diagnosed in about 25 % of patients with gastrinomas and 5–10 % in patients with insulinomas.

10.7.1.1 Clinical Manifestations (3Ps: Parathyroid, Pancreas, Pituitary)

- Hyperparathyroidism (parathyroid adenoma): **90 % of the patients**
  - Hypercalcemia with elevated PTH
- Endocrine tumors of the pancreas or duodenum: **30–80 % of the patients**
  - Elevated serum gastrin or insulin levels
- Anterior pituitary adenoma: **20–65 % of the patients**
  - Elevated prolactin, GH, or ACTH

Practical Pearls

- Parathyroid and pituitary lesions usually manifest before pancreatic lesions are found.
- Patients with duodenal gastrinomas have a better prognosis than patients with pancreatic gastrinomas.
- PNEN associated with MEN-1 have a lower rate of malignancy than sporadic tumors.
- They have a higher rate of postoperative recurrence and are a common cause of death in patients.
- Cutaneous tumors are also common in MEN-1: angiofibromas (face), collagenomas, and lipomas.

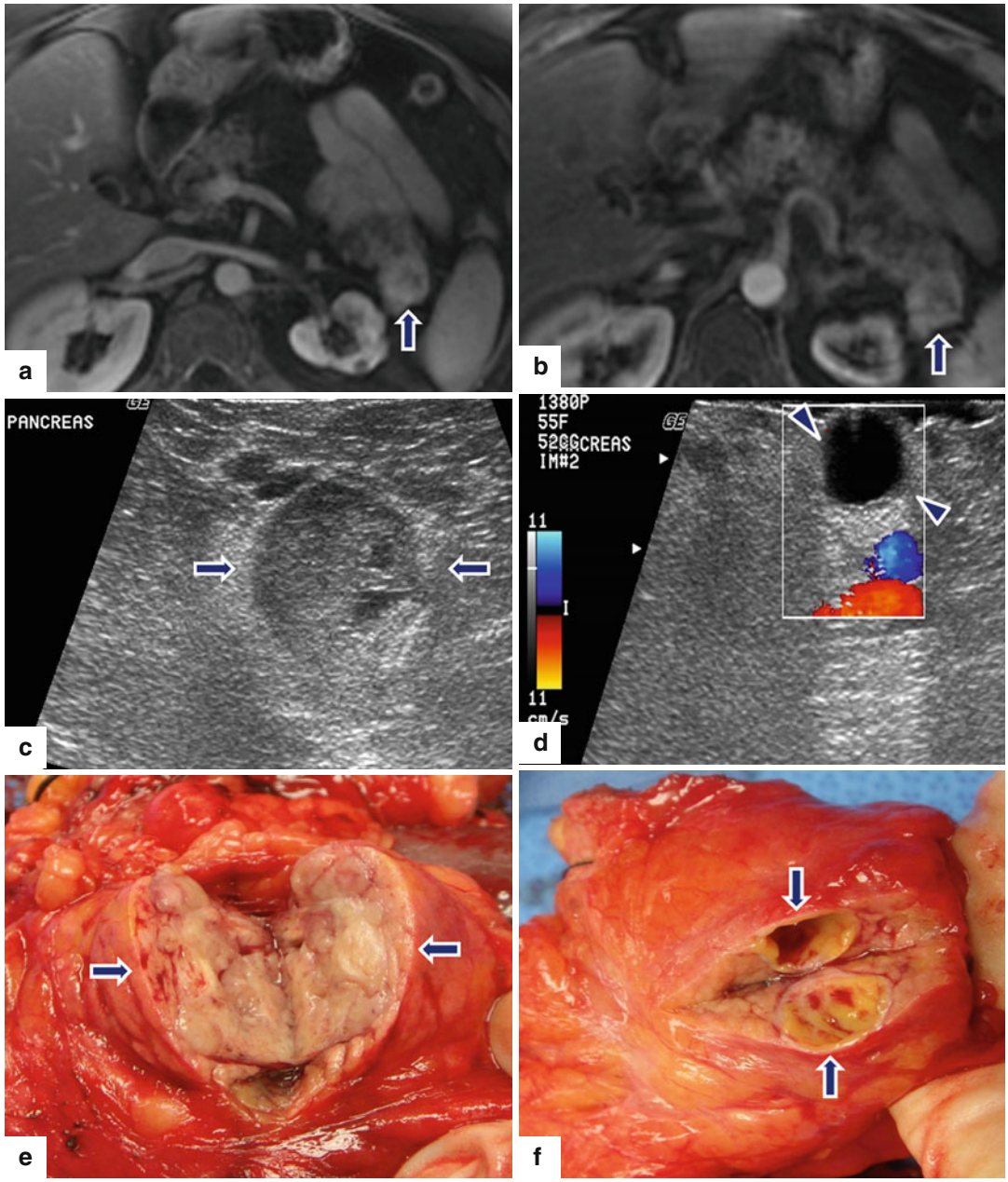

Fig. 10.83 Nonfunctional PNENs in MEN-1 syndrome on MR. A 63-year-old male with history of MEN-1 syndrome. Surveillance abdominal MR found an incidental pancreatic mass. Contrast-enhanced fat-suppressed T1-weighted images (**a**, **b**) display a hypervascular mass with heterogeneous signal intensity in the pancreatic tail (*arrows*). Note the atrophy of the left kidney. IOUS transverse (**c**, **d**) images confirm the presence of a solid mass in the pancreatic tail (*arrows*) and demonstrate an additional small cystic mass with a thick wall in the proximal pancreatic body (*arrowheads*). The patient underwent a distal pancreatectomy and splenectomy. Photograph of the bivalved pancreatic tail mass (**e**) displays a pale pink, fleshy tumor (*arrows*) and the photograph of the mass in the pancreatic body (**f**) displays a small cystic mass with a thick wall (*arrows*).

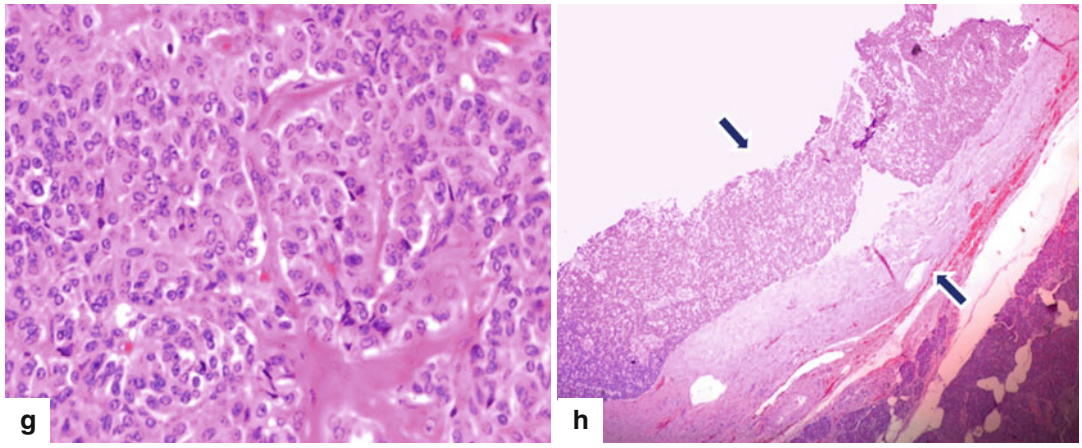

Fig. 10.83 (continued) Histological sections (**g**, **h**) demonstrate a cystic neuroendocrine tumor composed of round cells with ample eosinophilic cytoplasm. The tumor was surrounded by a thick fibrous capsule (*arrows*) (H&E, 20×, 4×)

10.7.2 Von Hippel-Lindau Syndrome (VHL) (Figs. 10.10 and 10.84)

- Autosomal dominant syndrome
- Prevalence: 1 in 36,000–39,000 people
- Caused by mutation of the VHL suppressor gene (located on chromosome 3p25)
- Patients develop multiple clear cell, benign and malignant tumors in multiple organ systems

Hallmark of This Condition

- Retinal and central nervous system hemangioblastomas
- Clear cell renal cell carcinomas
- Pheochromocytomas
- Pancreatic serous cystadenomas
- Pancreatic neuroendocrine neoplasms

PNEN in VHL

- Occurrence: 5.6–15 %
- Usually multiple neoplasms
- Synchronous pheochromocytomas (40 %)
- Synchronous cystic pancreatic disease (60 %)
- Age range: 16–42 years; mean age: 31.5 years
- Most of them are nonfunctional pancreatic neuroendocrine tumors (discovered on screening)
- Slow growing
- Frequency of metastatic disease is low

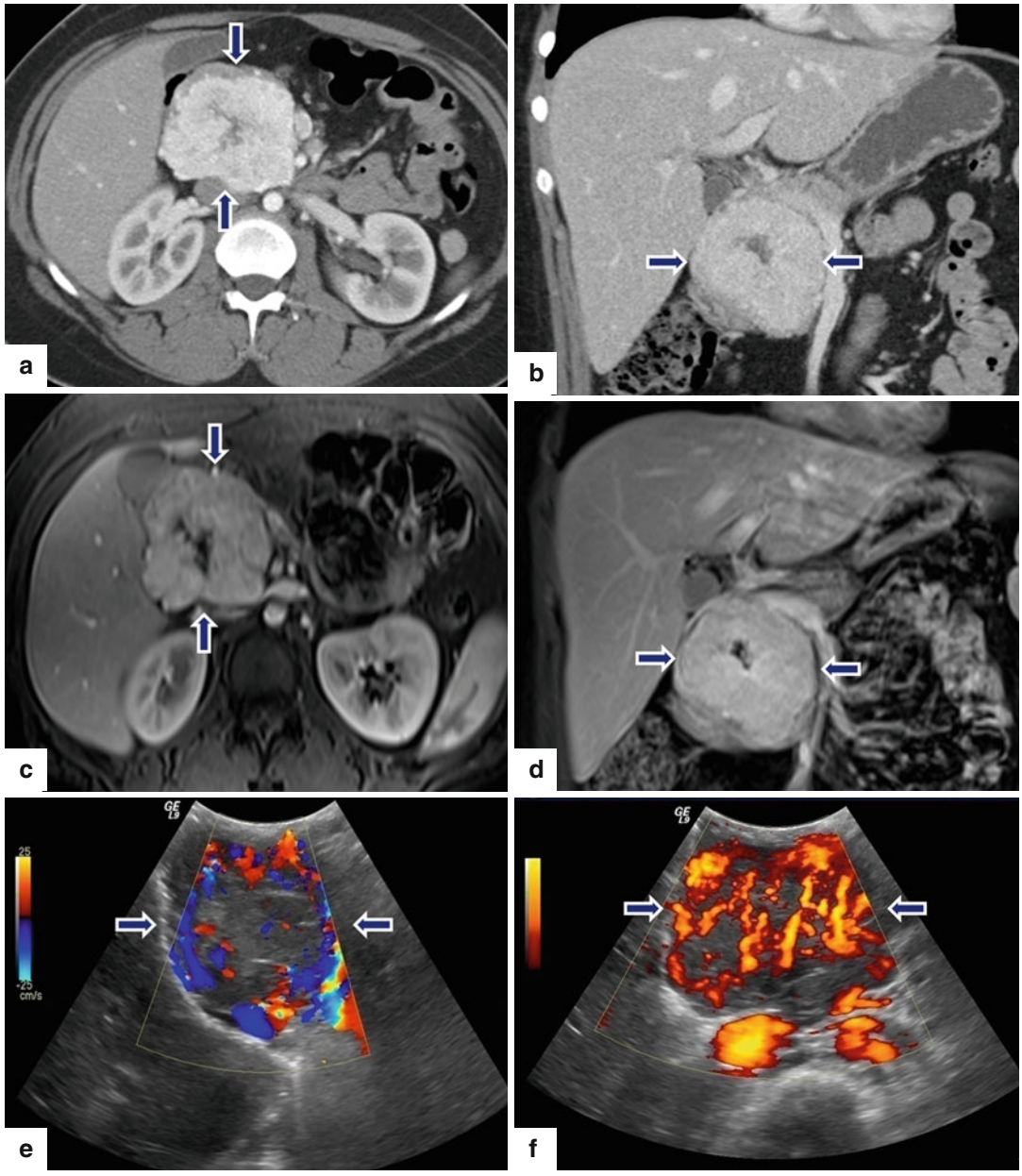

Fig. 10.84 Nonfunctional PNEN in von Hippel-Lindau syndrome. An 18-year-old asymptomatic female with history of von Hippel-Lindau disease. Surveillance abdominal CT found an incidental pancreatic mass. CECT axial (**a**) and coronal (**b**) images show a large, lobulated, well-circumscribed mass with central necrosis involving the head of the pancreas (*arrows*). Contrast-enhanced fat-suppressed gradient echo T1-weighted axial (**c**) and coronal (**d**) images confirm the presence of a large, hypervascular mass in the head of the pancreas (*arrows*). Note the absence of associated dilatation of the pancreatic duct and common bile duct. IOUS color Doppler (**e**) and power Doppler (**f**) images show a hypervascular pancreatic mass (*arrows*).

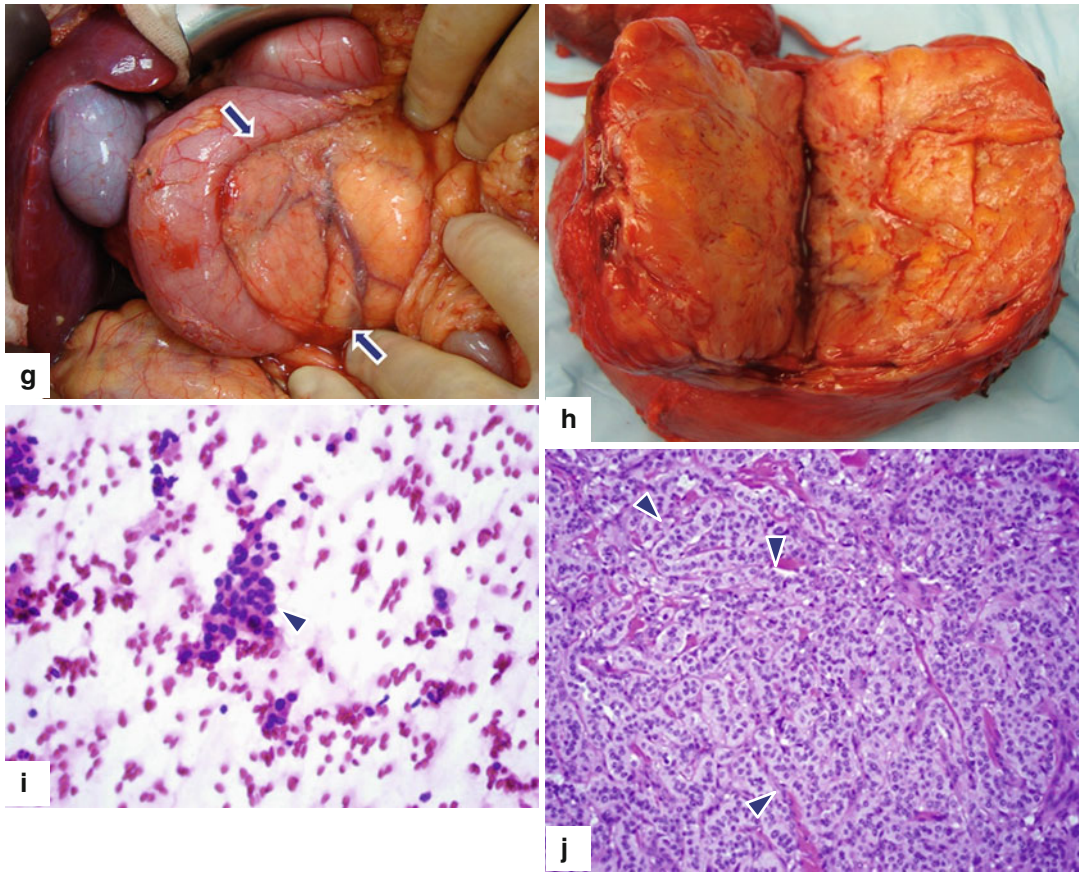

Fig. 10.84 (continued) Patient underwent a pancreaticoduodenectomy. Intraoperative photograph (**g**) shows a large, yellow mass with lobulated margins abutting the duodenum (*arrows*). Photograph of the bivalved specimen (**h**) shows a fleshy, yellow-tan, soft mass. Cytology imprint of the tumor (**i**) reveals mildly cohesive groups of cells (*arrowhead*) with round nuclei and "salt-and-pepper" chromatin in a bloody background. Histological section (**j**) reveals a solid tumor with cells arranged in a trabecular and ribbon-like pattern (*arrowheads*) (H&E, 10×)

10.7.3 Neurofibromatosis Type 1 (NFT1)

- Relatively common disorder occurring in 4,000–5,000 live births.
- Occurs upon alteration of the NF-1 gene on chromosome 15q11.2 which encodes neurofibromin.
- Neurofibromin acts as a tumor suppressor.
- Signs and symptoms present by 5 years of age.
- The most common manifestations are neurofibromas and café au lait skin macules, as well as functional neurological deficits and epilepsy.
- Other lesions: ganglioneuromas, gastrointestinal stromal tumors, pheochromocytomas (rare), and precocious puberty.
- Endocrine involvement: duodenal somatostatinomas (more common), pancreatic somatostatinomas, pancreatic gastrinomas, insulinomas, and nonfunctioning PNENs (rare).

10.7.4 Tuberous Sclerosis (TS)

- Autosomal dominant neurocutaneous multisystem disorder.
- Associated with mutations in two genes: the TSC1 gene at 9q34 that encodes hamartin and TSC2 at 16p13.3 that encodes tuberin.
- Most cases are due to sporadic de novo mutations, with no family history of the disease.
- Manifestations: apparent shortly after birth.
- Hamartomas manifest in almost every organ: the brain, skin, eyes, heart, kidneys, lungs, and skeleton.
- Disabling neurological features: epilepsy, mental retardation, and autism.
- The association of TS and pancreatic neuroendocrine neoplasms (PNENs) is not clear.
- Malignant PNENs have been reported in children.
- Functional PNENs have been reported to produce insulin or gastrin.

10.8 Poorly Differentiated Neuroendocrine Carcinomas (High-Grade Neuroendocrine Carcinomas)

- Rare
- Prevalence: 2–3 % of all PNENs
- Usually occur in older men (middle aged to elderly)
- Fatal within less than 1 year
- Usually large tumors at presentation: >5 cm in diameter
- Histologically, they are classified as small cell carcinoma and large cell carcinoma

10.8.1 Clinical Symptoms

- Abdominal pain
- Back pain
- Cachexia
- Jaundice (obstruction of biliary system)

10.8.2 Imaging (CT/MR) (Figs. 10.85 and 10.86)

- Large heterogeneous masses
- Well or poorly defined margins
- Obstruction of the pancreatic duct
- Obstruction of the common bile duct
- Liver metastases, hypervascular (homogeneous or heterogeneous)

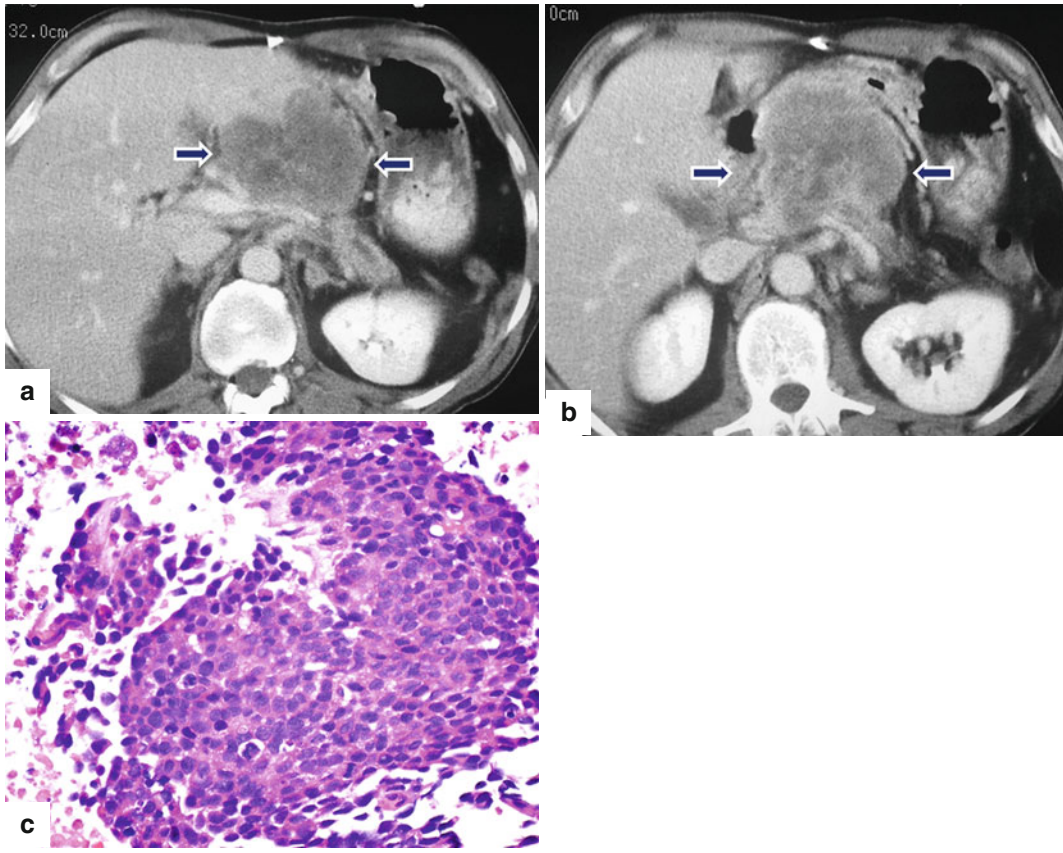

Fig. 10.85 Poorly differentiated PNEN on CT. A 57-year-old male with history of epigastric pain and weight loss. CECT axial (**a**, **b**) images demonstrate a large, infiltrative, ill-defined, heterogeneous mass involving the pancreatic body (*arrows*). Note the atrophy of the distal gland and the dilatation of the pancreatic duct. Histological section (**c**) demonstrates a poorly differentiated neuroendocrine carcinoma, small cell type (H&E, 40×)

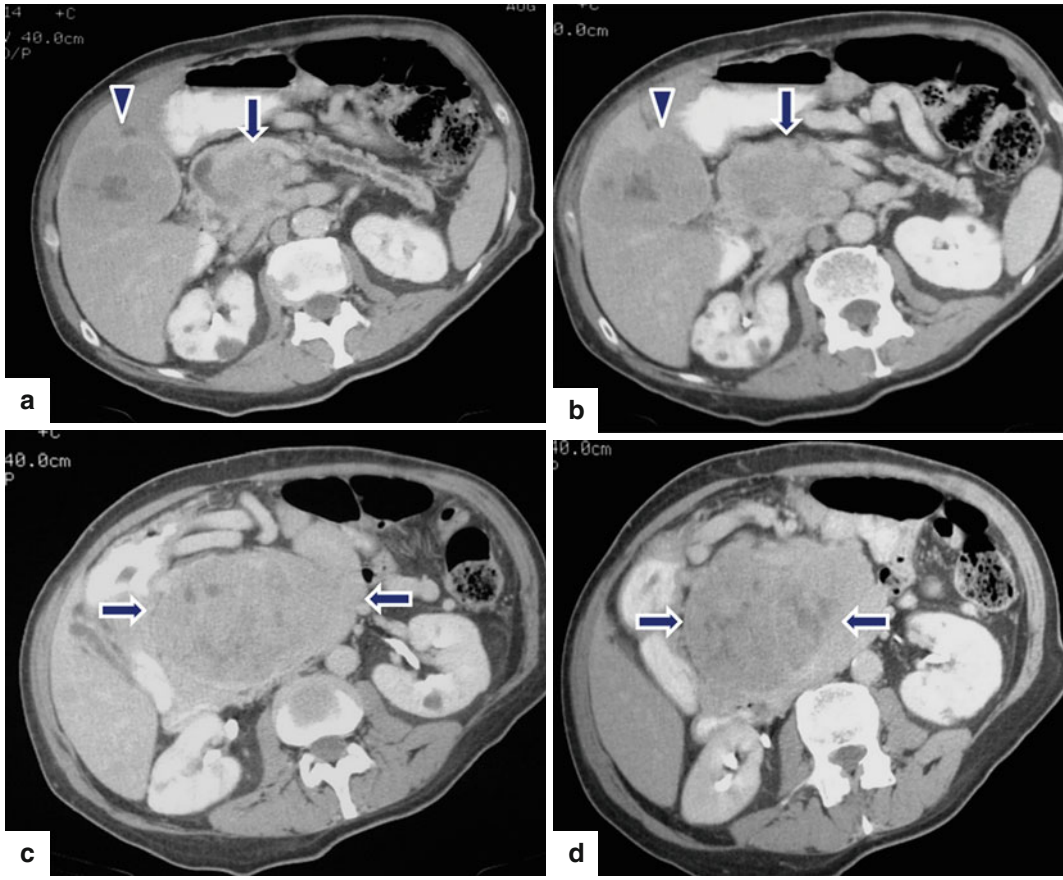

Fig. 10.86 Poorly differentiated PNEN on CT. A 65-year-old male with history of malaise, loss of appetite, and epigastric pain. CECT axial (**a**–**d**) images demonstrate a large mass with heterogeneous enhancement in the pancreatic head (*arrows*) associated with dilatation of the distal pancreatic duct and gland atrophy. Note the presence of a large, hypervascular, partially necrotic, metastatic deposit in the right lobe of the liver (**a**, **b**) (*arrowheads*)

10.9 Staging System of Pancreatic Endocrine Tumors

- The AJCC TNM system specific for pancreatic adenocarcinoma should be used.

The American Joint Committee on Cancer (AJCC) TNM Stage System	
T-primary tumor	
TX	Primary tumor cannot be assessed
T0	No evidence of primary tumor
T1	Tumor limited to the pancreas <2 cm
T2	Tumor limited to the pancreas <2 cm
T3	Tumor extends beyond the pancreas but without the involvement of the celiac axis or the superior mesenteric artery
T4	Tumor involves the celiac axis or the superior mesenteric artery (unresectable)
N-regional nodes	
NX	Regional nodes cannot be assessed
N1	No regional node metastases
N2	Regional node metastases
M-distant metastases	
MX	Distant metastases cannot be assessed
M0	No distant metastases
M1	Distant metastases (indicates the presence of any single or multiple metastases at any distant anatomic site including no regional nodes)

Stage 1a	Stage 1b	Stage IIa	Stage IIb	Stage III	Stage IV
T1,N0	T2,N0	T3,N0	T1–T3,N1	T4, any N, MO	Any T, M1

10.10 Treatment of PNEN: Surgery

- Remains the only curative treatment.
- Only approach that can achieve a complete cure in patients with NE tumors.
- In cases of metastases, surgery has been used to improve hormone-mediated symptoms, quality of life, and survival in certain groups of patients, as well as to reduce tumor bulk and prevent further local and systemic effects.
- Surgical resection of primary tumors, as well as lymph nodes and liver metastases, can improve survival.

Surgical Procedures

- **Enucleation** is the most common surgical procedure for sporadic, small, exophytic PNENs without metastases.
- **Distal pancreatectomy** for deep lesions in the body or tail of the pancreas.
- **Pancreatoduodenectomy** for lesions deep in the head of the pancreas.
- **Central pancreatectomy** is an alternative procedure for lesions deep in the body of the pancreas.
- Isolated metastatic disease can be excised.
- Debulking surgery improves symptoms and survival in these patients.
- **Liver transplantation** may provide palliation in young patients with metastatic disease (only to the liver).

Nonsurgical Procedures

- Hormonally related symptoms in patients with metastatic disease may be managed medically with octreotide or analogs such as lanreotide (symptomatic response occurs in 60–90 %).
- Alpha interferon may be helpful for refractory metastatic disease.
- Patients with gastrinomas that cannot be removed can be treated with long-term omeprazole therapy to alleviate the symptoms.
- Chemotherapy regimens for small cell carcinomas are used in patients with poorly differentiated PNEN.
- Hepatic metastases can be treated with hepatic transarterial chemoembolization (doxorubicin or adriamycin).
- Radiofrequency ablation and NanoKnife® of hepatic lesions are other alternatives used to treat hepatic metastases.
- **Radionuclide may be used to treat tumors with somatostatin receptors** (combination of octreotide, octreotate, or lanreotide with DOTA and a radionuclide such as yttrium 90 or lutetium 155). Therapeutic agents may be administered intravenously or directly into the hepatic artery.

10.11 Prognosis of PNEN

- Functioning tumors have a better prognosis than nonfunctioning tumors.
- Poorly differentiated neuroendocrine carcinomas have the worst prognosis.
- Prognosis of PNEN is much better than pancreatic adenocarcinomas.

Most Reliable Indicators of Malignancy and Poor Prognosis Are
- Extrapancreatic invasion
- Metastatic disease

Poor Prognostic Factors for PNEN
- Size larger than 2–4 cm
- Vascular or neural invasion
- High mitotic rate
- High Ki-67 proliferative index
- Necrosis
- Chromosomal loses or gains

Insulinomas Have the Best Prognosis
- Small
- No necrosis or invasion
- Survival rate similar to that of the general population

Non-insulinoma PNEN
- Recur or metastasize in 50–80 % of patients (survival rate 50–65 %)
  - After PNEN surgical resection: overall median survival is 58–95 months
  - Without surgical resection: overall median survival is 15–21 months

10.12 Teaching Points

Pancreatic neuroendocrine neoplasms (PNENs)	
Classification	**Nonfunctional PNEN** **Functional PNEN**
Pathology	**Macroscopic appearance**: well-circumscribed (majority) or poorly defined margins (malignant masses). Size 1–20 cm **Microscopic appearance**: cells with round or oval nuclei that have stippled, "salt-and-pepper" chromatin and eosinophilic granular cytoplasm **Immunohistochemical markers**: chromogranin A and synaptophysin positive. **Hormonal markers**: insulin, glucagon, somastostatin, gastrin, VIP, and/or PPP
World Health Organization (WHO) classification	Well-differentiated neuroendocrine neoplasm grade 1: less than 2 mitoses per 10 high-power fields and less than 3 % Ki-67 proliferative index Well-differentiated neuroendocrine neoplasm grade 2: 2–20 mitoses per 10 high-power fields and 3–20 % Ki-67 proliferative index Poorly differentiated neuroendocrine carcinoma (small cell carcinoma and large cell carcinoma): more than 20 mitoses per 10 high-power fields and more than 20 % Ki-67 proliferative index
Nonfunctional PNEN	
General	Most common PNEN Usually sporadic Mean age at presentation: 55 years 60 % malignant Slight female predominance Most common PNEN in MEN-1 and von Hippel-Lindau syndromes
Clinical presentation	Abdominal pain, weight loss, anorexia, nausea, abdominal mass, jaundice, pruritus Incidental finding on imaging
Laboratory evaluation	Elevation of serum chromogranin A (sensitivity 50 %)
Imaging	Average size: 5–6 cm Usually solitary, round or oval **Preferred imaging modalities**: CECT and octreoscan CT: hypervascular, homogeneous, or heterogeneous enhancement Rare: cystic changes or calcifications Signs of malignancy: poorly defined margins, vascular invasion, peripancreatic nodes, hypervascular hepatic metastases Octreoscan: radiotracer accumulation in tumor and/or metastases DD: pancreatic adenocarcinoma, metastases, solid papillary tumors of the pancreas, intrapancreatic spleen
Treatment	Resectable masses: surgical resection Unresectable masses: chemotherapy, alpha interferon, radionuclide to treat tumors with somatostatin receptors Liver metastases: hepatic artery chemoembolization, radiofrequency ablation or NanoKnife, liver transplant (young patients)
Functional PNEN	
Insulinoma	Most common functional PNEN Arise from β-cells Produces insulin Usually sporadic Mean age: 45 years Most benign 10 % are malignant
Clinical presentation	**Whipple's triad**: Low glucose level Symptoms and signs of hypoglycemia: dizziness or weakness, associated with fasting or exercise Symptoms are relieved by glucose

Laboratory	Inappropriately elevated insulin level (>5 mU/ml) in the presence of low glucose (<40 mg/dl) Insulin to glucose ratio >0.4 after an overnight fast May be found in MEN-1 and von Hippel-Lindau syndromes
Imaging	Tumor size:<2 cm Usually solitary Even distribution throughout the pancreas Multiple in MEN-1 syndrome **Preferred imaging modalities**: CECT and intraoperative ultrasound (IOUS) CT: hypervascular mass IOUS: hypoechoic, hypervascular mass
Treatment	Surgical resection
Gastrinoma	Second most common functional PNEN Produces gastrin Peak of incident: fifth decade Malignant behavior: 60–90 % Most sporadic 20–25 % associated with MEN-1 syndrome
Clinical presentation	Diarrhea (most common), epigastric pain, dysphagia, atypical ulcers, refractory to the treatment
Imaging	Most located in gastrinoma triangle 55 % arise in the duodenum **Preferred imaging modalities**: Endoscopic ultrasound (EUS), intraoperative ultrasound (IOUS), CECT, octreotide scan CECT: hypervascular mass Octreotide: accumulation of radiotracer in the primary tumor Metastases: peripancreatic nodes, liver (hypervascular)
Laboratory	Gastrin levels over 1,000 pg/ml
Treatment	Surgical resection Unresectable lesions: somatostatin analog, chemotherapy
Glucagonoma	Third most common PNEN Arise from α-cells Produces glucagon 40–60 years of age Usually sporadic Most malignant (50 %)
Clinical presentation	4Ds: dermatitis, diabetes, deep vein thrombosis, and depression
Laboratory finding	Serum glucagon 10–20 times above normal
Imaging	Most common location: body and tail of pancreas Size 5–6 cm **Preferred imaging modalities**: CECT and octreotide scan CECT: hypervascular mass, homogeneous or heterogeneous enhancement Octreotide: accumulation of radiotracer in the primary tumor Metastases: peripancreatic nodes, liver (hypervascular).
Treatment	Surgical resection, chemotherapy
Vasoactive intestinal peptide-secreting tumor (VIPoma)	Very rare Produces vasoactive intestinal polypeptide (VIP) Fifth and sixth decades Most malignant behavior Rarely associated with MEN-1 syndrome
Clinical presentation	Severe diarrhea (6–8 L per day)
Laboratory finding	Elevated fasting serum VIP level (>200 pg/ml)

Imaging	Most occur in the body and tail of the pancreas **Preferred imaging modalities**: CECT and octreotide scan CECT: hypervascular mass, homogeneous or heterogeneous enhancement Octreotide: accumulation of radiotracer
Treatment	Surgical resection Unresectable lesions: chemotherapy
Somatostatinoma	Less than 2 % of functional PNEN Arise from δ-cells Produces somatostatin Associated with neurofibromatosis type 1 and MEN-1 syndrome
Clinical presentation	Nonspecific (diabetes mellitus, steatorrhea, diarrhea, cholelithiasis, hypochlorhydria, and weight loss)
Laboratory finding	Fasting serum somatostatin levels are 50-fold higher than normal
Imaging	Most occur in the body and tail of the pancreas **Preferred imaging modalities**: CECT and octreotide scan CECT: hypervascular mass, homogeneous or heterogeneous enhancement Octreotide: accumulation of radiotracer
Treatment	Surgical resection Unresectable lesions: chemotherapy
Syndromes associated with PNEN	
Multiple endocrine neoplasm MEN-1	May have multiple microadenomas and nonfunctioning PNEN Gastrinomas (60 %); more common in the duodenum Insulinomas (20–30 %)
Von Hippel-Lindau syndrome	Most of them are rare, nonfunctional PNEN
Neurofibromatosis type 1	Duodenal somatostatinomas are more common
Tuberous sclerosis	Malignant PNEN in children Functional PNEN (gastrin, insulin)

Recommended References

Classification, epidemiology, clinical presentation, localization, and staging of pancreatic neuroendocrine tumors (islet-cell tumors). 2013. http://www.uptodate.com/contents/classification-epidemiology-clinical-presentation-localization-and-staging-of-pancreatic-neuroendocrine-tumors-islet-cell-tumors?detectedLanguage=en&source=search_result&search=classification,+epidemiology,+clinical+presentation,+localization,+and+staging&selectedTitle=1~150&provider=noProvider. Accessed 23 Sept 2013.

Classification, epidemiology, clinical presentation, localization, and staging of pancreatic neuroendocrine tumors (islet-cell tumors). 2014. http://www.uptodate.com/contents/classification-epidemiology-clinical-presentation-localization-and-staging-of-pancreatic-neuroendocrine-tumors-islet-cell-tumors. Accessed 19 Dec 2014.

Fidler JL, Johnson CD. Imaging of neuroendocrine tumors of the pancreas. Int J Gastrointest Cancer. 2001;30(1–2):73–85.

Halfdanarson TR, Rubin J, Farnell MB, Grant CS, Petersen GM. Pancreatic endocrine neoplasms: epidemiology and prognosis of pancreatic endocrine tumors. Endocr Relat Cancer. 2008;15(2):409–27.

Kartalis N, Mucelli RM, Sundin A. Recent developments in imaging of pancreatic neuroendocrine tumors. Annals of Gastroenterology: Quarterly Publication of the Hellenic Society of Gastroenterology. 2015;28(2): 193–202.

Lewis RB, Lattin Jr GE, Paal E. Pancreatic endocrine tumors: radiologic-clinicopathologic correlation. Radiographics. 2010;30(6):1445–64.

Marcos HB, Libutti SK, Alexander HR, et al. Neuroendocrine tumors of the pancreas in von Hippel-Lindau disease: spectrum of appearances at CT and MR imaging with histopathologic comparison. Radiology. 2002;225(3):751–8.

Memorial Sloan Kettering Cancer Center. Gastrointestinal neuroendocrine tumors: pancreatic neuroendocrine tumors. 2014. http://www.mskcc.org/cancer-care/adult/gastrointestinal-neuroendocrine-tumors/pancreatic-neuroendocrine-tumors. Accessed 19 Dec 2014.

Öberg K. Treatment of neuroendocrine tumours of the gastrointestinal tract. Oncología (Barc). 2004;27(4):57–61.

Wick MR, Graeme-Cook FM. Pancreatic neuroendocrine neoplasms: a current summary of diagnostic, prognostic, and differential diagnostic information. Am J Clin Pathol. 2001;115(Suppl):S28–45.